

DTIC FILE COPY

AD _____

2

AD-A219 667

MOLECULAR ORIGINS OF SELECTIVE TOXICITY
ANNUAL/FINAL REPORT

Richard L. Schowen and Ildiko M. Kovach

1 November 1987

U.S. ARMY MEDICAL RESEARCH AND DEVELOPMENT COMMAND
Fort Detrick, Frederick, Maryland 21701-5012

Contract No. DAMD17-83-C-3199

The University of Kansas
The Center for Biomedical Research
Campus West, Lawrence, Kansas 66046

DTIC
ELECTE
MAR 26 1990
S B D

Approved for public release; distribution unlimited.

The findings in this report are not to be construed as an official
Department of the Army position unless so designated by other autho-
rized documents.

00 08 12A 077

REPORT DOCUMENTATION PAGE

Form Approved
OMB No 0704-0188
Exp Date Jun 30 198

1a REPORT SECURITY CLASSIFICATION Unclassified		1b. RESTRICTIVE MARKINGS	
2a SECURITY CLASSIFICATION AUTHORITY		3 DISTRIBUTION/AVAILABILITY OF REPORT Approved for public release; distribution unlimited	
2b DECLASSIFICATION/DOWNGRADING SCHEDULE		5. MONITORING ORGANIZATION REPORT NUMBER(S)	
4. PERFORMING ORGANIZATION REPORT NUMBER(S)		7a. NAME OF MONITORING ORGANIZATION	
6a NAME OF PERFORMING ORGANIZATION The University of Kansas The Center for Biomedical Research	6b OFFICE SYMBOL (If applicable)	7b ADDRESS (City, State, and ZIP Code)	
5c. ADDRESS (City, State and ZIP Code) Campus West, Lawrence, KS 66046		9 PROCUREMENT INSTRUMENT IDENTIFICATION NUMBER Contract No. DAMD17-83-C-3199	
8a NAME OF FUNDING SPONSORING ORGANIZATION U.S. Army Medical Research & Development Command	8b OFFICE SYMBOL (If applicable)	10. SOURCE OF FUNDING NUMBERS	
3c. ADDRESS (City, State, and ZIP Code) Fort Detrick Frederick, Maryland 21701-5012		PROGRAM ELEMENT NO 61102A	PROJECT NO 3M1- 61102BS11
		TASK NO EF	WORK UNIT ACCESSION NO 012
1. TITLE (Include Security Classification) Molecular Origins of Selective Toxicity			
2 PERSONAL AUTHOR(S) Schowen, Richard L.; Kovach, Ildiko M.			
13a TYPE OF REPORT Annual/Final	13b TIME COVERED FROM 83/9/15 TO 87/5/31	14 DATE OF REPORT (Year, Month, Day) 1987 November 1	15 PAGE COUNT 120
6 SUPPLEMENTARY NOTES Annual covers period of September 15, 1986-May 31, 1987			
7 COSATI CODES		18 SUBJECT TERMS (Continue on reverse if necessary and identify by block number)	
FIELD	GROUP	SUB-GROUP	RA5, Serine hydrolase inhibition, acetylcholinesterase organophosphates, isotopic probes for acetylcholinesterase inhibition by organophosphates, Toxicity, Catalysis
06	01		
06	20		
19 ABSTRACT (Continue on reverse if necessary and identify by block number) SERINE PROTEASE, ENZYMES The major findings from the overall study are the following: 1. Organophosphorus (OP) compounds recruit the full one-proton catalytic potential of acetylcholinesterase (AChE) in the course of the inhibition stage. AChE was found in the course of this research to be distinct from the serine proteases (see below) in possessing only a one-proton catalytic entity. 2. The inhibition sequence for AChE and other serine hydrolases by OP agents involves not only the actual phosphorylation step ("chemical step") but also kinetically significant induced-fit steps ("physical step(s)").			
20 DISTRIBUTION/AVAILABILITY OF ABSTRACT <input type="checkbox"/> UNCLASSIFIED/UNLIMITED <input checked="" type="checkbox"/> SAME AS RPT <input type="checkbox"/> DTIC USERS		21 ABSTRACT SECURITY CLASSIFICATION Unclassified	
22a NAME OF RESPONSIBLE INDIVIDUAL Mrs. Mary F. Bostian		22b TELEPHONE (Include Area Code) 301/663-7325	22c OFFICE SYMBOL SGRD-RM1-S

3. All OPs recruit part but not all of the acid-base catalytic power of every serine protease examined in the initial inactivation (phosphorylation) step. This is reflected in the normal solvent isotope effects and linear proton inventories. Thus one-proton catalysis is recruited. This is typical of small substrates of these enzymes, which also give one-proton catalysis. On the other hand, the two-proton catalysis recruited by polypeptide substrates is not seen with OP inhibitors.

4. OP compounds attacking AChE pass through a transition state with (a) incomplete Ser-O---P bond formation as signaled by the solvent isotope effect (protolytic one-proton general-base catalysis recruited by the OPs) and a substantial excess of bond-making by Ser-O over fission of P-O [in ArO-bearing agents], as indicated by the inverse secondary-D isotope effects; and (nevertheless) (b) considerable P-O fission as indicated by the large oxygen-18 kinetic isotope effect. Taken together, these data strongly suggest that the inactivation reaction is concerted.

5. Aging of the OP-inactivated AChE involves electrophilic catalysis of carbonium-ion formation, probably by proton donation from an enzymic histidinium function to the oxygen of the alkyl---O breaking bond, as indicated by normal solvent isotope effects, normal (although small) secondary isotope effects in the departing alkyl group, and full incorporation of solvent oxygen-18 in the alcohol product of aging.

Nucleophilic reactivation by 2-PAM appears to be a simple acylation process at P, as indicated by the lack of solvent isotope effects. On the other hand, TMB4 shows both kinetic complexity and an inverse solvent isotope effect, consistent with the involvement of a protein reorganization in the course of reactivation.

PERSONNEL SUPPORTED BY THE CONTRACT

1. Ildiko M. Kovach, Ph.D. Associate Scientist, Center for Biomedical Research, University of Kansas: Co-Principal Investigator
2. Richard L. Schowen, Ph.D. Solon E. Summerfield Professor of Chemistry and Biochemistry, University of Kansas: Co-Principal Investigator
3. Andrew Bennet, Ph.D. Research Associate, Center for Biomedical Research, University of Kansas
4. Joan Harmon-Ashley Huber, Ph.D. Research Technician, Center for Biomedical Research, University of Kansas
5. Mark Larson, B.S. Research Assistant, Center for Biomedical Research, University of Kansas (currently medical student, University of Kansas Medical Center)
6. Jeffrey Bibbs, B.S. Graduate Research Assistant, Department of Chemistry, University of Kansas; Ph.D., 1989.

Accession For	
NTIS GRA&I	<input checked="" type="checkbox"/>
DTIC TAB	<input type="checkbox"/>
Unannounced	<input type="checkbox"/>
Justification	
By _____	
Distribution/	
Availability Codes	
Dist	Avail and/or Special
A-1	



Foreword

Citations of commercial organizations and trade names in this report do not constitute an official Department of the Army endorsement or approval of the products or services of these organizations.

Table of Contents

	Page
Foreword	1
A. Problem	6
B. Background	9
C. Approach	14
D. Results	17
1. Syntheses of Organophosphorus Inhibitors	17
2. Analysis of Labeled Inhibitors	19
3. Kinetic Methods	26
4. Rates, Solvent Isotope Effects and Proton Inventories for the Inhibition of Serine Hydrolases by OPs	28
5. Acetylation and Deacetylation of AChE by Phenyl Acetate	64
6. ^{18}O -Leaving Group and β -D Isotope Effects	64
7. Hydrolytic Reactions of 4-Nitrophenyl 2-Propyl Methylphosphonate (IMN)	74
8. Solvent Isotope Effects for the Aging and Spontaneous Reactivation of 2-Propyl Methylphosphonyl-AChE	74
9. ^{18}O -Exchange in the Aging of Soman-inhibited AChE from the Electric Eel	80
10. Solvent Isotope Effect for the Nucleophilic Reactivation of AChE Inhibited by Sarin	80
11. Chemical Model Reactions for Aging	88
12. Molecular Graphics Modeling of the Interactions of OP Agents with Serine Proteases	89
E. Discussion	93
1. Rates, Solvent Isotope Effects and Proton Inventories for AChE Inhibition by OPs	93
2. Kinetic Isotope Effect Probes for the Inactivation of AChE	95
3. Acetylation and Deacetylation of AChE by Phenyl Acetate	95
4. Inhibition of Serine Proteases	96
5. Comparison of AChE and Serine Protease Catalysis	98
6. Nonenzymic Hydrolysis of Phosphonate Esters	99
7. Solvent Isotope Effects for the Aging of AChE Inhibited by Sarin	99
8. ^{18}O Exchange Studies of Aging of the Soman-Inhibited AChE	100
9. Solvent Isotope Effects for the Nucleophilic Reactivation of the Sarin-inhibited AChE	100
10. Chemical Modeling of Aging	100
11. Molecular Graphics Modeling of the Interactions of OP Agents with Serine Proteases	100

F. Experimental Procedures	102
G. References	109
H. Distribution List	114

Figures

1. Rosenberry's model of the acetylcholinesterase active site.	10
2. Schematic representation of the chymotrypsin active site.	11
3. Comparison of transition states for acyl transfer and phosphoryl transfer.	13
4. HPLC recording of IMN and impurities	20
5. Calibration of fluoride ion concentration	21
6. Burst kinetics of chymotrypsin with MUTMAC	23
7. Calibration of fluorescence intensity	24
8. Inhibition of chymotrypsin by soman (CH ₃)	25
9. First-order rate constants for the inhibition of AChE by soman	31
10. Substrate dependence of the inverse first-order rates of inhibition of AChE by soman.	32
11. Eyring plot for the inhibition of AChE from <u>Electrophorus electricus</u> by soman.	34
12. First-order rate constants for the inhibition of AChE by NPN.	36
13. Plot of relative AChE activities against PA, (v_t/v_0) as a function of time ($e^{-k_h t}$), after inhibition by NPN.	37
14. Inverse first-order rates of inhibition of AChE by MPN.	39
15. Dependence of the first-order rate constants of inhibition of AChE by MPN concentrations.	40
16. pL-Rate profile for the inhibition of α -chymotrypsin by NPN.	42
17. First-order rate constants for the inhibition of chymotrypsin by soman as a function of soman concentration.	44
18. Proton inventory for the reaction of chymotrypsin with soman.	52
19. Proton inventory for the inactivation of chymotrypsin and elastase by NPN.	53
20. Proton inventory for the inactivation of chymotrypsin, elastase and subtilisin by MPN.	54
21. pH Dependence of the phosphorylation of trypsin.	56
22. Proton inventory for the inactivation of subtilisin and trypsin by NPN.	58
23. Proton inventory for the reaction of subtilisin BPN' with soman.	62
24. Proton inventory for the reaction of phenyl acetate with Eel AChE.	68
25. Proton inventory for the reaction of phenyl acetate with AChE (RBC).	69
26. Inactivation of AChE by IMN	70
27. Inactivation of AChE by soman	71
28. Inactivation of AChE by sarin	72
29. pH Dependence of the aqueous hydrolysis of IMN	75
30. Phosphate-catalyzed hydrolysis of IMN	76
31. Phosphate-catalyzed hydrolysis of IMN at three temperatures	77
32. Eyring plots for the phosphate-catalyzed hydrolysis of IMN	78
33. Reactivation and aging of 2-propyl methylphosphonyl-AChE	81

34.	Aging of 2-propyl methylphosphonyl-AChE	82
35.	Aging of L ₆ -2-propyl methylphosphonyl-AChE	83
36.	Mass fragmentogram for aging of soman-inhibited AChE	85
37.	Reactivation of 2-propyl methylphosphonyl-AChE with 2-PAM	86
38.	AChE activity recovered by TMB ⁴ after inhibition by sarin	87
39.	Evaluation of the first-order rate constants for reactivation from data in Figure 38	90
40.	DFP-inhibited trypsin active site and specificity pocket	91
41.	4-Nitrophenyl trypsin O-serinyl propylphosphonate	92

Tables

I.	Bimolecular Rate Constants and Solvent Isotope Effects for the Reaction of Organophosphorus Agents with AChE.	29
J.	Temperature Dependence of the Second-Order Rate Constants for Inhibition of Eel AChE by Soman.	33
III.	Bimolecular Rate Constants and Rate Ratios for the Reaction of Organophosphorus Agents with RBC AChE in HOH, DOD and HOH:DOD = 1:1.	41
IV.	Dependence on pL (L = H,D) of Inhibition Rate Constants for Chymotrypsin.	43
V.	Primary Data for Chymotrypsin Inhibition by Soman.	46
VI.	Primary Data for Chymotrypsin Inhibition by NPN.	47
VII.	Primary Data for Chymotrypsin Inhibition by MPN.	48
VIII.	Inhibition Rate Constants for Serine Proteases with Soman in Binary Mixtures of Protium and Deuterium Oxides (Atom Fraction of Deuterium).	49
IX.	Inhibition Rate Constants for Serine Proteases with NPN in Binary Mixtures of Protium and Deuterium Oxides (Atom Fraction of Deuterium).	50
X.	Inhibition Rate Constants for Serine Proteases with MPN in Binary Mixtures of Protium and Deuterium Oxides (Atom Fraction of Deuterium).	51
XI.	Dependence on pL (L = H,D) of Inhibition Rate Constants for Trypsin ^a with NPN in HOH and DOD Solvents at 25.00 ± 0.05 °C, $\mu = 0.29$.	55
XII.	Primary Data for Trypsin Inhibition by NPN.	57
XIII.	Primary Data for Subtilisin Inhibition by MPN.	59
XIV.	Primary Data for Subtilisin Inhibition by Soman.	60
XV.	Primary Data for Subtilisin Inhibition by NPN.	61
XVI.	Primary Data for Elastase Inhibition by MPN.	63
XVII.	Primary Data for Elastase Inhibition by NPN.	65
XVIIIa.	Second-order Rate Constants and Solvent Isotope Effect Information for Inactivation of Serine Proteases by NPN at 25 °C and Appropriate pL.	66
XVIIIb.	Second-order Rate Constants and Solvent Isotope Effect Information for Inactivation of Serine Proteases by MPN at 25 °C and Appropriate pL.	66
XIX.	Kinetic Parameters in Mixed Isotopic Waters for Hydrolysis of 0.8-8.2 mM Phenyl Acetate by Acetylcholinesterases at pH 7.60 and Equivalent at 25.00 ± 0.05 °C.	67
XX.	Second-order Rate Constants for Inactivation of Acetylcholinesterase.	73
XXI.	Activation Parameters for Nonenzymic Hydrolysis of IMN.	79

- XXII. First-order Rate Constants and Isotope Effects for the Aging of L₆-2-Propyl Methylphosphonyl-AChE (Electric Eel, L=H,D) in pH 6.43 (pD 6.93), 0.13 M Phosphate Buffer. 84
- XXIII. Pseudo-First-Order Rate Constants and Solvent Isotope Effects for the Reactivation of 2-Propyl Methylphosphonyl-AChE (Electric Eel) by Oximes in pH 7.60 (pD 8.10), 0.05 M Phosphate Buffer at 25°C. 84

A. Problem

The overall objective of this project was to learn how organophosphorus compounds (OPs) recruit the catalytic apparatus in the active site of serine hydrolases. Mechanistic investigations were planned for all four characteristic phases of enzyme-OP interactions, i.e., inhibition, aging, spontaneous reactivation, and nucleophilic reactivation. The synthesis of two new inhibitors, bis-4-nitrophenyl 2-propylphosphonate (NPN) and methyl 4-nitrophenyl 2-propylphosphonate (MPN), an investigation of the inhibition of acetylcholinesterases (AChEs) from the electric eel by organophosphorus reagents, and a brief study of model systems for the mechanism of aging were accomplished in the first year.¹ In the second year the inhibition of serine proteases by the agents and confirmation of the mechanism of aging were the chief targets. The inquiry into the recruitment of the AChE acid-base catalytic apparatus has been extended to the inhibition of AChE from human erythrocytes and to the nature of deacetylation of AChEs in the physiologically important reaction. Inactivation of acetylcholinesterase (AChE) by organophosphorus reagents and the mechanism of aging, spontaneous reactivation and nucleophilic reactivation of inhibited AChE have been the main targets of our third year of investigations. Specific features of the problem are detailed below.

1. The Role of Acid-base Catalysis in Inhibition

The sensitivity of the acid-base catalytic mechanism used by hydrolytic enzymes to the structure of the inhibitor and to the inhibitor-induced conformation changes reveals much with respect to the ability of an inhibitor to utilize such an enzyme's acid-base catalytic mechanism. AChE presents an especially interesting case of an evolutionarily highly developed enzyme that has brought its catalytic (chemical) steps to such a level of perfection that the rate-limiting process remains the encounter between the enzyme and its natural substrate.¹² Under such circumstances, acid-base catalysis is not observable by customary mechanistic probes. Some organophosphorus inhibitors exhibit rates of reactions with AChE that approach those of the natural substrate. Among the serine proteases, chymotrypsin has been studied the most extensively with organophosphate (OP) inhibitors and seems to show similar behavior. The question is then whether powerful inhibitors behave similarly to the natural substrate or more like some other type of substrates with respect to the manifestation of acid-base catalysis by hydrolases. Also, reactions of AChE and selected serine proteases should be studied with toxicants of different potency and in comparison with different substrates to unravel the rules for the activation of enzyme catalytic power, particularly the use of acid-base catalysis. The study of the acid-base catalytic apparatus is approached by rate measurements in protium oxide (HOH), deuterium oxide (DOD), and their mixtures--a method called proton inventory. This approach is detailed in Section C.

2. The Role of Acid-Base Catalysis in Aging and Reactivation

How important protonic reorganization is in the processes of aging and spontaneous and nucleophilic reactivation should also be studied for a complete understanding of where AChE actually fails in catalyzing dephosphorylation but catalyzes aging, in some cases, instead. A related question is the site of bond breaking in the the course of aging of AChE

inhibited by OP compounds of different structures.

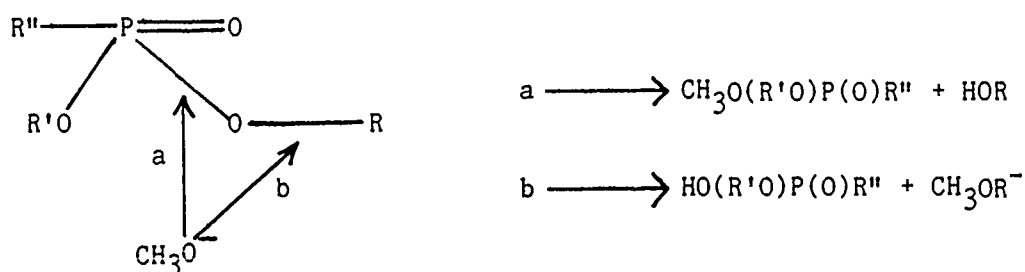
3. Isotope Effects Using Labeled Inhibitors

How effective a particular inhibitor might be at simulating the natural substrate at the transition state and whether its interaction with the enzyme involves structural alterations similar to those seen with natural substrates are critical questions addressed by these investigations of the molecular mechanisms of inhibition.

The extent of bond breaking, bond making, and the geometry at the transition state for the inactivation of AChE can be assessed by the measurement of a series of heavy atom and secondary deuterium isotope effects. The same information for the appropriate nonenzymic reactions for the OP compounds can provide a good basis for comparison. The results can be analyzed in the context of mobilization of the catalytic power of the enzyme to attain a certain structure or distortion for a degree of rate acceleration. The geometry of the transition state for the aging reaction can also be tested with the use of secondary isotope effects. This information would particularly be helpful in establishing the extent of carbonium ion character of any of the dealkylation process.

4. Model Reactions for Aging Reactions

The nature of bond fission in the aging process of some phosphonylated hydrolases has been a largely unanswered problem. A phosphonylated hydrolase containing a labile alkoxy substituted at the central phosphorus can undergo nucleophilic attack at the phosphorus or at the carbon. The two processes differ in their pH dependence because the attack at P depends on concentration of the basic species that enters the rate-determining step. In the other process a rate-determining carbonium ion formation is believed to be accompanied by an acid-catalyzed departure of the phosphonate hemiester group. The etheral oxygen, however, is not a particularly good H-bond acceptor in some cases and, therefore, the ion pair mechanism involving the base that traps the weak carbonium ion can also be a viable route. This condition may be mimicked in methanol methoxide since attack by path a, at phosphorus, versus attack by path b, at carbon, leads to different sets of easily detectable products. That is, path a leads to the alcohol along with a methoxy alkylphosphonate derivative, while pathway b leads to the methyl ester and the phosphonic acid as shown below:



Scheme 1.

5. Molecular Modeling of Inactivation of Serine Proteases

Serine proteases have shown some specificity for the structural characteristics of phosphonate esters. With the availability of the Brookhaven data base for the x-ray structures of some of these enzymes, visual inspection of the likely interactions between enzyme and inhibitor as well as molecular mechanics calculations of the interaction energies involved can be now accomplished. Such information will be of great use in the understanding of the driving force behind specificity for OP inhibition of serine hydrolases.

B. Background

OPs as a class owe their toxicity³⁻⁷ to their extraordinary ability to activate the catalytic machinery of the target enzyme toward its own destruction. The thesis that it is the enzyme catalytic machinery that brings about hydrolytic rate enhancements of OPs in the order of 10^{10-17} is supported by the fact that only enzymes are capable of such enhancements. This activation occurs to a varying degree with different hydrolases and it is also strongly dependent on structural features of the inhibitors^{6,8}. The extent of toxicity is further related to how well the catalytic apparatus is used in each of the three levels of enzyme operation, i.e., in activation, aging, and reactivation. From a therapeutic point of view, the catalytic participation in nucleophilic reactivation is also important. What components of an enzyme's catalytic apparatus are involved in each elementary step of the inhibition process can be inferred from structural models and dynamic data.

Structural features of the active sites of AChE and chymotrypsin are shown in Figures 1 and 2, respectively. Three-dimensional structural data are not available for AChE, but, based on the most exhaustive dynamic investigation, the most thorough model was proposed by Rosenberry. Figure 1 presents Rosenberry's model^{2b} including sites involved in the induced-fit conformational changes that are believed to accompany binding and catalysis. All elements--the charge relay system ($\text{CO}_2\text{..HIm..HO}^-$); the anionic site A^- ; a nearby tryptophan T, creating a cationic bridging group; an acidic group HZ; the hydrophobic areas V; and peripheral sites $\text{P}_1\text{...P}_4$ --affect the catalytic process. Although the identity of the general-base catalytic group has not been proven, the presence of a histidine and an acid residue at the active site have lately been shown in the primary structure of AChE.⁹ The active site picture of chymotrypsin (Figure 2) has been constructed according to the x-ray structural data.¹⁰ The hydroxyl of serine which acts as a nucleophile in the catalytic activity of chymotrypsin is shown at the top of the diagram and leads into the catalytic triad (marked "acid-base catalytic machinery"). Other important subsites are the oxyanion-hole, the binding pocket and the specificity pocket, which interacts with the C_1 side chain of the scissile amino acid residue. Further N-acyl interactions between residues of the substrate and enzyme residues Trp 215 and Gly 216 also arise when the natural substrate binds. These structural features for chymotrypsin explain perfectly well the dynamic data that have been compiled in decades. Consequently, similarities and differences in the dynamic behavior of the two enzymes, AChE and chymotrypsin, are justifiably interpreted in light of what is known about the structure of chymotrypsin.

Dynamic information on the nature of the chemistry catalyzed by hydrolases. There has been a wealth of information published in recent years about the action of hydrolytic enzymes, including those of greatest interest in the toxicity of organophosphorus agents, on natural and unnatural substrates. AChE has been shown to react with unnatural substrates through a rate-limiting, induced-fit conformational change(s) in lieu of the enzyme-substrate interactions found for the natural substrate.^{2,11} Deacylation is rate-limiting at saturation for the natural substrate, while unnatural acetyl derivatives can give rise to rate-limiting acylation as a result, perhaps, of failures to fit in the acylation transition states.¹² These conclusions were drawn from the magnitude of

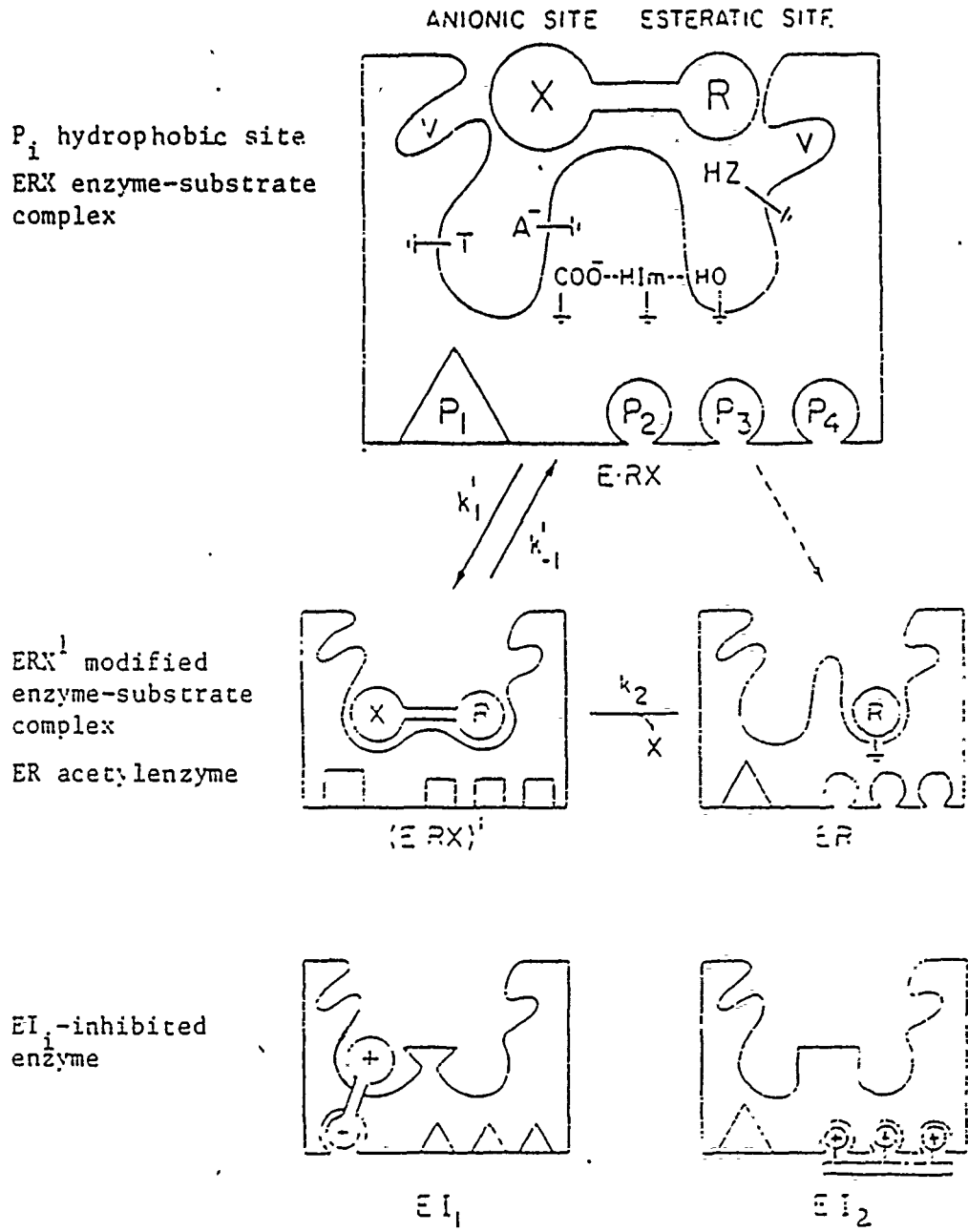


Figure 1. Rosenberry's model of the acetylcholinesterase active site.

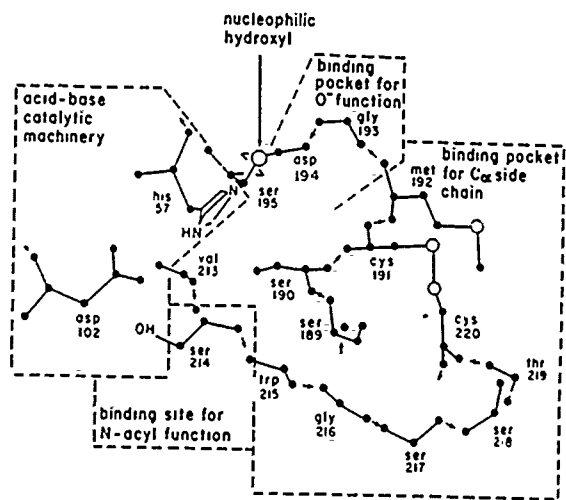
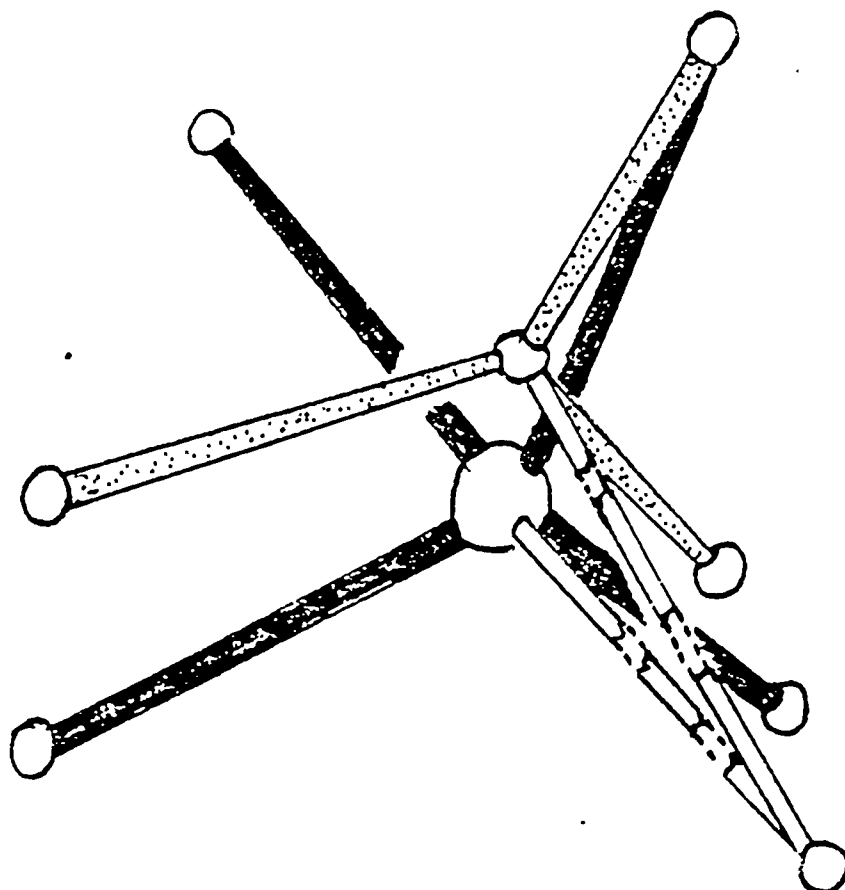


Figure 2. Schematic representation of the chymotrypsin active site.

reaction rates, that of the solvent isotope effects, studies of the temperature dependence of acylation and deacylation and solvent effects.¹³ Particularly convincing evidence for the way in which enzyme-substrate interactions generate catalytic power has been presented^{10,14} for digestive proteases. It is clear from these studies that interactions of the enzyme with the substrate-derived structure in the transition state were sensitive to the exact composition of the substrate, even at some distance from the site of covalent change. Both our results and those of Hunkapiller et al.¹⁴ added further support to the view that the more a substrate possesses the structural features of the natural substrate, the more enzymic subsites participate in catalysis, i.e., the more fully the catalytic power of AChE^{11,15} or other hydrolase enzyme¹⁶⁻¹⁷ is called upon. This is reflected, for example, in the number and nature of proton bridges in the course of catalysis. This powerful approach, the inventory and characterization of the nature of proton bridges in the course of the inhibition process by OPs, is a major component of this project and mostly used in the phase reported herein. Whether or not and to what degree the general acid-base catalytic apparatus is used in inhibition will also further test Rosenberry's model and expand the scope of the best mode for AChE.

The degree to which an unnatural substrate (or an inhibitor) may utilize the enzyme catalytic power may depend on the degree to which it simulates the positions of groups in the natural substrate during the transition state for the enzymic reaction. The key to the selective toxicity exhibited by organophosphorus agents must then be that they accomplish a substantial recruitment in the inactivation step, and occasionally in the aging step, while they often fail to achieve even a small recruitment in the reactivation steps. This conclusion follows from the irreversible nature of the inhibition by OPs or, in kinetic terms, from the observation of large rate enhancements in phosphorylation, some in aging, but very little in reactivation.¹⁸ It is reasonable then that the transition state for the inactivation of a target enzyme by an organophosphorus agent should be one which places ligand groups of the phosphorus in places that simulate the positions of at least some of the structural features of the natural substrate in order to interact with catalytic groups such as the acid-base machinery.¹⁸ Figure 3 is a comparative illustration of putative structures for the acyl-transfer transition state (bonds to carbon ligands stippled) and the phosphorus-displacement transition state (bonds to phosphorus ligands in heavy black). The acyl-transfer transition state is very "early"; as suggested by secondary isotope effects the nucleophilic bond order is 0.1.¹⁹ The phosphorus transition state is presumed to be a trigonal bipyramid.^{18,20} The serine residue is superimposed for both structures at the lower right. By virtue of the substantially longer bonds to phosphorus than to carbon and of the proposed quasi-trigonal-bipyramidal nature of the transition state for inhibition, as opposed to the quasi-tetrahedral transition state for acyl transfer, there seems to be enough resemblance between the structures to superimpose one further ligand and bring two others into the same general spatial regions.



LEGEND: Structures drawn with the Oakridge Thermal Ellipsoid Programs (ORTEP, a computer plotting technique) for possible enzymic transition states for acyl transfer (stippled bonds, "early" structure with nucleophilic bond order 0.1) involving the natural substrate and for displacement at phosphorus (heavy black bonds, trigonal-bipyramidal structure) involving an organophosphorus toxin. The nucleophilic serine oxygen of the enzyme is represented at lower right and is superimposed for the two structures. Note that a second ligand can be exactly superimposed, while two others can be brought into the same general regions of space.

Figure 3. Comparison of transition states for acyl transfer and phosphoryl transfer.

C. Approach

1. Selection of Enzymes and Substrates

The target enzymes were AChE from the electric eel and from human blood erythrocytes as well as trypsin, chymotrypsin, porcine elastase, thrombin, and subtilisin BPN'. For comparison, data on the nonenzymatic hydrolysis of OPs, as well as reactions of AChE from electric eel were used in the proton inventory studies for acylation and deacylation by phenyl acetate. The latter experiments were necessary for the comparison (vide supra) of the results with those of appropriate substrate reactions. The other target enzymes were also planned to be included in the proton inventory studies for comparison between AChEs and the structurally well-characterized serine proteases. Host-guest interactions at the active site in the OP-adducts were modeled with molecular graphics. The x-ray coordinates for β -trypsin inhibited by diisopropylfluorophosphate were used for our modeling studies.

Phosphonate inhibitors with fluoride (soman and sarin) and 4-nitrophenyl leaving groups and with different alkyl substituents were used to examine the effect of a variety of ligand interactions with the crucial enzyme subsites that are presumed to induce catalytic recruitment in the activation process. Essential information about the protonic involvement by AChEs in the physiologically rate-determining deacetylation has also been obtained.

2. Solvent Isotope Effects and Proton Inventories²¹

Rate ratios in water and heavy water, i.e., solvent isotope effects of appropriate kinetic parameters, are excellent, well-tested tools for the measure of the participation of acid-base catalysis in the rate-limiting process. A related technique, the "proton inventory," is a study of the rate dependence of a parameter on the composition of the mixtures of isotopic waters. This technique can aid in assessing the number of protons that participate in catalysis as transferring protons from enzymic residues or from solvating water molecules. In optimal situations the chemical character, i.e., identity, of the active site residues participating in the proton relay may also be inferred.

Enzymes, the most complex of catalysts, may involve more than a single protonic site in their acid-base catalytic function. It is therefore very desirable to select out from solvent isotope effects, if possible, the component contributions of individual sites. Studies of rates in the mixtures of isotopic waters serves this purpose well. The Gross-Butler²¹ equation given below relates the dependence of a particular rate parameter to the atom fraction of deuterium, n , in the solvent mixtures;

$$V_n = V_0 \frac{TS}{\prod_i (1-n+\phi_i^T)} / \frac{RS}{\prod_j (1-n+\phi_j^R)} \quad (1)$$

where

V_n = Velocity in a binary solvent
 V_o = Velocity in water
 n = Atom fraction of deuterium
RS = Reactant state
TS = Transition state
 ϕ^R = RS fractionation factor
 ϕ^T = TS fractionation factor

Here the TS product is over transition-state isotopic fractionation factors and the RS product, over reactant-state factors. The fractionation factors are in essence inverse equilibrium isotope effects K_D/K_H for exchange between a bulk water site and a particular structural site of reactants or transition state. The most common simplifications of this equation involve the assumption of a unit fractionation factor of most reactant states and the assumption that one or two active-site units contribute in most hydrolytic enzymes. Equations (a) and (b) describe these situations, respectively.

$$V_n = V_o(1-n+n\phi^T) \quad (a)$$

$$V_n = V_o(1-n+n\phi_1^T)(1-n+n\phi_2^T) \quad (b)$$

More complex models can also be derived from the general expression.

A simplified approach²¹ to an estimate of fractionation factors and the number of protonic sites participating at the TS is from a three-point determination of rate parameters in protium oxide (HOH), deuterium oxide (DOD) and their 1:1 mixture.

Results of a proton-inventory experiment on the pH-independent kinetic constant of interest are the kinetic isotope effects (inverse fractionation factors) at contributing sites in the catalytic transition state and in some cases in the effective reactant states too. Interpretation of the isotope effects and the number of contributing sites in the action of organophosphorus inhibitors is most meaningful in comparison to the same information obtained with the natural (and other) substrates.

3. ¹⁸O⁻ and β -Deuterium Isotope Effects

The determination of the ^{16,18}O effect for the leaving aryloxy ion permits an estimate of the bond order to the inactive enzyme.²¹⁻²³ Comparison with effects for nonenzymic transition states permits determination of whether the enzyme alters this aspect of the transition state. In principle, the effect may be determined either directly, with the use of precision spectrophotometric kinetics,^{24,25} or competitively, by mass spectrometry.²⁶ Both techniques have been used by Kirsch and his collaborators²⁵⁻²⁷ for alkoxy leaving-group ¹⁸O isotope effects in the action of β -glycosidase. In AChE inhibition, the product released is at the nanomolar level for practical purposes; therefore, product isolation could create a major problem, whereas separate rate measurements for each

isomeric compound in the presence of a substrate modifier is a viable method. In the case of the nonenzymic reaction, the competitive technique involving mass spectrometry is the more promising option.

The CH_3/CD_3 effect for substitution on phosphorus in phosphonates is suggested by some model studies^{28,29} as a possible indicator of the change in electrical charge at phosphorus on conversion of the effective reactant state to the effective transition state. If the effect is sufficient in magnitude and variability, it could then be employed to determine the degree to which the charge at P is altered by the enzyme in various transition states, and the degree to which it responds to the structure of the reactant or of the target enzyme. The measurements for AChE inactivation can be made by the same spectrophotometric technique. For the hydrolysis of the compounds involved, standard kinetic methods such as spectrophotometry or F^- ion detection, in the case of fluoridates, can be used.

4. Studies of Aging and of Spontaneous and Nucleophilic Reactivation

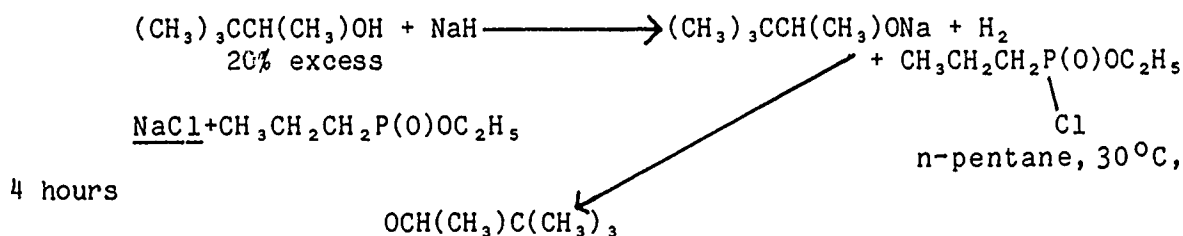
The question of the site of bond breaking in the aging reaction involving branched alcoholic ligands on P such as with soman and sarin has been aimed at with labeling studies. Earlier reports on tritium labeling experiments support C-O bond cleavage when isopropyl³⁰ and pinacolyl³¹ groups are involved. We approached the problem by mass spectral product analysis of extracts of reaction mixtures in which inhibited AChE had been allowed to age in H_2^{18}O . Rate measurements for aging and spontaneous and nucleophilic reactivation in water and heavy water are used to shed light on the participation of the acid-base apparatus of AChE in these processes.

D. Results

1. Synthesis of Organophosphorus Inhibitors

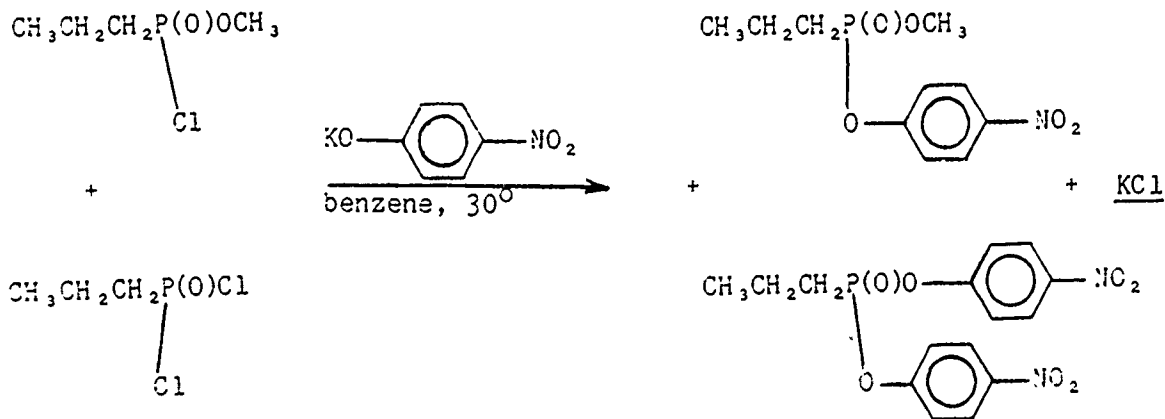
a. **Methyl and ethyl n-propylphosphonochloridates** were made from n-propylphosphonodichloridate and methanol or ethanol in pentane at 20°C under N₂ with lutidine catalyst.

b. **Ethyl pinacolyl n-propylphosphonate (EPPP)** was prepared by coupling ethyl n-propylphosphonochloridate and Na pinacolate in n-pentane under N₂ atmosphere;



The NaCl was centrifuged out and the supernatant removed into a distillation flask. The solvent and pinacolyl alcohol were removed and the phosphonate distilled out at 95°C, 1.2 Hg mm.

c. **Methyl p-nitrophenyl n-propylphosphonate (MPN)** and **bis p-nitrophenyl n-propylphosphonate (NPN)** were synthesized from 70% methyl n-propylphosphonochloridate and 30% n-propylphosphonodichloridate with K-p-nitrophenolate in benzene;³²



The KCl was filtered out, the benzene was removed and the residue was treated with cold methanol. NPN was filtered out of methanol as clean white crystals. After recrystallization from ethylacetate, it was characterized by mp (132-135°C) and by hydrolyzing it to p-nitrophenol, which yielded 102% p-nitrophenolate calculated from molar absorptivity and absorbance at 400 nm. MPN was purified by separation on preparative silica gel thin layer chromatography (TLC) plates from a benzene solution. A clear yellow oil was obtained. Hydrolysis to p-nitrophenol and spectroscopic analysis of a sample showed the presence of 5% p-nitrophenol, which could not be removed by feasible techniques because of the lability of MPN.

(ODS Hypersil 150 x 4.7 mm, 2.5 μ particle size) with methanol-water gradient elution before each experiment. The 4-nitrophenol equivalent product of basic hydrolysis was measured spectrophotometrically at 400 nm.³²

III. Purification of IMN

Basic hydrolysis of the ^{16}O and ^{18}O isomers of IMN obtained by synthesis revealed that some fast-hydrolyzing impurity coextracted with the ^{18}O -labeled compound. Addition of Tris base did not effect the hydrolysis rate; thus coextraction of Tris from the buffered aqueous extract could not have caused the faster hydrolysis of the ^{18}O isomer of IMN observed at the outset of the reaction. To rectify the problem, the compounds were further purified by HPLC separation of the impurities on an ODS Hypersil column with water-methanol gradient elution. Figure 4 shows the HPLC recording of the signal from a UV detector of the eluting components. IMN elutes with a retention time of 14 minutes, while the impurity present in the ^{18}O isomer elutes at 20 minutes. The aqueous eluent of each of the isomers of IMN was extracted with methylenechloride, dried over anhydrous MgSO_4 and evaporated to dryness. The pure compounds were then taken up in absolute methanol for stock solutions for kinetic measurements.

2. Analysis of Labeled Inhibitors

Precise determination of the amount of intact inhibitor in the reaction mixture for kinetics is particularly essential for the measurement of small isotope effects by direct rate measurements of the individual isomers. In such direct rate studies, the rates are directly proportional to the concentration of the inhibitor.

Stock solutions of IMN were prepared in 10^{-3} M concentrations in methanol. Known aliquots of these solutions were hydrolyzed in 0.1 M NaOH solution at 25°C and the release of 4-nitrophenol followed at 400 nm. The total amount of IMN was calculated from the total absorbance change. A 1:1 mixture of the stock solutions of the two isomers was also prepared for mass spectral analysis by evaporating the solvent from the mixture and redissolving it in methylenechloride for introduction into the mass spectrometer. The $^{16}\text{O}:^{18}\text{O}$ ratios for the molecular ions was used for the concentration ratio in the kinetic experiments, i.e., for isotope effect calculations.

Stock solutions of soman and sarin unlabeled and deuterium labeled in the β -position from the phosphorus were made up in water in 2×10^{-5} M solution from the dilute stock solutions provided by USAMRICD. A further dilution of the 2×10^{-5} M solutions with dilute HCl (pH 4.0) was necessary for kinetic measurements. The latter solutions, however, are too dilute for analysis. Thus, the 2×10^{-5} M solutions of sarin and soman isomers were hydrolyzed with dilute base and were diluted to 8×10^{-6} M with a pH=5.8 0.015 M phthalate buffer prepared with 0.05 M KNO_3 . The fluoride-selective electrode was standardized with 10^{-6} - 10^{-4} M solutions serially diluted from a 0.1 M NaF standard solution with the buffer used for the samples. Figure 5 shows the calibration curve. From the mV readings at 25°C of the sample solutions, the following total F^- concentrations were calculated with a 2% reproducibility, but probably slighter accuracy:

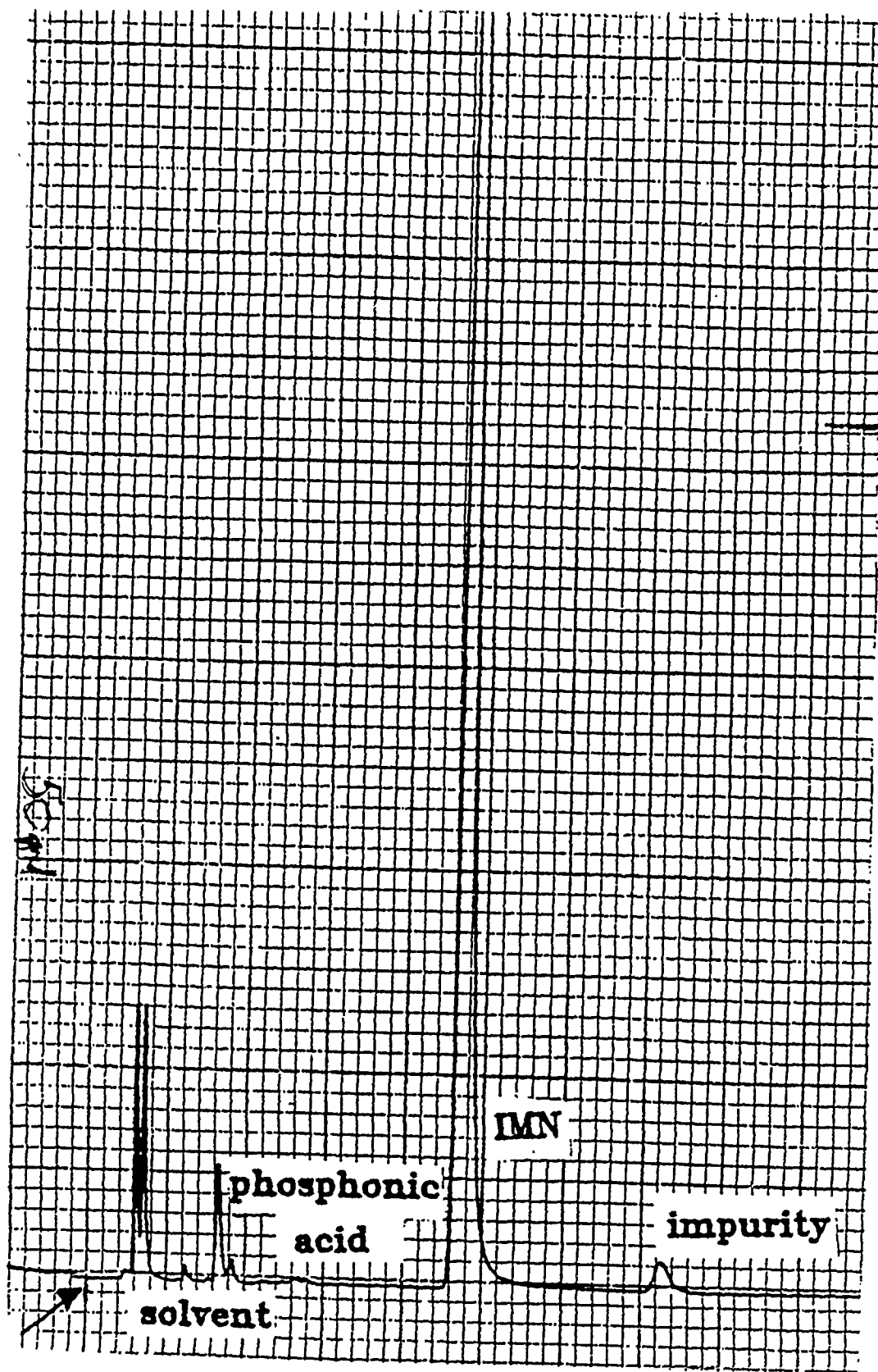


Figure 4. HPLC-recording of IMN and impurities.

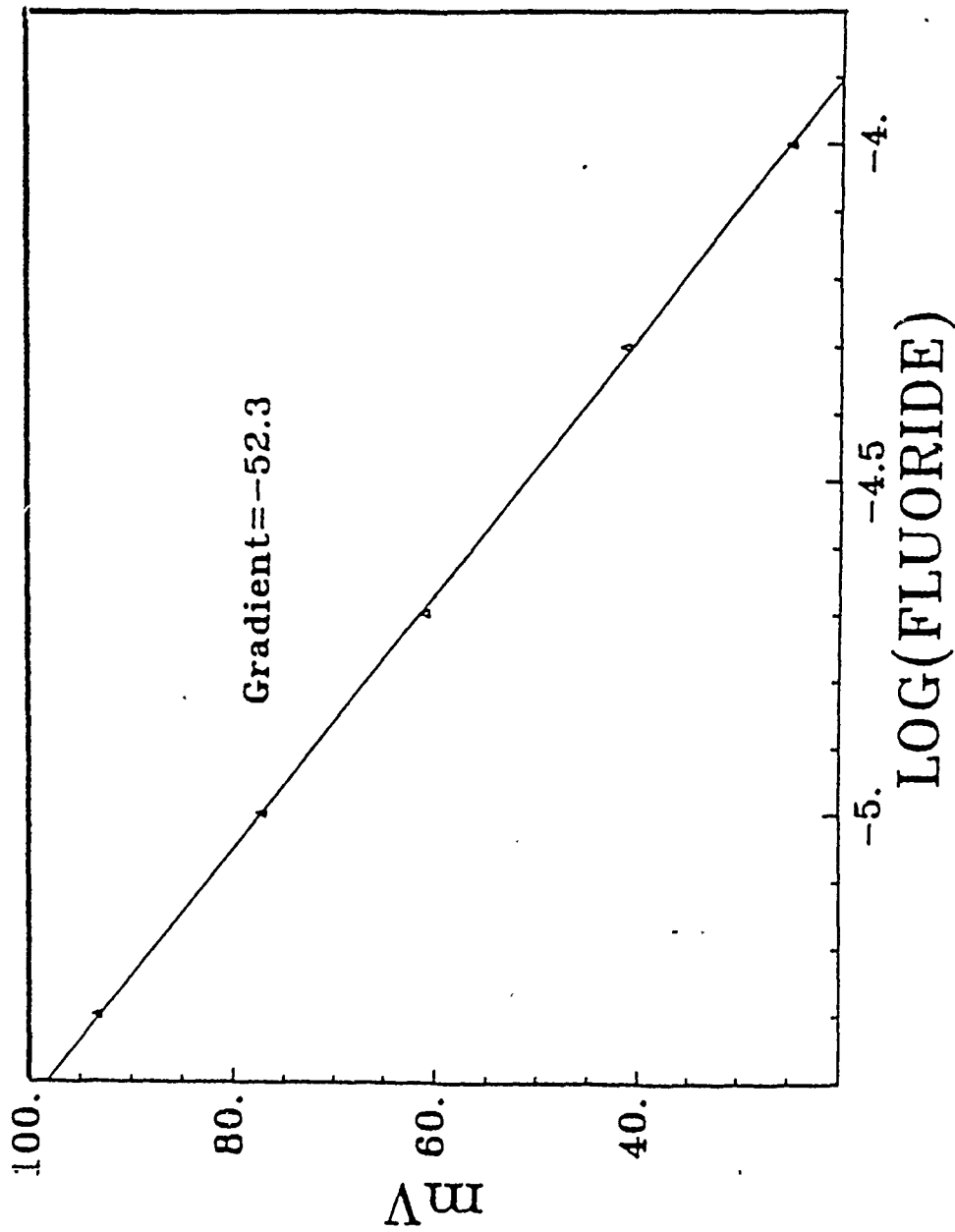


Figure 5. Calibration of fluoride ion concentration.

soman	1.83×10^{-5} M
soman- β D ₃	1.19×10^{-5} M
sarin	3.98×10^{-5} M
sarin- β D ₃	2.90×10^{-5} M

In independent experiments, 5 ml of a 2×10^{-4} M solution of each agent prepared in a pH 5.8, 0.015 M phthalate (0.05 M KNO₃) buffer was hydrolyzed and the F⁻ release monitored by the same selective electrode. The initial F⁻ concentration was estimated from extrapolation to zero time. An aliquot of the sample was also hydrolyzed in strong base to check the total F⁻ concentration of the sample. The % mol fractional F⁻ content in the solution of the agents is as follows:

soman	2.0 ± 2 %
soman- β D ₃	0.05 ± 2 %
sarin	<8.0 ± 2 %
sarin- β D ₃	1.5 ± 2 %

Thus, within the limits of this technique, ± 2% precision, the F⁻ content of the stock solutions of the agents were 0.05% - 8 mol%. This analytical technique gives information only about the type of decomposition that results in the release of F⁻.

Since acid-catalyzed hydrolysis of OP compounds that have a branched alcoholic group can also deplete the concentration of active inhibitor, a measurement of intact OP ester concentration had to be developed. The analytical technique involves the use of an excess of chymotrypsin over the inhibitor. The active site concentration of chymotrypsin, on the other hand, can be determined with precision by using highly sensitive fluorimetric techniques. The fluorophor of our choice is 7-hydroxy 4-methylcoumarin (MU), which is released from its p-(NNN-trimethylammonium) cinnamate ester (MUTMAC) upon displacement by serine at the active site of chymotrypsin. Figure 6 demonstrates the burst of fluorescence intensity upon the instantaneous release of MU observed with a 3×10^{-8} M chymotrypsin solution. The two upper traces or "burst" correspond to a large increase in fluorescence intensity due to the "burst" of MU before chymotrypsin inhibition. The lower "burst" is a smaller rise of fluorescence intensity after chymotrypsin inhibition. The difference in fluorescence intensity between the upper and the lower traces is then proportional to the active sites of chymotrypsin inhibited which in return is stoichiometrically equivalent to the concentration of the inhibitor. The linear dependence of fluorescence on concentration in the range 50-1000 nM reagent is shown in Figure 7.

The concentration of 6×10^{-6} M soman stock solutions has been determined with a twofold excess of chymotrypsin, by the difference in the concentrations of chymotrypsin active sites in diluted solutions of uninhibited and inhibited chymotrypsin, respectively. The inhibition was effected by a 10 minute incubation of enzyme and inhibitor at 25°C. Under these circumstances only the S-P(-)-isomer of soman reacts with chymotrypsin, which isomer is also the only appreciable inhibitor of AChE in our kinetic experiments. Figure 8 shows the linear dependence of fractional inhibition of a chymotrypsin solution on increasing soman concentrations. The same stock solutions were used for kinetic measurements.

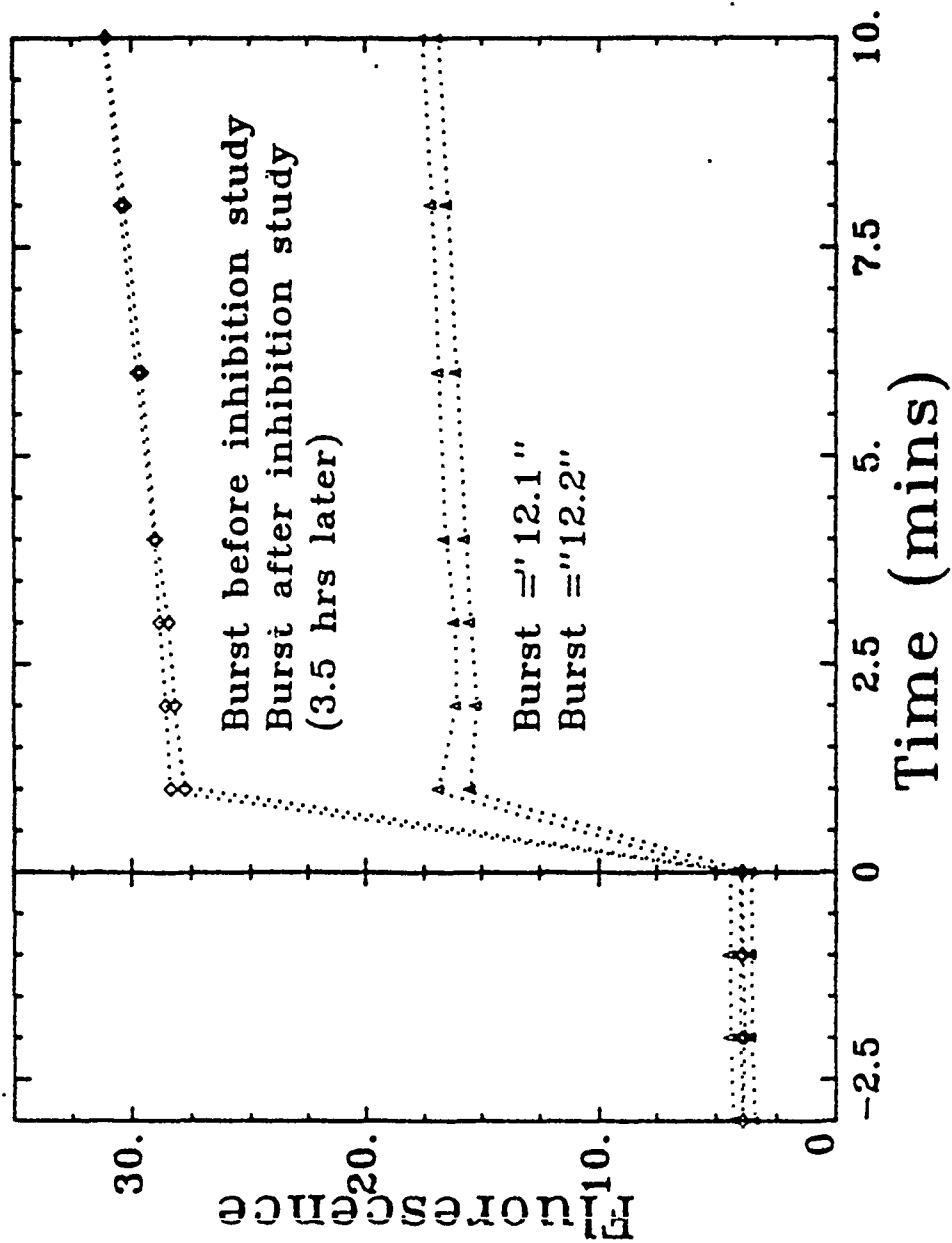


Figure 6. Burst kinetics of chymotrypsin with MUTMAC.

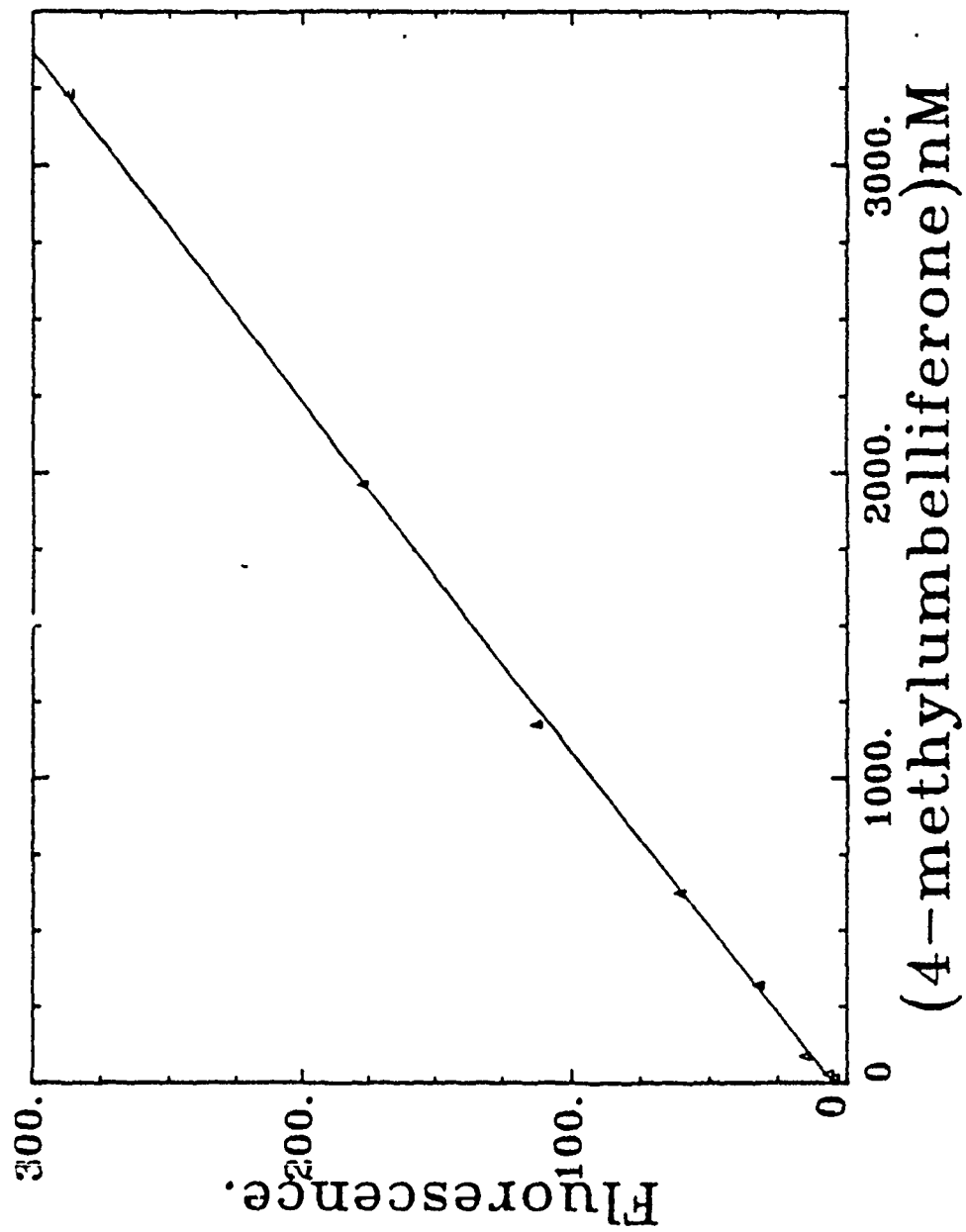


Figure 7. Calibration of fluorescence intensity.

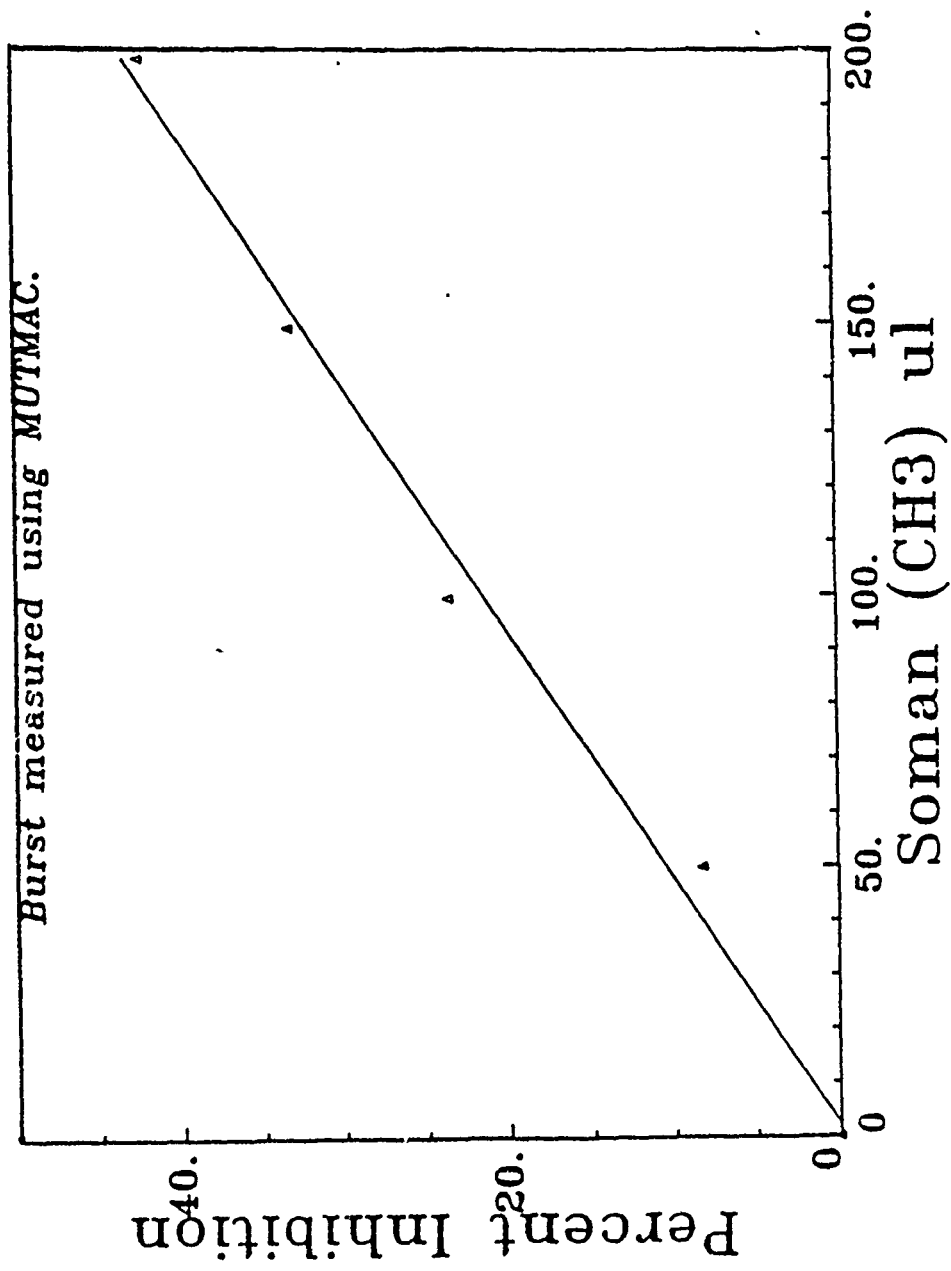


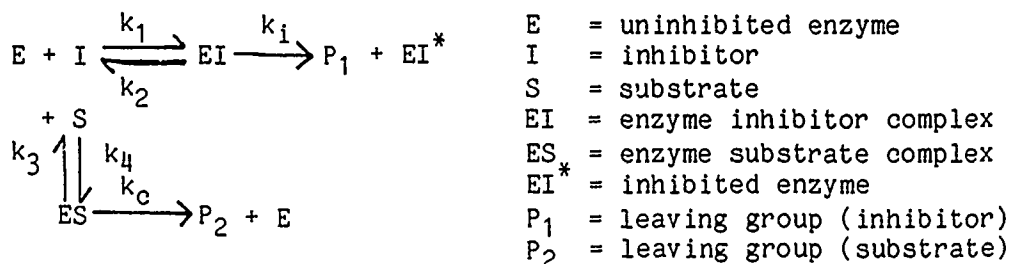
Figure 8. Inhibition of chymotrypsin by soman (CH₃).

The concentrations of both isomers of sarin stock solutions were determined in 10^{-4} M stock solutions. The incubation time was raised to 20 minutes with chymotrypsin until reactions of both isomers were complete. Since only one of these, the S-P(-)-isomer, reacted with AChE under our experimental conditions, the half of the concentration measured with chymotrypsin was used in the analysis of the AChE inhibition data. For kinetic measurements with AChE, the stock solutions had to be diluted 100 times.

3. Kinetic Methods

The derivation of the rate law for the competitive irreversible inhibition technique in the presence of a substrate with the appropriate characteristics is given below:³⁴

The enzyme is engaged in parallel reactions. One involves the inhibitor, which produces the inhibited enzyme adduct and the leaving group, P_1 . The other reaction is with the substrate that is being turned over by the available free enzyme, the product of which is the leaving group of the substrate, P_2 . Either the depletion of the substrate or the production of P_2 can be monitored by some analytical technique. In most cases, as in ours, the departure of a chromogenic leaving group is followed by spectroscopic techniques.



The two differential equations of interest are 2, for the production of the chromogenic leaving group of the substrate, and 3, for the production of the dead enzyme. The mass balance, summarizing the distribution of uninhibited enzyme [E] ($E = E_0 - EI^*$) among the free [E_f] and modified [ES] and [EI] forms, is given in eq. 4.

$$dP_2/dt = k_c[ES] \quad 2$$

$$dEI^*/dt = k_i[EI] \quad 3$$

$$E = [E_f] + [ES] + [EI] \quad 4$$

As is customary in derivations for enzyme kinetics, E_f and EI in terms of ES are readily derived from steady-state approximations;

$$[E_f] = [ES]K_m/[S] \quad \text{and} \quad [EI] = [ES]K_m/[S]\{[I]/K_i\}$$

$$\text{where } K_m = \{k_4 + k_c\}/k_3 \quad \text{and} \quad K_i = \{k_2 + k_i\}/k_1$$

and upon substitution into eq. 4, eq. 5 is obtained:

$$E = [ES] \{ K_m/[S] + K_m/[S] \{ [I]/K_i \} + 1 \} \quad 5$$

or

$$[ES] = E[S]K_i / \{ [I]K_m + K_mK_i + [S]K_i \} \quad 6$$

Substitution of 6 into 2 gives 7, the rate of product release as a function of the also time-dependent concentration of uninhibited enzyme (E_t).

$$dP_2/dt = E_t k_c [S] K_i / \{ [I]K_m + K_mK_i + [S]K_i \} \quad 7$$

The distribution of the different forms of enzyme as a function of time, on the other hand, is governed by eqs. 2, 3, and 4. Therefore, eq. 3 is also expressed in terms of steady-state parameters of enzyme kinetics as follows: Since $[E_f] = [EI]K_i/[I]$, $[ES] = [EI][S]/K_m \{ K_i/[I] \}$ and $E = E_0 - EI^*$ are also true, thus;

$$[EI] = \{ E_0 - EI^* \} [I] K_m / \{ [I] K_m + K_m K_i + [S] K_i \} \quad 8$$

and

$$dEI^*/dt = \{ E_0 - EI^* \} k_i [I] K_m / \{ [I] K_m + K_m K_i + [S] K_i \} \quad 9$$

The analogies between eqs. 7 and 9 are readily recognizable. Provided that $[S] = [S_0]$ and $[I] = [I_0]$, where $[S_0]$ and $[I_0]$ are the initial concentrations, through the reaction:

$$k_{obs} = k_i [I_0] K_m / \{ [I_0] K_m + K_m K_i + [S_0] K_i \} \quad 10$$

After separation of terms (eq. 11) and integration between limits, $t = 0$; $EI^* = 0$ and t ; EI^*_t , eq. 12 is obtained:

$$dEI^* / \{ E_0 - EI^* \} = k_{obs} dt \quad 11$$

$$\ln(E_0 / \{ E_0 - EI^* \}) = k_{obs} t \text{ or } \ln(E_t / E_0) = -k_{obs} t \quad 12$$

Now, the time-dependent product formation can also be related to the initial concentration of enzyme E_0 , by substitution of eq. 12 in the exponential form, $E_t = E_0 \exp(-k_{obs} t)$, into eq. 7 (eq. 13).

$$dP_2/dt = E_0 \exp(-k_{obs} t) k_c [S_0] K_i / \{ [I_0] K_m + K_m K_i + [S_0] K_i \} \quad 13$$

i.e.,

$$dP_2/dt = \text{const} \exp(-k_{obs} t)$$

Separation of terms and integration of eq. 13 between the limits $t = 0$; $P_2 = 0$; and t ; P_{2t} yields eq. 14.

$$P_{2t} = \{ \text{const} / k_{obs} \} \{ 1 - \exp(-k_{obs} t) \} \quad 14$$

and at infinite time,

$$P_{2\infty} = \text{const} / k_{obs} = E_0 k_c [S_0] K_i / k_i [I_0] K_m \quad 15$$

Since the denominator for the constant in eq. 13 and that of k_{obs} in eq. 10 are identical, they cancel out in eqs. 14 and 15. In these equations, the concentration of product released in time is related to experimentally

definable kinetic parameters and concentrations factored by the fraction of reaction progress $\{1 - \exp(-k_{\text{obs}}t)\}$ in the simplified form of eq. 16.

$$P_{2t} = E_0 k_c [S_0] K_i / \{k_i [I_0] K_m\} \{1 - \exp(-k_{\text{obs}}t)\} \quad 16$$

Evaluation of Microconstants. A convenient expression for the determination of the second-order (k_i/K_i) and first-order (k_i) rate constants is obtained by inversion of eq. 10 and separation of terms as in eq. 17.

$$1/k_{\text{obs}} = 1/k_i + (K_i/k_i/[I_0])(1 + [S_0]/K_m) \quad 17$$

In the broadest application, particularly when inhibition is studied at a level of about half saturation of the enzyme with the inhibitor, a plot of k_{obs}^{-1} versus $[I_0]^{-1}$ gives k_i^{-1} as intercept and $(1 + [S_0]/K_m)K_i/k_i$ as slope. A knowledge of $[S_0]/K_m$ or a replot of a series of slopes against corresponding values of $[S_0]$ can lead to a determination of K_i . Alternatively, if $K_i/[I_0] > 1$, a plot of k_{obs}^{-1} versus $[S_0]$ approximates $K_i/k_i[I_0]$ as intercept and $K_i/k_i[I_0]K_m$ as slope. In the reverse case, if $K_i/[I_0] < 1$, a plot of k_{obs}^{-1} versus $[S_0]$ approximates k_i^{-1} as intercept and $K_i/k_i[I_0]K_m$ as slope.

Linear least-squares techniques were used throughout these studies for data work-ups of this kind. The line in each figure is drawn across calculated points in this report. In almost all cases, k_i is so large and K_i is so small that traditional kinetic measurements are limited to the concentration range (well) below K_i and, therefore, the only parameter that can be obtained with acceptable precision is k_i/K_i .

4. Rates, Solvent Isotope Effects and Proton Inventories for the Inhibition of Serine Hydrolases by OPs

a. Reactions of Acetylcholinesterase from the Electric Eel

AChE inhibition by NPN, MPN, IMN and sarin were studied at pH 7.70 in 0.05M phosphate buffer containing 5% methanol at 25°C in the absence and presence of a good substrate, phenyl acetate (PA). The inhibition by soman was studied only in the presence of PA and 1% methanol, because the rapidity of the reaction rendered the technique of sampling for residual AChE activity by drawing aliquots unfeasible.

PA has been chosen to assay for remaining enzyme activity as a function of time after inhibition, or as a competitor for AChE catalysis, because of its ideal characteristics as a good chromogenic substrate with greater stability to aqueous hydrolysis than substituted analogs of phenyl esters. The release of phenol on enzymic hydrolysis of PA is easily followed at 275 nm, where $\Delta\epsilon = \epsilon_{\text{phenol}} - \epsilon_{\text{PA}} = 1340 \text{ cm}^{-1} \text{ M}^{-1}$.^{2,3} The rate parameters for PA hydrolysis by AChE at pH = 7.70 in 0.05 M phosphate buffer and 5% methanol have been found to be $k_{\text{cat}} = 1.76 + 0.09 \times 10^4 \text{ s}^{-1}$ and $K_m = 2.6 + 0.2 \text{ mM}$, in good agreement with reported values.^{8,9} The nonenzymic hydrolysis rates of PA were measured to be $k = 3.82 \times 10^{-6} \text{ s}^{-1}$ and $1.99 \times 10^{-6} \text{ s}^{-1}$ at pH = 7.70 and pD = 8.25 in HOH and DOD buffered in 0.05 M phosphate of an acid:base ratio of 3:1. The pseudo-first-order rate constants (k_{obs}) were fitted to eq. 17. The summary of the rate data with standard errors is given in Table I.

TABLE I. Bimolecular Rate Constants and Solvent Isotope Effects for the Reaction of Organophosphorus Agents with AChE.^a

Agent	$k(\text{HOH}), \text{M}^{-1} \text{s}^{-1}$	$k(\text{DOD}), \text{M}^{-1} \text{s}^{-1}$	$k_n(0.5), \text{M}^{-1} \text{s}^{-1}$	$\frac{k(\text{HOH})}{k(\text{DOD})}$	$\frac{k(n=0.5)}{k(\text{DOD})}$
Soman	$(1.67 \pm 0.2) \times 10^6$	1.2×10^6	1.41×10^6 ^{c,d}	1.41 ± 0.14 ^{c,d}	1.25×0.12 ^d
Sarin	$(4.8 \pm 0.10) \times 10^5$	$(3.78 \pm 0.14) \times 10^5$		1.27 ± 0.80	
IMN	8130 ± 380	6520 ± 100		1.25 ± 0.06	
MPN	354 ± 26	236 ± 21	303 ± 6 ^d	1.50 ± 0.17 ^e	1.17 ± 0.03 ^d
NPN	7.32 ± 0.1	5.77 ^d		1.3 ± 0.1	

^a pH 7.7, 0.05 phosphate buffer, 25°C

^b $n = 0.5$; HOH:DOD = 1:1

^c Estimate from measurements at two inhibitor concentrations

^d Calculated from k_{obs} at one inhibitor concentration

^e The value of $k(\text{HOH})/k(\text{DOD}) = 1.43 \pm 0.03$ was obtained at the same MPN concentration at which the $n = 0.5$ data were collected.

I. Inhibition by Soman

Aliquots of a diluted solution of soman at pH 4.5 (HCl) were pre-equilibrated with a 10 μ l aliquot of a methanolic solution of PA and the appropriate amount of buffer at pH 7.7. Introduction of AChE initiated the reaction. Figure 9 shows a representative plot of k_{obs} versus soman concentration, all at 1 mM PA. The experimental points are best fitted by a straight line: saturation of AChE with soman is not likely to occur in the concentration interval studied.

Figure 10 demonstrates the substrate dependence of the reaction at soman = 10^{-8} M in water where linear behavior is observed. Corresponding lines in a water and heavy water mixture of 1:1 and in heavy water, as defined by measurements at two PA concentrations, are also indicated.

Since the solvent isotope effects are quite small, a multipoint dependence of the rate constants on n , the mol fraction of DOD in HOH, would not give much refinement of the characteristics of the proton transfers involved, over the deductions that can already be made from these data at hand.

The substrate-independent inhibition rate constants and solvent isotope effects are tabulated as a function of temperature in Table II and the Eyring plot for the data is given in Figure 11. From the least squares slopes and intercepts $\Delta H^* = 7.3 \pm 0.6$ and $\Delta S^* = -4 \pm 2$ eu in H_2O and $\Delta H^* 7.1 \pm 0.4$ and $\Delta S^* = -6 \pm 1$ eu in D_2O were calculated.³⁵

II. Inhibition by Sarin and IMN

The inhibition of AChE by these compounds was studied in the presence of 8.2 mM PA while the concentration of the inhibitor was varied in the manner described below for the secondary isotope effect studies.

III. Inhibition by NPN

i. Direct inhibition by NPN in the absence of substrate was carried out with 5-8 units of AChE in a total volume of 1.0-1.2 ml and NPN concentrations 7.17, 3.22, and 1.79×10^{-5} M. The inhibitor was introduced from an acetonitrile stock solution in a volume to result in 5% acetonitrile in the incubation mixture. The progress of inhibition was followed by drawing 0.1 ml aliquots of the incubation mixture and diluting them with a 5 mM solution of buffered PA to 1.0 ml. This test for remaining enzyme activity was allowed to develop to 2-3% hydrolysis of the PA and the zero order rates were calculated from traces recorded in time. These velocities were further corrected for aqueous hydrolysis of PA under the same conditions; this correction remained 2% below of the enzymic rates. Fractional enzyme activities were calculated by dividing remaining AChE activities (v_t) by the activity of the uninhibited enzyme toward PA (v_0). NPN exhibited a sluggish reaction in this concentration range, below its saturation solubility at pH 7.70; therefore, reactions had to be followed for 1-2 hours to cover 3-4 half lives. Under this circumstance, aqueous hydrolysis depletes NPN substantially. The following kinetic scheme can account for these results:

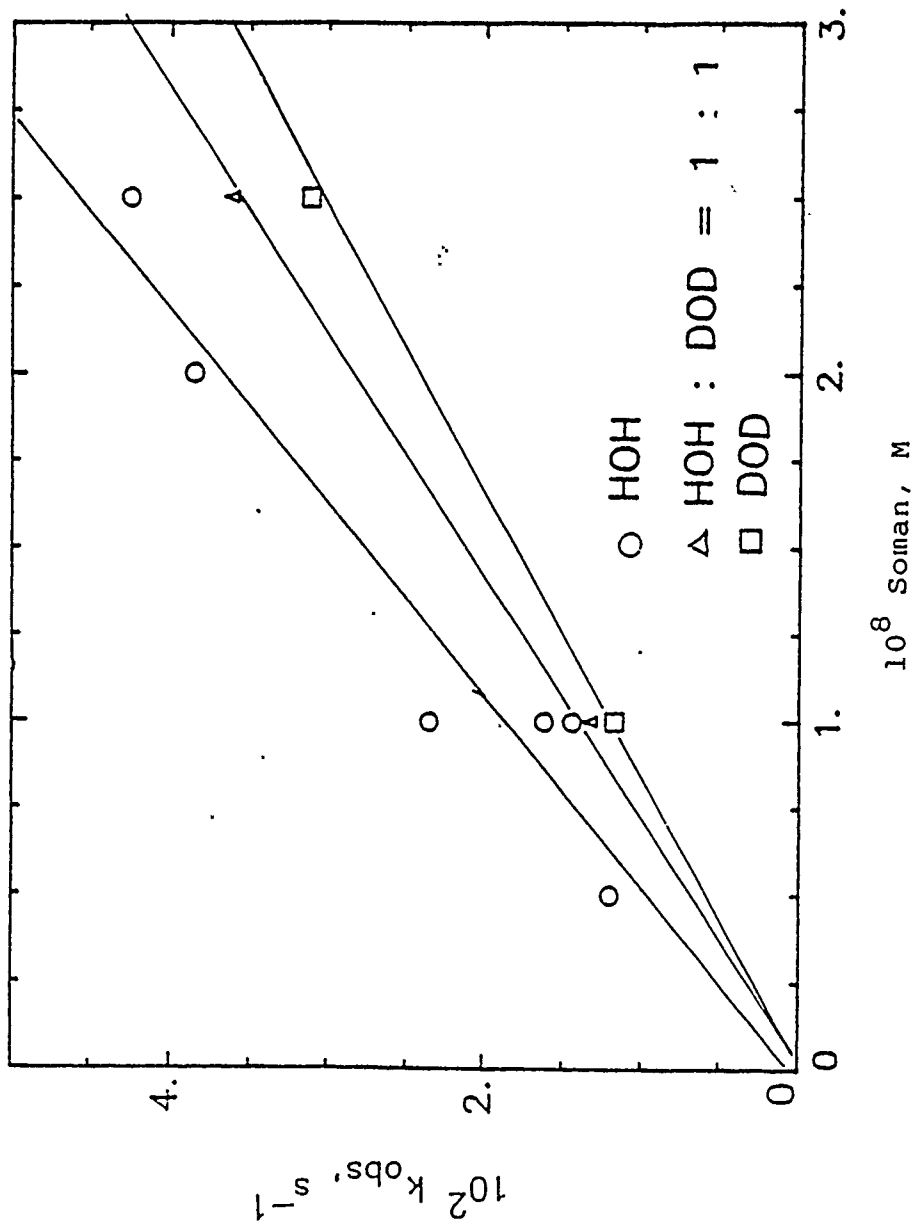


Figure 9. First-order rate constants for the inhibition of AChE by soman.

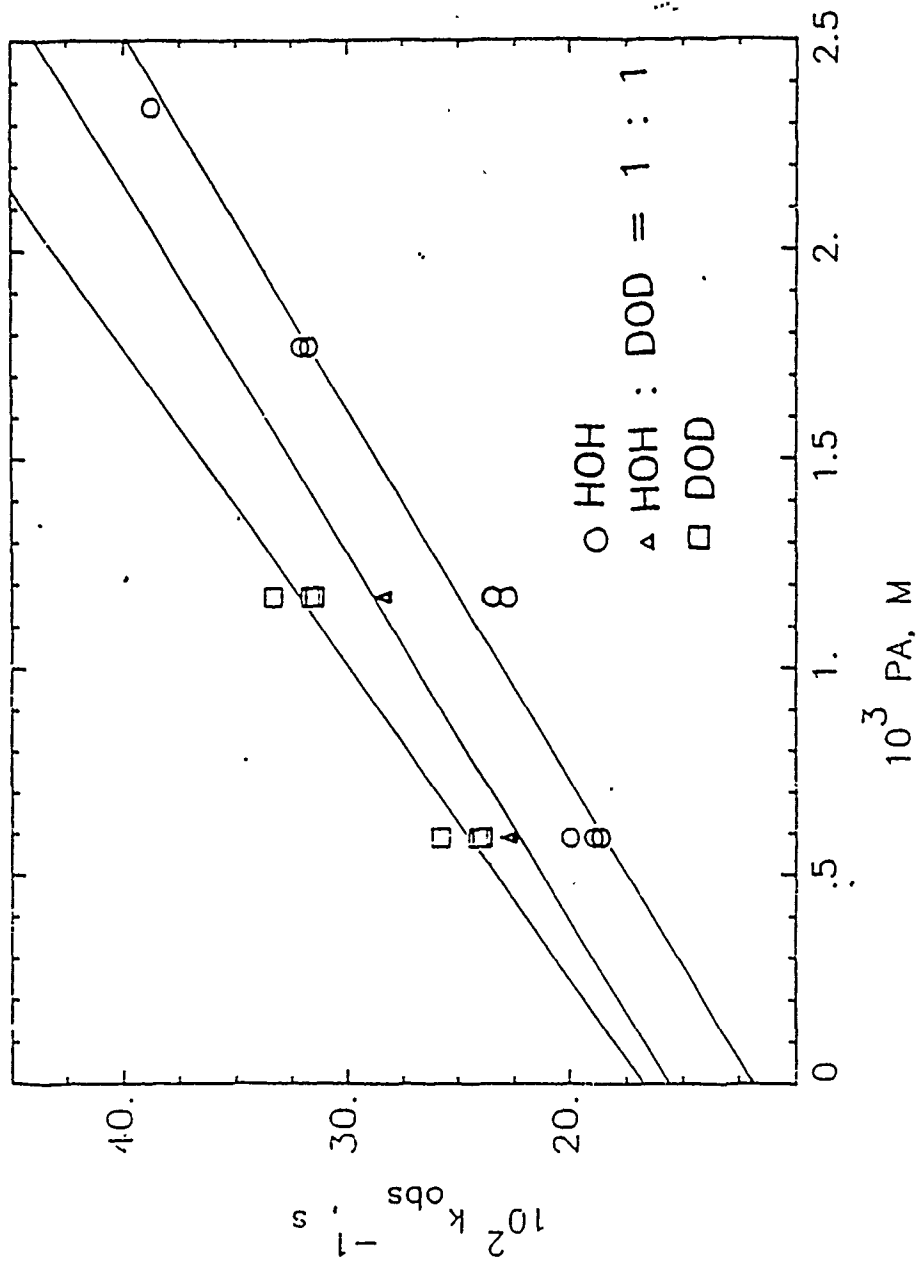


Figure 10. Substrate dependence of the inverse first-order rates of inhibition of AChE by soman.

TABLE II. Temperature Dependence of the Second-Order Rate Constants for Inhibition of Eel AChE by Soman.

Temperature, °C ^a	$10^{-3}k_i(\text{HOH}),$ $\text{M}^{-1}\text{s}^{-1}$	$10^{-3}k_i(\text{DOD}),$ $\text{M}^{-1}\text{s}^{-1}$	$k(\text{HOH})/k(\text{DOD})$
5.0	794 ± 66	617 ± 32	1.29 ± 0.12
15.0	1420 ± 41		
20.0	2117 ± 20	1578 ± 78.5	1.34 ± 0.10
25.0	3020 ± 120	2152 ± 76.2	1.41 ± 0.07
35.0	4181 ± 300	3159 ± 270	1.33 ± 0.12
45.0	6097 ± 360	4541 ± 313	1.34 ± 0.11

^aAccurate to ± 0.1°C

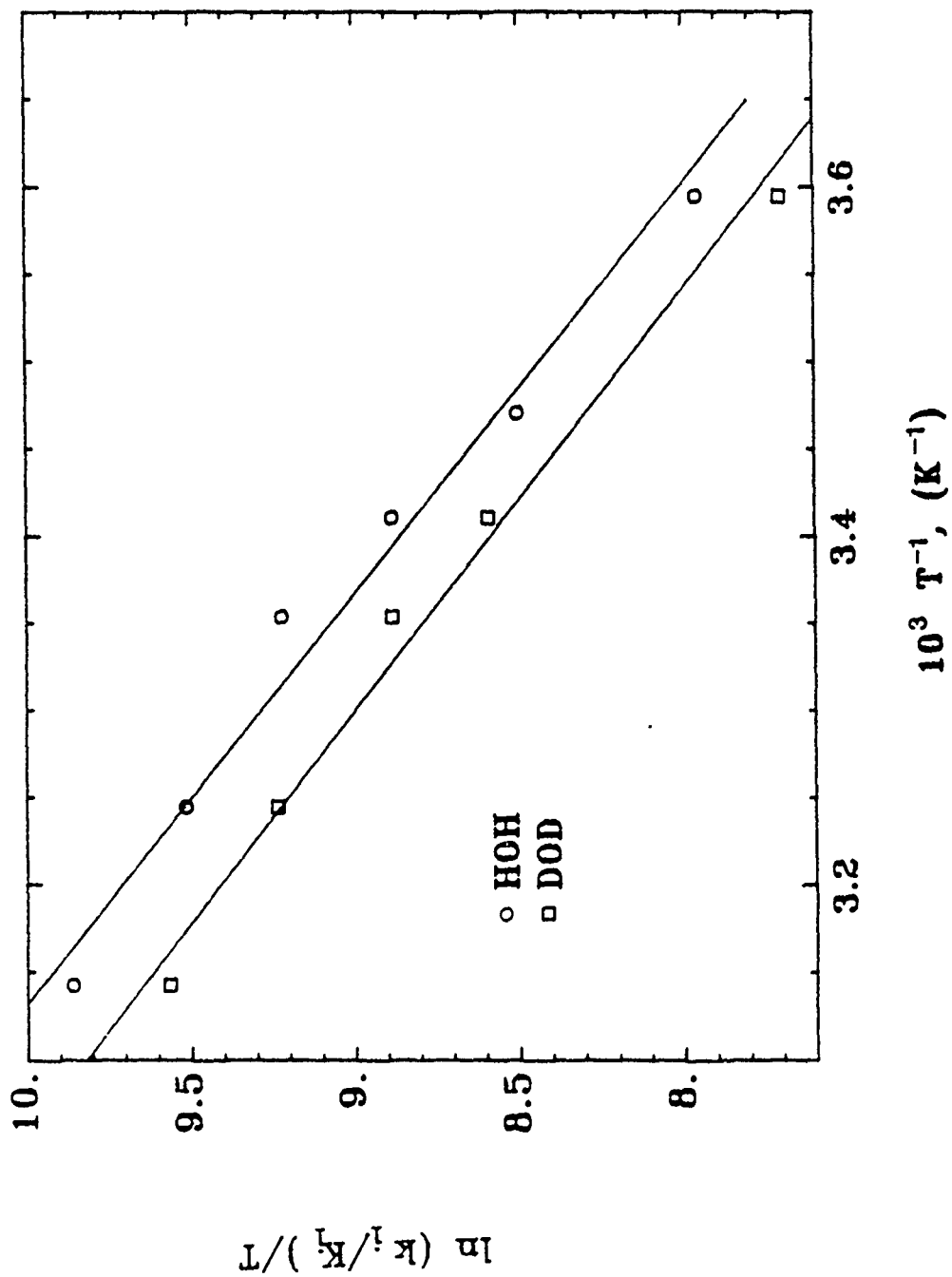
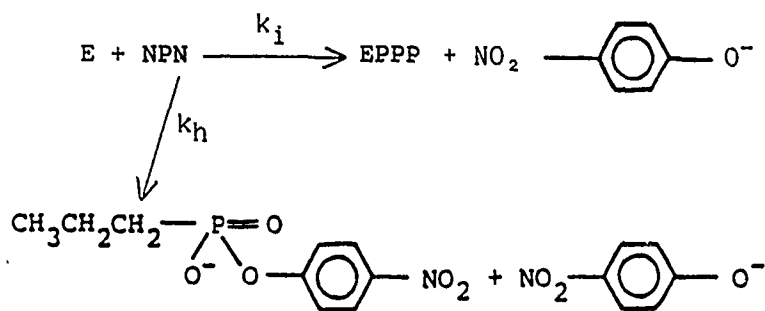


Figure 11. Eyring plot for the inhibition of AChE from Electrophorus electricus by soman.



$$\frac{dE}{dt} = k_i [E][I_0] \quad 18$$

$$\int_0^t \frac{d[E]}{[E_0]} = k_i [I_0] \int_0^t e^{-k_h t} dt \quad 19$$

$$\ln \frac{[E_t]}{[E_0]} = \frac{k_i}{k_h} [I_0] (e^{-k_h t} - 1) = \ln \frac{v_t}{v_0} \quad 20$$

A plot of $\ln(v_t/v_0)$ versus $(e^{-k_h t} - 1)$ gives $k_i [I_0]/k_h$ as the slope. $k_h = 9.07 \times 10^{-5} \text{ s}^{-1}$ in water and $9.00 \times 10^{-5} \text{ s}^{-1}$ in heavy water at pH = 7.70, pD = 8.24 in 0.05 M phosphate buffer. Corrected values of the slopes at different NPN concentrations (k_{obs}) were plotted against I_0 and the second-order rate constant of inhibition was calculated to be $7.32 + 0.10 \text{ M}^{-1} \text{ s}^{-1}$ (Figure 12). Inhibition studies were carried out in HOH and DOD buffers parallel at each $7.19, 5.18,$ and $3.22 \times 10^{-5} \text{ M}$ NPN concentrations. One of these is shown in Figure 13 at $7.19 \times 10^{-5} \text{ M}$ NPN. The ratios of the inhibition constants in HOH to those in DOD were somewhat larger than unity, 1.2-1.3, with up to 10% errors inherent in this technique.

ii. Results of the measurements of k_i in the presence of protective substrate are only preliminary, because the acetonitrile content in these reaction mixtures was 5-10% as a result of the direct introduction of NPN stock solutions into the enzyme assay solutions. Acetonitrile and similar organic solvents at this level interfere with these kinds of measurements and complicate interpretation of the data. Optimization of the reaction conditions involving only methanolic stock solutions is under way.

IV. Inhibition by MPN

i. Inhibition studies in the absence of substrate were conducted in the same manner as described for NPN, but for much shorter periods of time, since MPN proved to be a much better inhibitor of AChE than NPN. Nonenzymic hydrolysis of MPN is slower than that of NPN at pH 7.70 in 0.05 M phosphate buffer, yielding $k_{\text{obs}} = 9.51 \times 10^{-6} \text{ s}^{-1}$. This allows the calculation of 2% decomposition of MPN in about 30 minutes, the duration of the experiments. Thus, parallel hydrolysis was not included in the reaction scheme and the simple first-order rate law was used:

ii. Measurements of k_i in the presence of PA with 5% methanol as a co-solvent at PA concentrations of 0.5-2.5 mM with a series of MPN concentra-

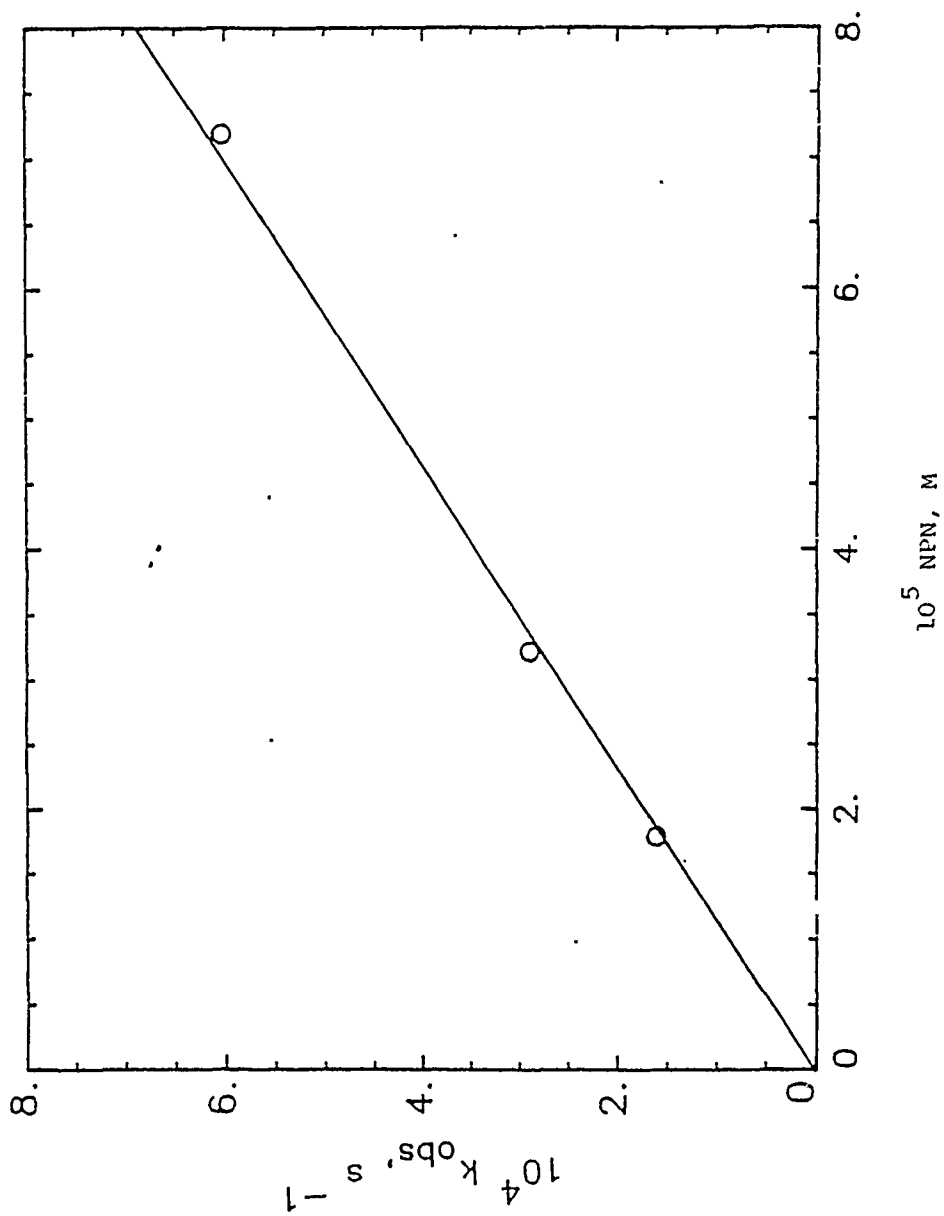


Figure 12. First-order rate constants for the inhibition of AChE by NPN.

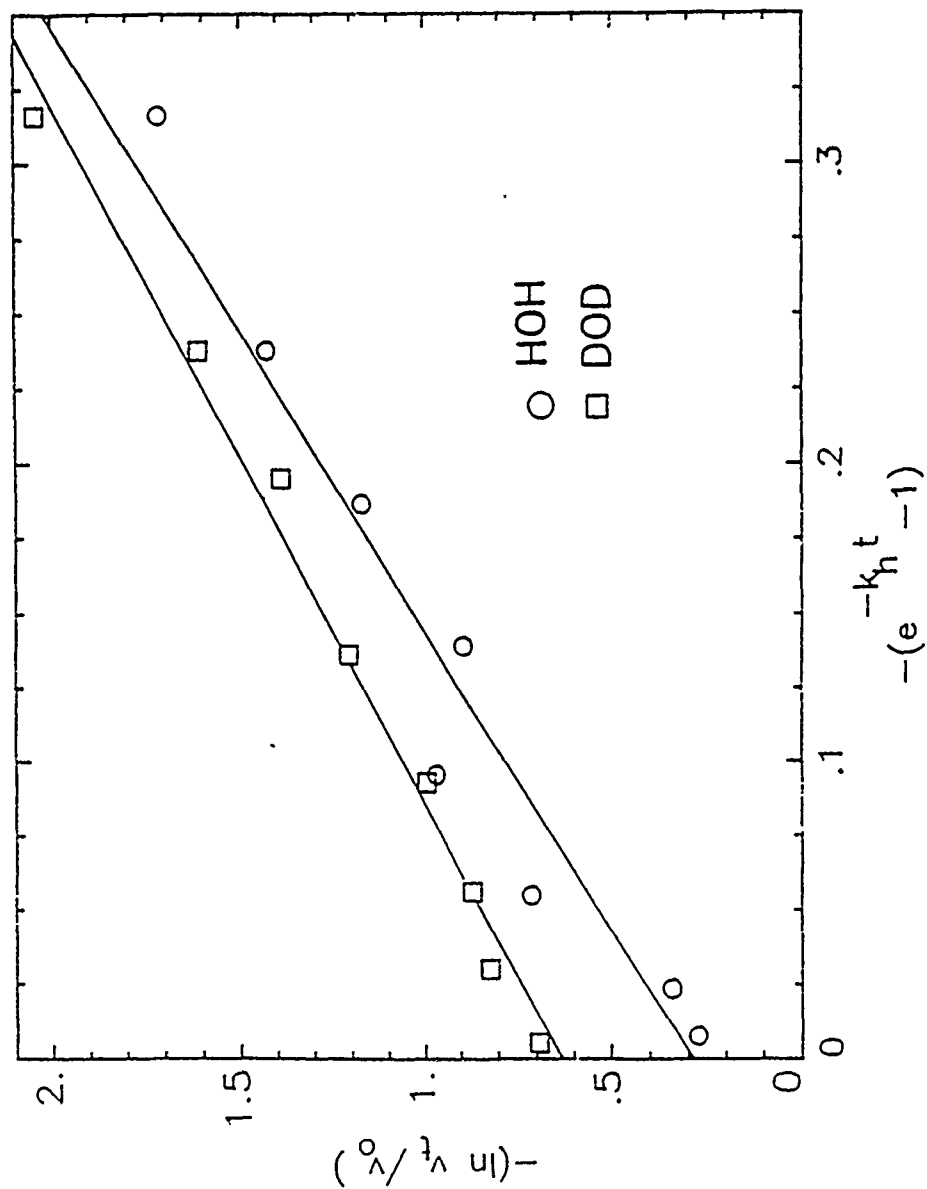


Figure 13. Plot of relative AChE activities against PA, (v_t/v_o) as a function of time $(e^{-k_h t} - 1)$, after inhibition by NPN.

tions ($0.7-12 \times 10^{-5}$ M) in HOH and DOD were mostly successful. In case inhibition was less than 85%, as with some of the lower concentrations, poor first-order kinetics was observed and the data had to be discarded. Figure 14 shows the PA dependence of the observed rate constants in HOH, in DOD, and in the 1:1 mixture of the two. Figure 14 shows that linear behavior is conserved at least until 3 mM PA and, therefore, eq. 17 describes adequately the characteristics of competitive substrate protection. Figure 15 demonstrates the substrate-independent rate constants as a function of MPN concentration for HOH and DOD. The points are best represented with a straight line within their experimental errors; i.e., there is no evidence of AChE saturation by MPN up to about 10^{-4} M. The second-order rate constants calculated from the slopes are somewhat less than those obtained in the preliminary measurements without substrate.

The solvent isotope effect calculated from these data is larger than that calculated with the other inhibitors in this study. To further characterize the nature of protonic participation in the inhibition process, measurements were repeated in HOH, DOD, and the 1:1 mixture with 2×10^{-5} M MPN. The data are given in Table I.

b. Inhibition of AChE from Human Erythrocytes

Kinetic measurements were made with PA 0.5-1.8 mM ($0.2-0.8 K_m$), AChE 0.0125 unit/ml and either with 4×10^{-8} M soman or with $1.45-5.63 \times 10^{-5}$ M MPN in H₂O, D₂O and, in one case, in their 1:1 mixture, in pL 7.40, 0.05 M phosphate buffer at 25°C. The MPN dependence of inhibition showed a small trend toward saturation. Table III gives second-order inhibition constants (k_i) and solvent isotope effects measured at an MPN concentration of 2.96×10^{-5} M.

c. Inhibition of Chymotrypsin

Measurements of the inhibition of chymotrypsin by soman and NPN gave good results in the presence of the chromogenic substrate Glu-Leu-Phe-4-nitroanilide (GLP). The rate parameters for GLP hydrolysis by chymotrypsin at pH=7.2 in 0.05 M phosphate buffer and 1% acetone have been found to be $k_{cat}=10.6 \text{ s}^{-1}$ and $K_m \sim 1 \text{ mM}$. The nonenzymic hydrolysis rates of GLP in H₂O and D₂O under these conditions are negligible. The substrate-independent second-order inhibition constants were again obtained from the fit of a series of k_{obs} values at different substrate concentrations or inhibitor concentrations to eq. 17.

The pL dependence of phosphorylation of chymotrypsin shows a maximum at pH ~7.2-7.6 in H₂O and at pD ~7.7-8.1 in D₂O as demonstrated for NPN in Figure 16 from the data in Table IV. These rates were determined singly or in duplicate (Table IV) and at low substrate concentrations where the substrate dependence is negligible. Phosphorylation of chymotrypsin by diisopropyl fluorophosphate shows the same pH dependence. In the concentration range $10^{-4}-10^{-5}$ M, where it is practical to work with GLP, the substrate dependence of the pseudo-first-order rate constant was not noticeable with soman and very small with NPN. Figure 17 shows the soman dependence when GLP is 1.05×10^{-4} and chymotrypsin is 3×10^{-6} M at $25.00 \pm 0.05^\circ\text{C}$ in H₂O. There is no evidence of saturation of chymotrypsin with the inhibitors under the conditions of our studies.

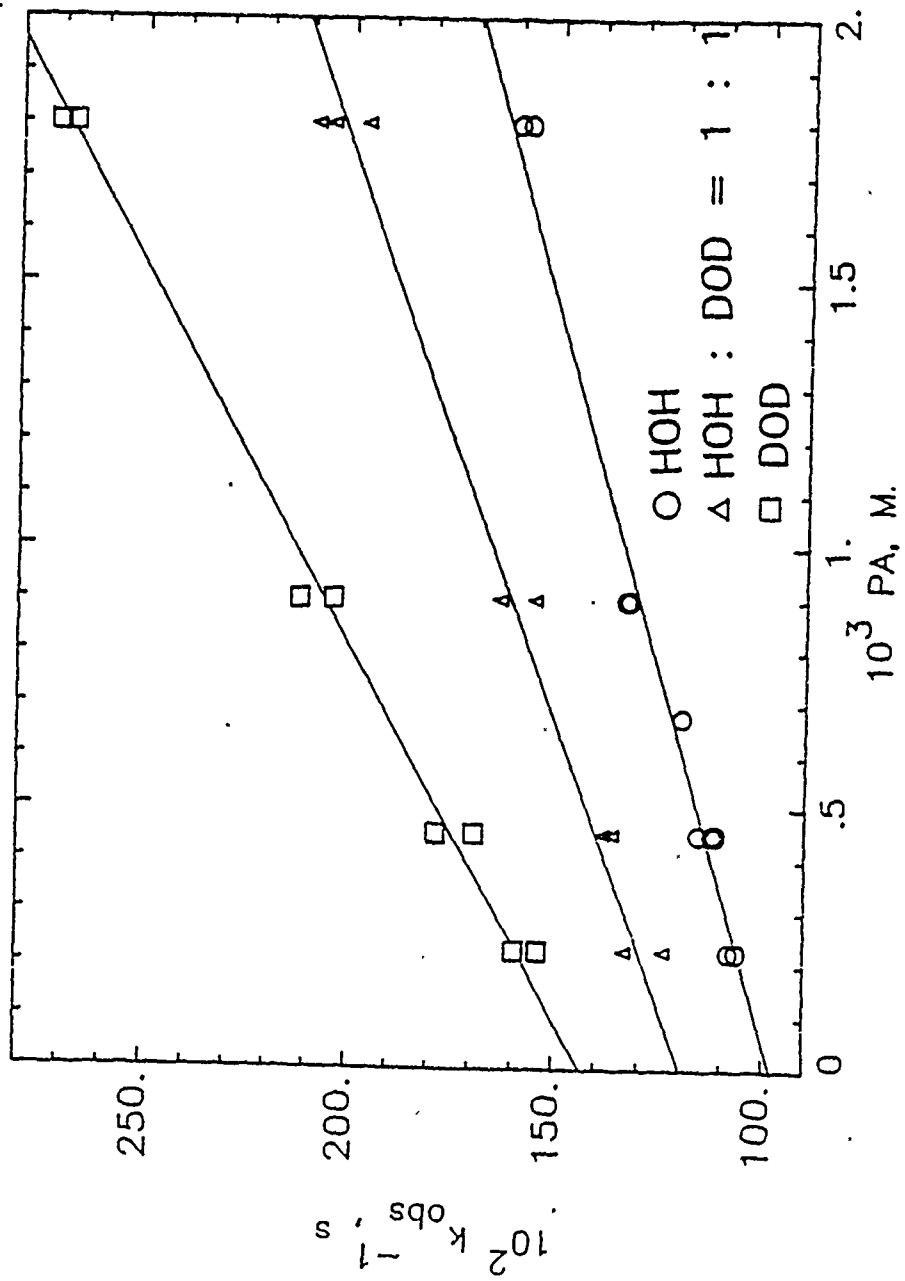


Figure 14. Inverse first-order rates of inhibition of AChE by MPN.

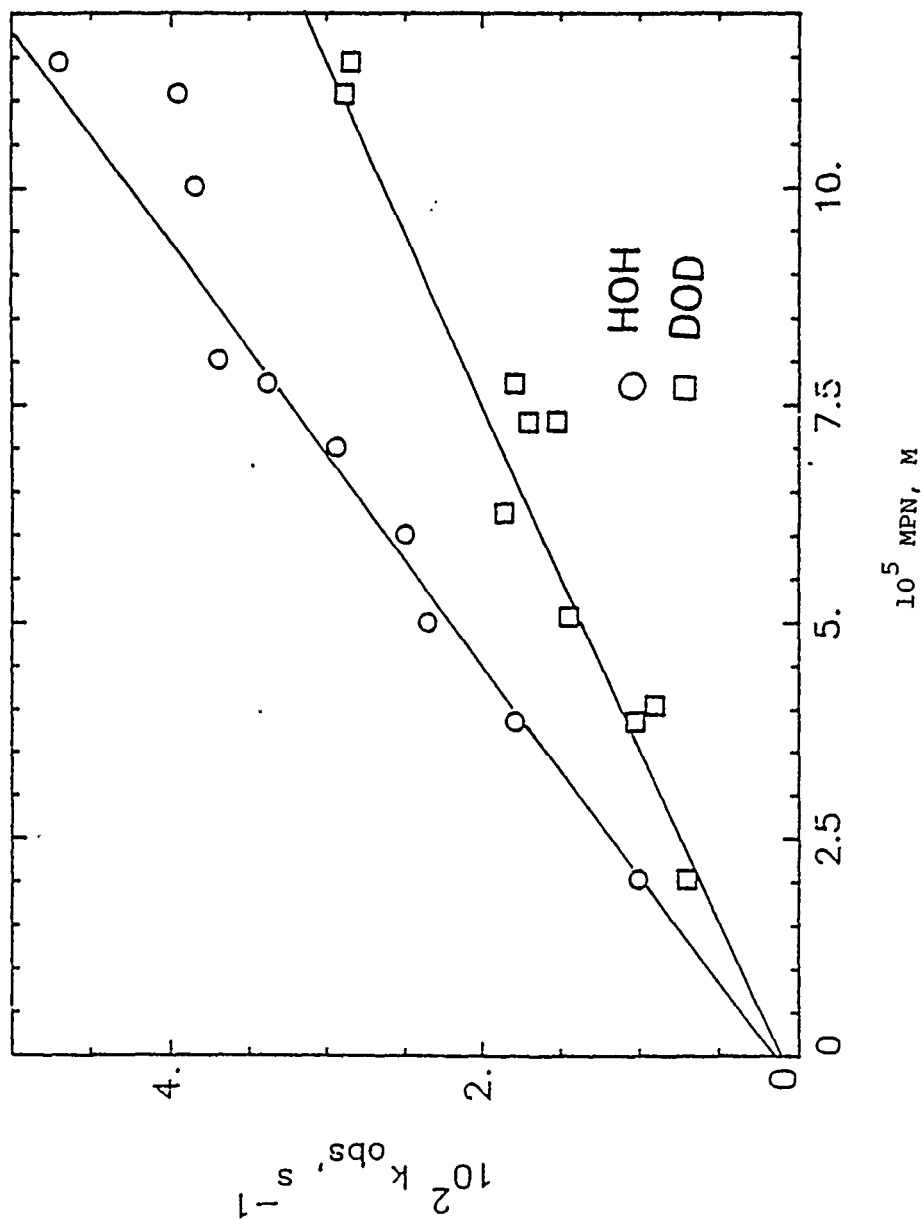


Figure 15. Dependence of the first-order rate constants of inhibition of AChE by MPN concentrations.

TABLE III. Bimolecular Rate Constants and Rate Ratios for the Reaction of Organophosphorus Agents with RBC AChE in HOH, DOD and HOH:DOD = 1:1.

Agent	$k(\text{HOH}), \text{M}^{-1}\text{s}^{-1}$	$k(\text{DOD}), \text{M}^{-1}\text{s}^{-1}$	$k_{\text{H}}(0.5), \text{M}^{-1}\text{s}^{-1}$	$\frac{k(\text{HOH})}{k(\text{DOD})}$	$\frac{k(n=0.5)}{k(\text{DOD})}$
Soman	$6.71 \pm 0.21 \times 10^5$	$4.31 \pm 0.43 \times 10^5$	5.63×10^5	1.556 ± 0.17	1.192
MPN	922 ± 50	608 ± 3.6	---	1.50 ± 0.10	---

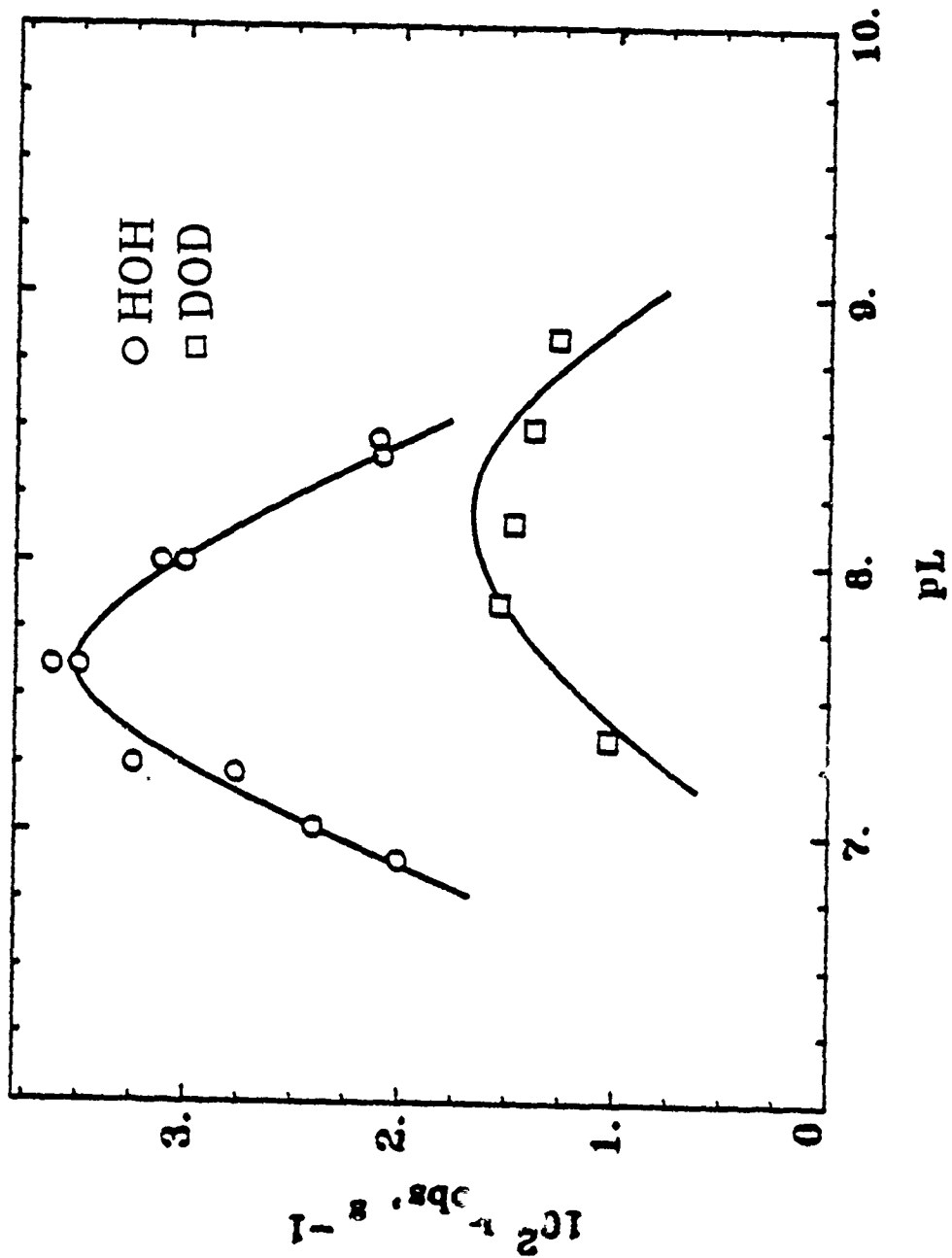


Figure 16. pL-Rate profile for the inhibition of α -chymotrypsin by NPN.

TABLE IV. Dependence on pL (L = H,D) of Inhibition Rate Constants for Chymotrypsin. 1.13×10^{-5} M NPN in HOH and DOD solvents at 25.00 ± 0.05 °C, $\mu = 0.29$ (KCl), GLP 5×10^{-5} M.

pL		$10^5 k_{\text{obs}}, \text{ s}^{-1}$
HOH,	pH	
	6.90	2010
	7.02	2402
	7.22	2766
	7.25	3245
	7.61	3502, 3630
	8.00	3010, 3121
	8.40	2093
	8.46	2110
DOD,	pD	
	7.35	1030
	7.85	1541
	8.15	1476
	8.84	1275

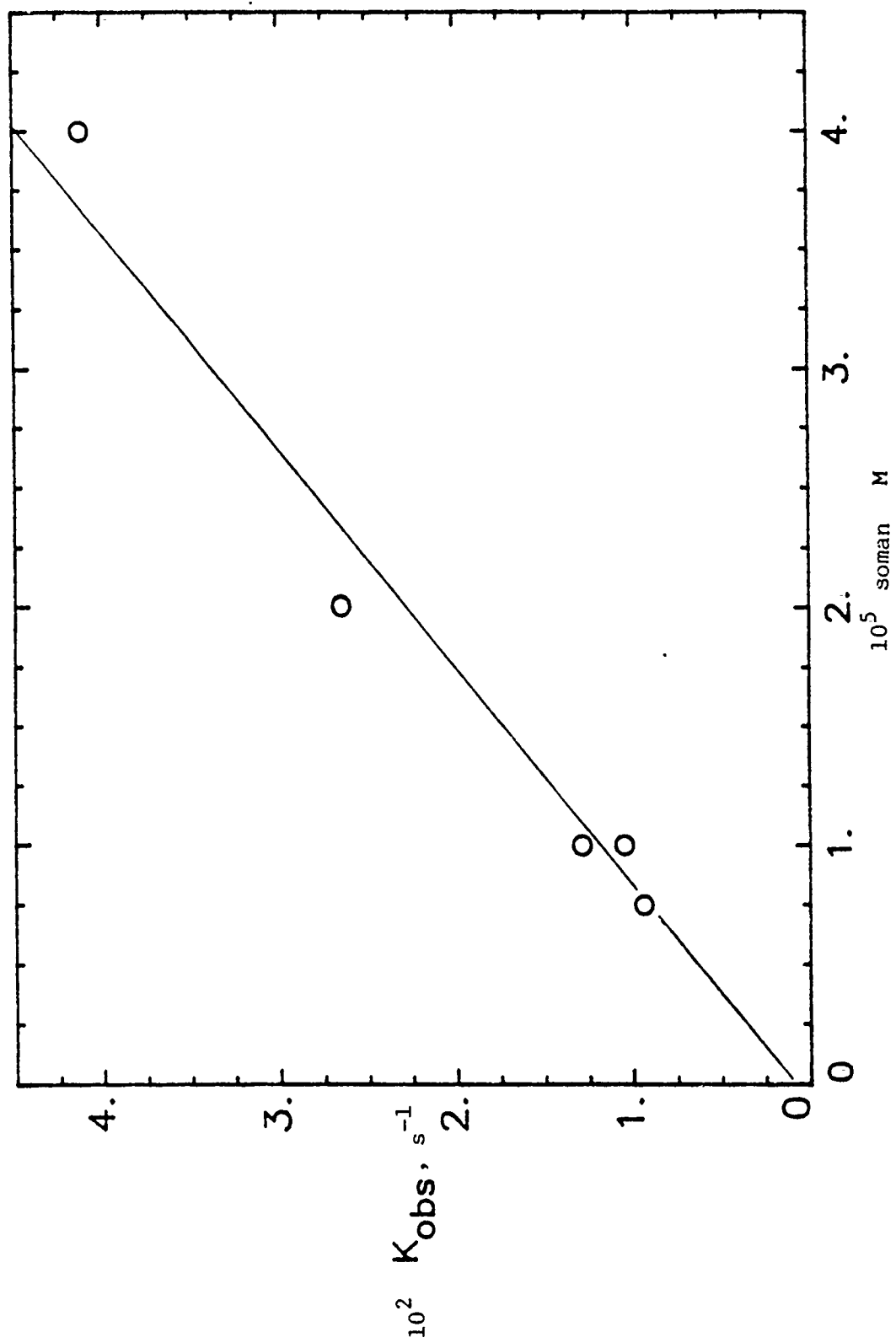


Figure 17. First-order rate constants for the inhibition of chymotrypsin by soman as a function of soman concentration.

Rate measurements of the inhibition of chymotrypsin by MPN were carried out at pH 6.9 in HOH and pD 7.45 in DOD buffered with 0.05 M phosphate. These reactions were so sluggish that initial rate studies of 10^{-3} M chymotrypsin solutions with MPN were the only workable approach.

Reaction conditions and first-order data are tabulated for the inhibition by soman in Table V, by NPN in Table VI, and by MPN in Table VII. The substrate concentration (S) used for each set of experiments is indicated in the table captions or in a separate column (c.f. Table V) in units of M and the order of magnitude is indicated by the factor preceding S, according to the convention of the Journal of the American Chemical Society. The data were collected at inhibitor concentrations below saturation but high enough that the substrate dependence was negligible (as at $S = 0$). Either the average of a given number of experiments is given in a table or each single k_{obs} value is reported. The values of k_i/K_i calculated from these data are tabulated in Tables VIII, IX and X, and the corresponding proton inventory plots are in Figures 18, 19 and 20. In these and all other plots and tables, n always represents the atom fraction of deuterium in the respective reaction mixture.

d. Inhibition of Trypsin

Trypsin is not inhibited by MPN to an appreciable degree. The progress of inhibition by NPN was followed under pseudo-first-order conditions when trypsin was in 25-fold excess. The pH dependence of phosphorylation of trypsin (Table XI and Figure 21) approached an asymptote at $\text{pH} > 8.2$; $\text{pD} > 8.6$ to the analogy of acylation. A more extensive determination of the pH dependence is technically complicated by the increasing background hydrolysis of the inhibitors and is not required for the location of the pH optimum, where proton inventories are preferentially measured. The proton inventory data are given in Tables XII and IX and in Figure 22.

e. Inhibition of Subtilisin BPN'

The very slow inhibition by MPN was followed by initial rates (v_0 in Ms^{-1} units) of less than 5% of inhibition. The proton inventory data, v_0 values as a function of n , the atom fraction of deuterium, are tabulated in Tables XIII and IX and portrayed in Figure 20.

Studies of inhibition by soman and NPN were carried out in competition with GLP as an adequate chromogenic substrate of subtilisin BPN'. It is interesting that no dependence of inhibition on the concentration of GLP could be observed in either case. The data are tabulated in Tables XIV and VIII for soman and in XV and IX for NPN. The corresponding proton inventories are given in Figs. 23 and 22.

f. Inhibition of Porcine Elastase

The sluggish inhibition by MPN was followed by initial rates as described for subtilisin BPN'. The proton inventory data are listed in Tables XVI and X and portrayed in Figure 20.

The rate of inhibition of elastase by NPN was followed in the presence of the chromogenic substrate n-succinyl-Ala-Ala-Ala-4-nitro-

TABLE V. Primary Data for Chymotrypsin Inhibition by Soman.

Enzyme: α -Chymotrypsin 2×10^{-6} M^a, Sigma Lot No. 31F-80751
 Substrate: GLP, 10^{-5} M, gift of Professor Barth et al., IK8472
 Inhibitor: Soman, 4×10^{-5} M; source: USAMRDC
 Buffer: Phosphate, 0.05 M, Fisher Lot No. 730871
 Ionic Strength: 0.15 M, 1% acetone
 Temperature: $25.00 \pm 0.05^\circ\text{C}$

n	pL	$10^5 k_{\text{obs}}, \text{s}^{-1}$	No. of experiments
0.00	7.44	4120 ± 123	(4)
0.252	7.46	3670 ± 115	(4)
0.495	7.48	3010 ± 167	(4)
0.746	7.51	2600 ± 155	(4)
1.000	7.54	1938 ± 57	(7)

^aActive site titration by 4-nitrophenyl acetate

TABLE VI. Primary Data for Chymotrypsin Inhibition by NPN.

Enzyme: α -Chymotrypsin, 4×10^{-7} M, Sigma Lot No. 31F-80751

Substrate: GLP, gift of Professor Barth et al., IK8472

Inhibitor: NPN, 1.5×10^{-5} M, Source: synthesis IK8417

Buffer: Phosphate, 0.05 M, Fisher Lot No. 730871

Ionic Strength: 0.15 M, 1% MeOH, 4% acetone

Temperature: $25.00 \pm 0.05^\circ\text{C}$

n	$10^4 S, \text{M}$	pL	$10^5 k_{\text{obs}}, \text{s}^{-1}$
0.00	5	7.40	3130, 3120
0.00	1	7.40	3700, 3540, 3540, 3860, 3640
0.239	5	7.43	2830, 2930
0.239	1	7.43	3300, 3460
0.521	5	7.48	2560, 2560
0.521	1	7.48	2680, 2670
0.712	5	7.51	2360, 2240
0.712	1	7.51	2680, 2540
1.000	5	7.53	1780, 1760
1.000	1	7.53	1970, 1990

TABLE VII. Primary Data for Chymotrypsin Inhibition by MPN.

Enzyme: α -Chymotrypsin $1.66 \times 10^3 \text{ M}^a$, Sigma Lot No. 31F-80751

Inhibitor: MPN, $3.6 \times 10^{-5} \text{ M}$; source: synthesis IK8417

Buffer: Phosphate, 0.05 M, Fisher Lot No. 730871

Ionic Strength: 0.15 M, 1% MeOH

Temperature: $25.00 \pm 0.05^\circ\text{C}$

n	pL	$10^{10} V_0, \text{ Ms}^{-1}$	No. of experiments
0.00	6.90	260 ± 5	(3)
0.25	6.92	233 ± 8	(3)
0.50	6.95	196 ± 2	(3)
0.75	6.97	164 ± 11	(3)
1.00	7.02	123 ± 1	(3)

^aActive site titration by 4-nitrophenyl acetate

TABLE VIII. Inhibition Rate Constants for Serine Proteases with Soman in Binary Mixtures of Protium and Deuterium Oxides (Atom Fraction of Deuterium).

System	$k_i/K_i, \text{M}^{-1}\text{s}^{-1} \pm \text{SD} (n)$
α -Chymotrypsin pH = 7.44 and corresponding pL, $\mu = 0.15 \text{ M}$	1030 \pm 30 (0.00); 902 \pm 29 (0.252) 753 \pm 42 (0.495) 650 \pm 38 (0.746); 484 \pm 16 (1.000)
Subtilisin BPN' pH = 8.40 and corresponding pL, $\mu = 0.017 \text{ M}$	20.5 \pm 4.2 (2.00); 17.0 \pm 3.5 (0.252) 15.0 \pm 0.3 (0.485); 12.4 \pm 0.1 (0.720); 10.1 \pm 1.4 (0.950); 9.6 \pm 2.0 (0.950)

TABLE IX. Inhibition Rate Constants for Serine Proteases with NPN in Binary Mixtures of Protium and Deuterium Oxides (Atom Fraction of Deuterium).

System	$k_i/K_i, M^{-1}s^{-1} \pm SD (n)$
α -Chymotrypsin pH = 7.40 and corresponding pL, substrate $1-5 \times 10^{-4}$ M $\mu = 0.15$ M	2261 \pm 59(0.00); 985 \pm 52(0.24); 1651 \pm 78(0.52); 1522 \pm 32(0.72); 1178 \pm 17(1.00)
Trypsin pH = 8.42 and corresponding pL, $\mu = 0.031$ M A different solution of Trypsin (see Table XI)	263.7 \pm 8(0.00); 234.4 \pm 7(0.25); 200.6 \pm 4(0.50); 170.6 \pm 5(0.75); 144.5 \pm 3(1.00); 277.4 \pm 3(0.00); 149.7 \pm 1(1.00)
Subtilisin BPN ¹ pH = 8.39 and corresponding pL, substrate 5×10^{-5} M $\mu = 0.017$ M	1325 \pm 49(0.00); 1190 \pm 58(0.227); 1190 \pm (0.278); 1016 \pm 23(0.495); 881(0.722); 885 \pm 12(0.773); 748 \pm 6(0.95); 713 \pm 7(1.00)
Elastase pH = 8.43 and corresponding pL, substrate $1.25-6.25 \times 10^{-4}$ M $\mu = 0.017$ M	1839 \pm 40(0.00); 1521 \pm 27(0.253); 1385 \pm 25(0.495); 1213 \pm 23(0.747); 1123 \pm 21(1.00)

TABLE X. Inhibition Rate Constants for Serine Proteases with MPN in Binary Mixtures of Protium and Deuterium Oxides (Atom Fraction of Deuterium).

System	$10^3 k_i/K_i, M^{-1}s^{-1} \pm SD (n)$
α -Chymotrypsin pH = 7.40 and corresponding pL, $\mu = 0.15 M$	435 \pm 8(0.00); 390 \pm 12(0.25); 326 \pm 1(0.50); 273 \pm 14(0.75); 205 \pm 2(1.00)
Subtilisin BPN' pH = 8.40 and corresponding pL, $\mu = 0.034 M$	2570 \pm 15(0.00); 2310 \pm 30(0.20); 1890 \pm 29(0.50); 1460 \pm 38(0.75); 1310 \pm 31(1.00)
Elastase pH = 8.43 and corresponding pL, $\mu = 0.034 M$	3190 \pm 200(0.000); 2870 \pm 138(0.238); 2340 \pm 11(0.500); 2020 \pm 115(0.750); 1670 \pm 55(1.000)

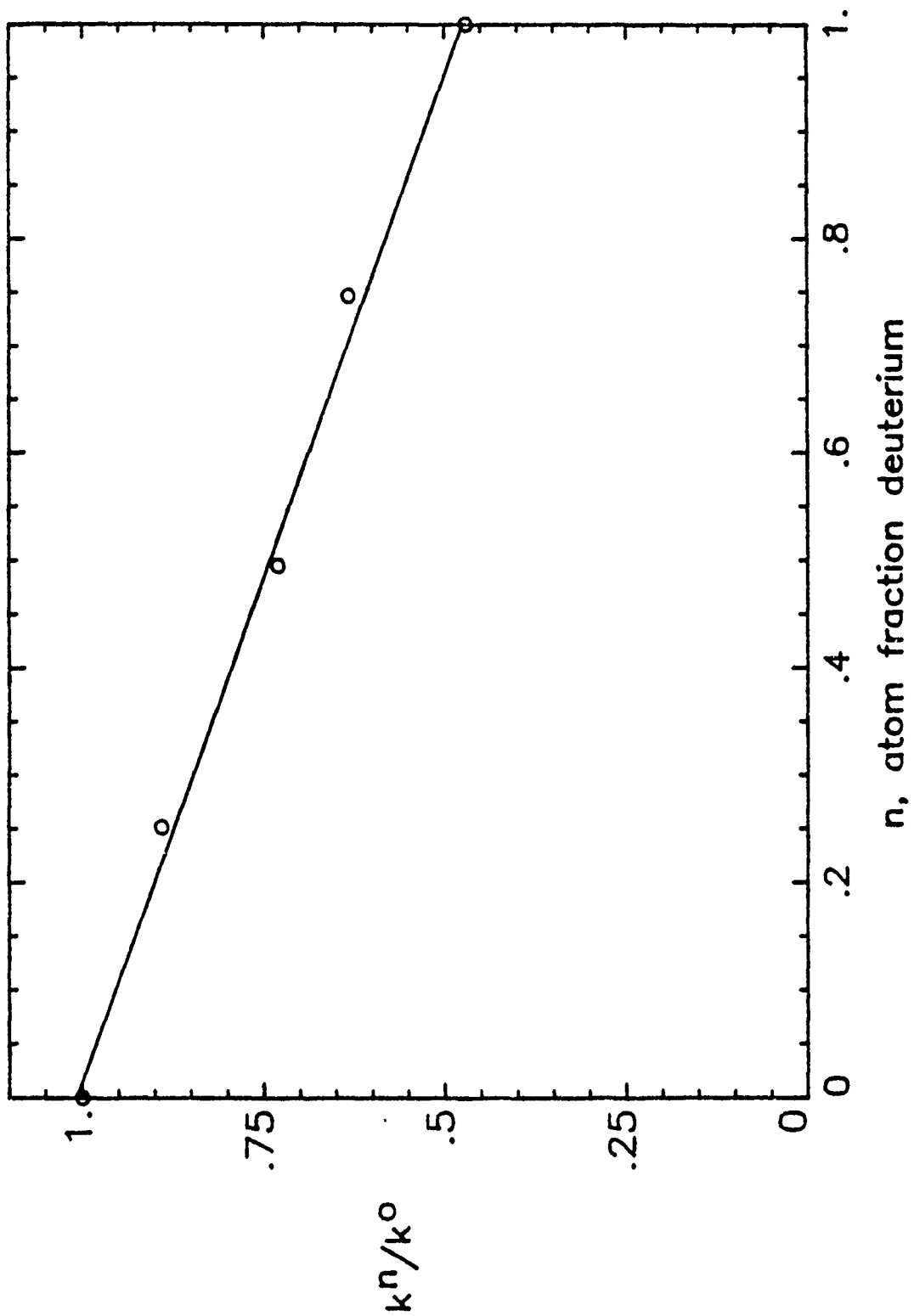


Figure 18. Proton inventory for the reaction of chymotrypsin with soman.

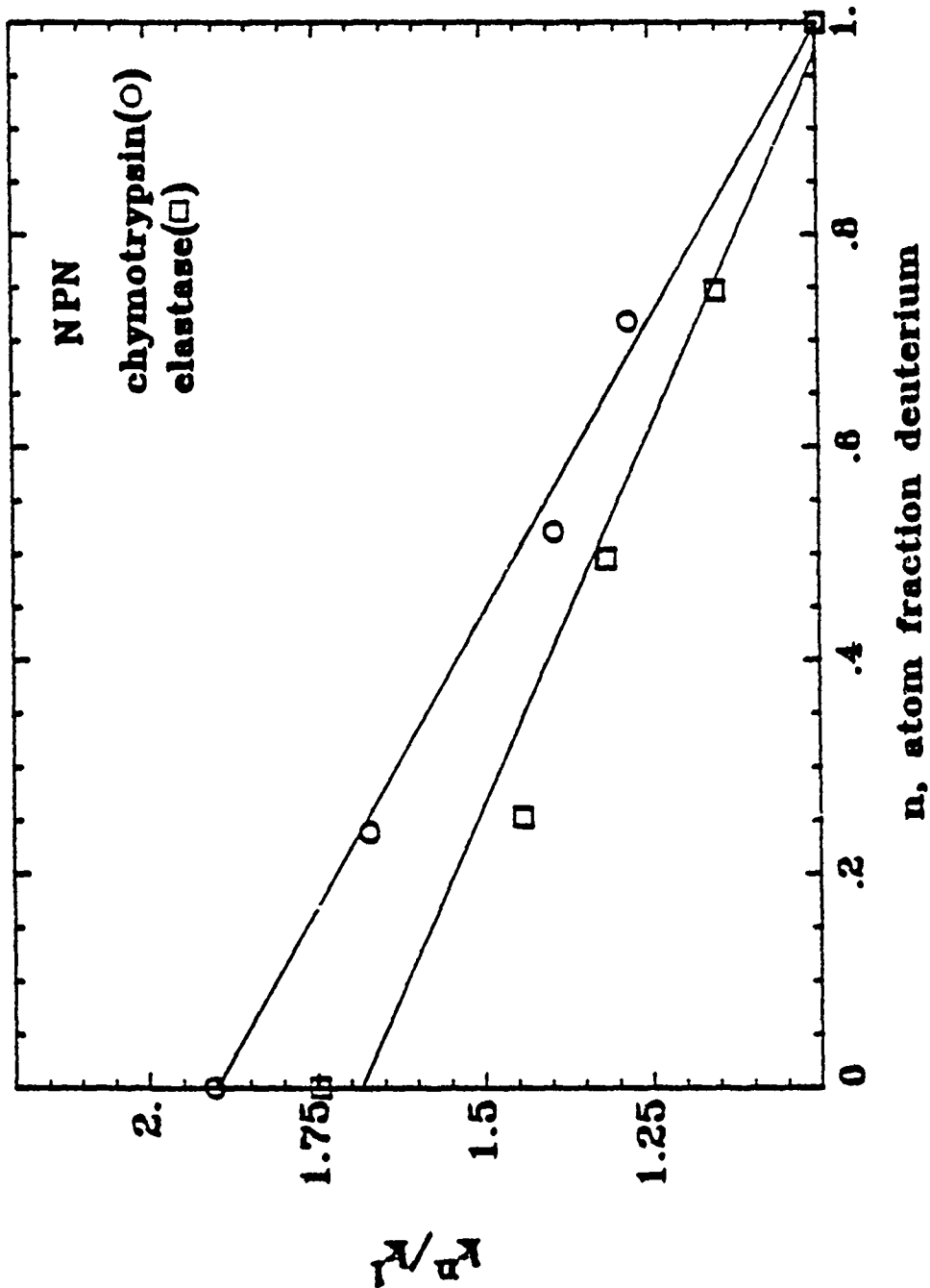


Figure 19. Proton inventory for the inactivation of chymotrypsin and elastase by NPN.

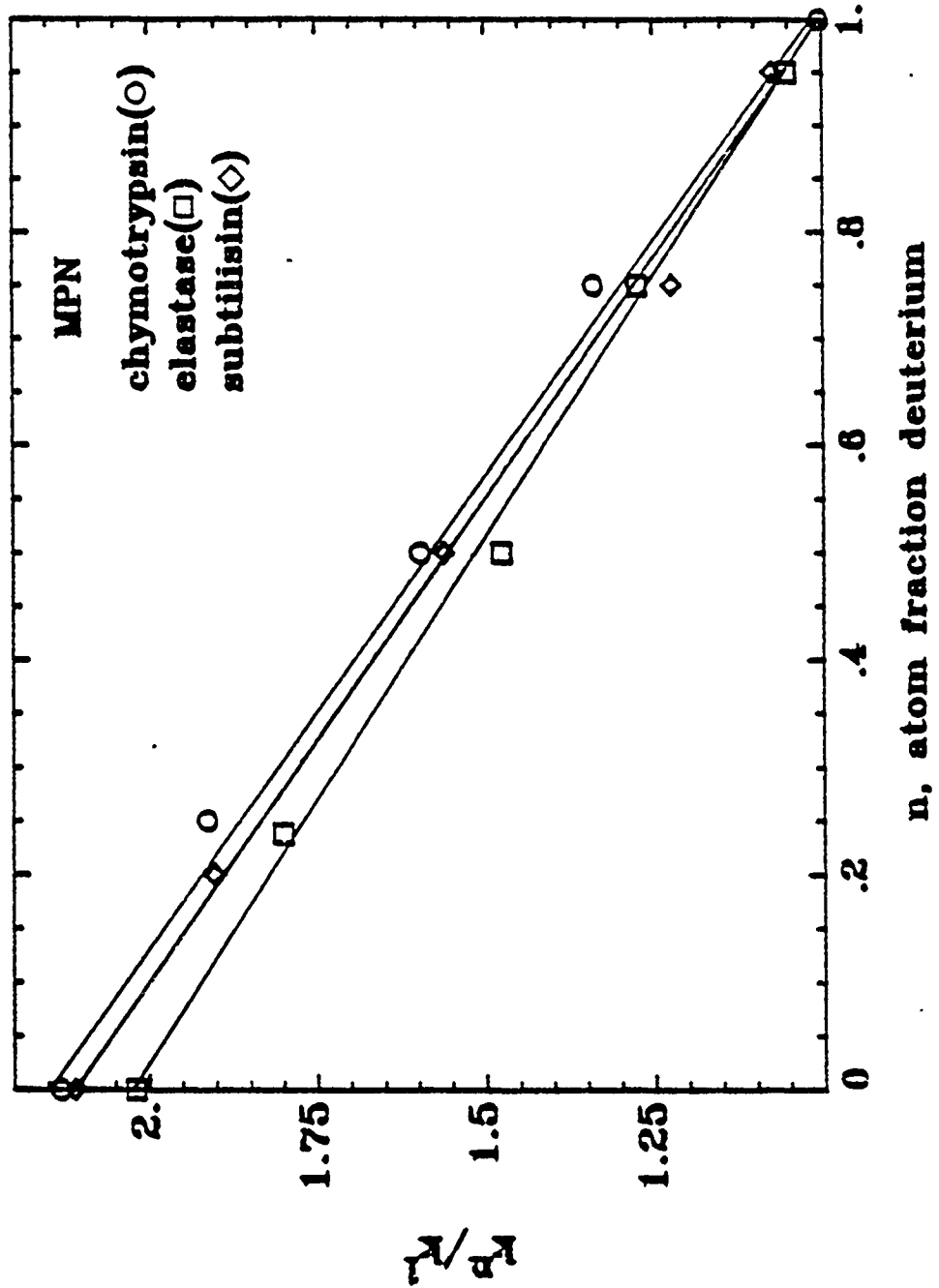


Figure 20. Proton inventory for the inactivation of chymotrypsin, elastase and subtilisin by MPN.

TABLE XI. Dependence on pL (L = H,D) of Inhibition Rate Constants for Trypsin^a with NPN in HOH and DOD solvents at 25.00 ± 0.05°C, μ = 0.29 (KCl).

pL		$k_i/K_i, M^{-1}s^{-1}$
HOH,	pH	
	7.10	131.6
	7.28	176.7
	7.58	214.8
	8.00	295.3
	8.04	282.3
	8.28	312
	8.45	315, 294
	8.90	288, 298
DOD,	pD	
	7.35	47.3, 51.1
	7.74	81.4
	8.14	95.2
	8.35	112.1, 115.2
	8.79	155.5
	9.38	175.3

^a31 mg/ml = 1.307 × 10⁻³ M calculated with MW = 23,800

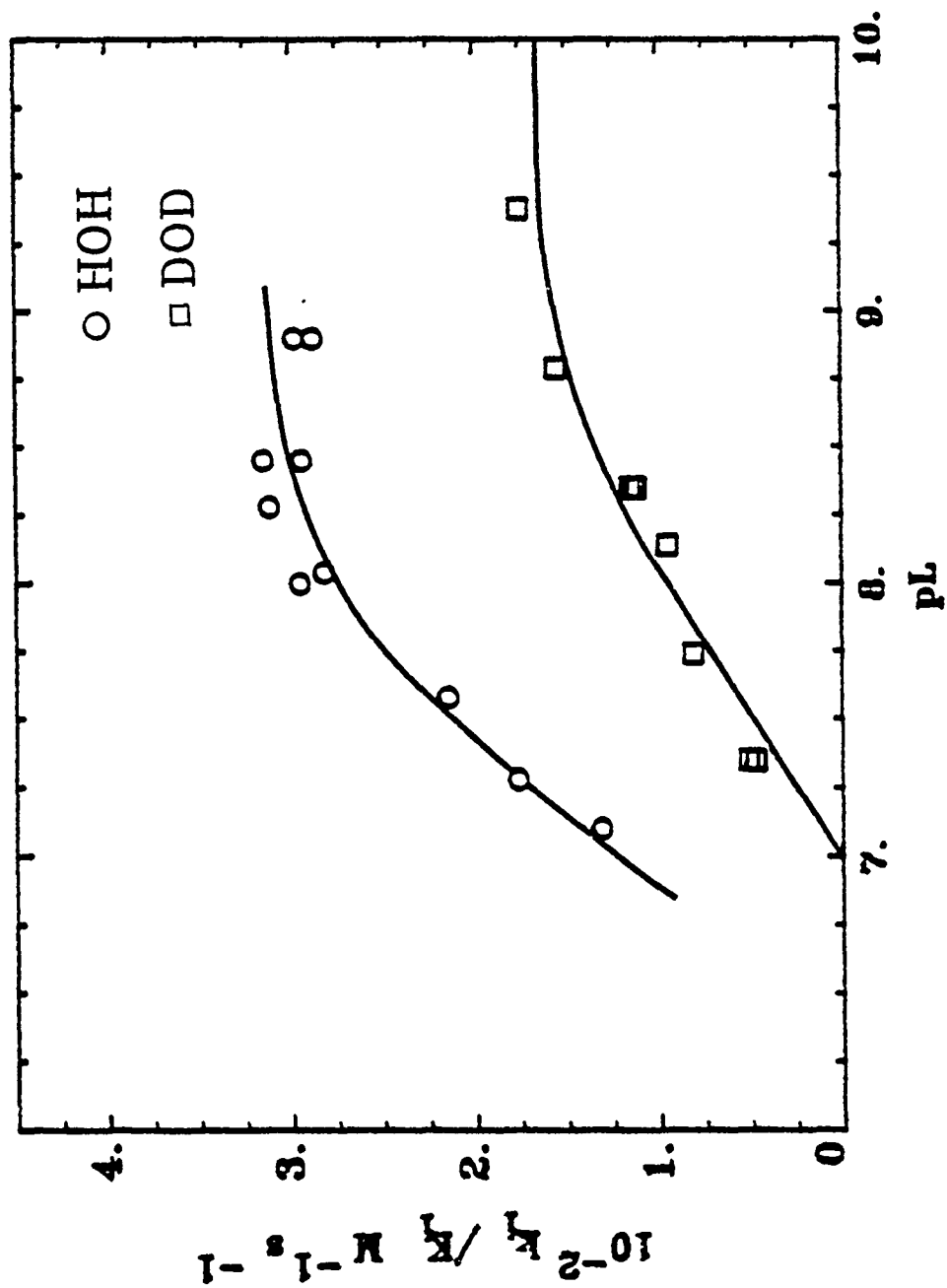


Figure 21. pH Dependence of the phosphorylation of trypsin.

TABLE XII. Primary Data for Trypsin Inhibition by NPN.

Enzyme: Trypsin 10^{-4} M,^a Sigma Lot No. 546-8220

Inhibition: NPN, 4.6×10^{-6} M, Source: synthesis IK8417

Buffer: Trizma 0.09 M, Sigma Lot No. 32F-5010

Ionic Strength: 0.031 M, 1% MeOH

Temperature: $25.00 \pm 0.05^\circ\text{C}$

n	pL	$10^5 k_{\text{obs}}, \text{s}^{-1}$	No. of Experiments
0.00	8.42	2769 ± 86	(8)
0.250	8.46	2438 ± 80	(4)
0.500	8.48	2106 ± 44	(4)
0.750	8.54	1791 ± 52	(4)
1.00	8.60	1517 ± 32	(5)
*0.00	8.42	3079 ± 31	(4)
*1.00	8.58	1617 ± 11.3	(4)

*Higher enzyme activity

^aCalculated from weight with MW = 23,800

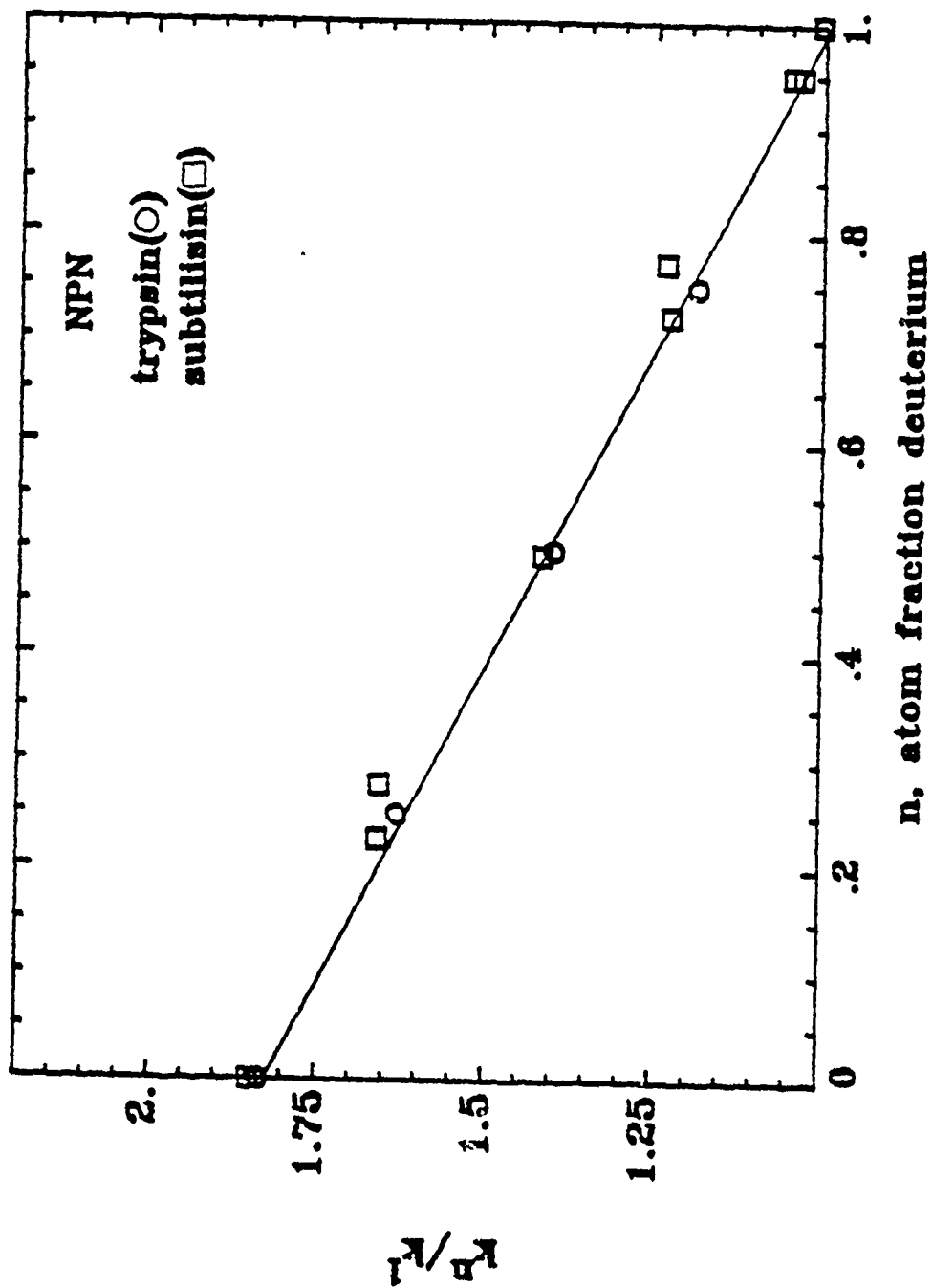


Figure 22. Proton inventory for the inactivation of subtilisin and trypsin by NPN.

TABLE XIII. Primary Data for Subtilisin Inhibition by MPN.

Enzyme: Subtilisin BPN', 2.7×10^{-5} M,^a Sigma Lot No. 123F-0316

Substrate: GLP, 10^{-4} M, gift of Professor Barth et al., IK8472

Inhibitor: MPN, 1.51×10^{-5} M, Source: synthesis IK8417

Buffer: Trizma, 0.1 M, Sigma Lot No 32F-5010

Ionic strength: 0.034 M, 2% MeOH

Temperature: $25.00 \pm 0.05^\circ\text{C}$

n	pL	$10^{11}V_0, \text{Ms}^{-1}$	No. of Experiments
0.00	8.40	1058 ± 6	(4)
0.200	8.41	955 ± 22	(4)
0.500	8.45	776 ± 15	(4)
0.750	8.48	604 ± 9	(4)
0.950	8.50	541 ± 6	(4)

^aActive site titration by MPN

TABLE XIV. Primary Data for Subtilisin Inhibition by Soman.

Enzyme: Subtilisin BPN', 8×10^{-7} M,^a Sigma Lot No. 123F-0316

Substrate: GLP, 10^{-4} M, gift of Professor Barth et al.,
IK8472

Inhibitor: Soman, 10^{-4} M, Source: USAMRDC

Buffer: Trizma, 0.05 M, Sigma Lot No. 32F-5010

Ionic strength: 0.017 M, 1% acetone

Temperature: $25.00 \pm 0.05^\circ\text{C}$.

n	pL	$10^5 k_{\text{obs}}, \text{s}^{-1}$	No. of experiments
0.00	8.40	205 ± 42	(3)
0.252	8.44	170 ± 35	(2)
0.485	8.46	150 ± 3	(2)
0.720	8.51	124 ± 1	(2)
0.950	8.55	101 ± 14	(3)
0.950	8.55	96 ± 20	(2)

^aActive site titration by MPN

TABLE XV. Primary Data for Subtilisin Inhibition by NPN.

Enzyme: Subtilisin BPN¹, 10^{-6} M,^a Sigma Lot No. 123F-0316

Substrate: GLP, 5×10^{-5} M, gift of Professor Barth
et al., IK8472

Inhibitor: NPN, 1.733×10^{-5} M, Source: synthesis IK8417

Buffer: Trizma, 0.05 M, Sigma Lot No. 32F-5010

Ionic strength: 0.017 M, 1% MeOH, 2% acetone

Temperature: $25.00 \pm 0.05^\circ\text{C}$.

n	pL	$10^5 k_{\text{obs}}, \text{s}^{-1}$	No. of experiments
0.00	8.39	2187 ± 13	(7)
0.227	8.39	1963 ± 96	(3)
0.278	8.40	1962	
0.495	8.40	1676 ± 43	(3)
0.722	8.42	1453	
0.773	8.44	1460 ± 20	(3)
0.950	8.49	1234 ± 10	(2)
1.000	8.49	1189, 1165	

^aActive site titration by MPN

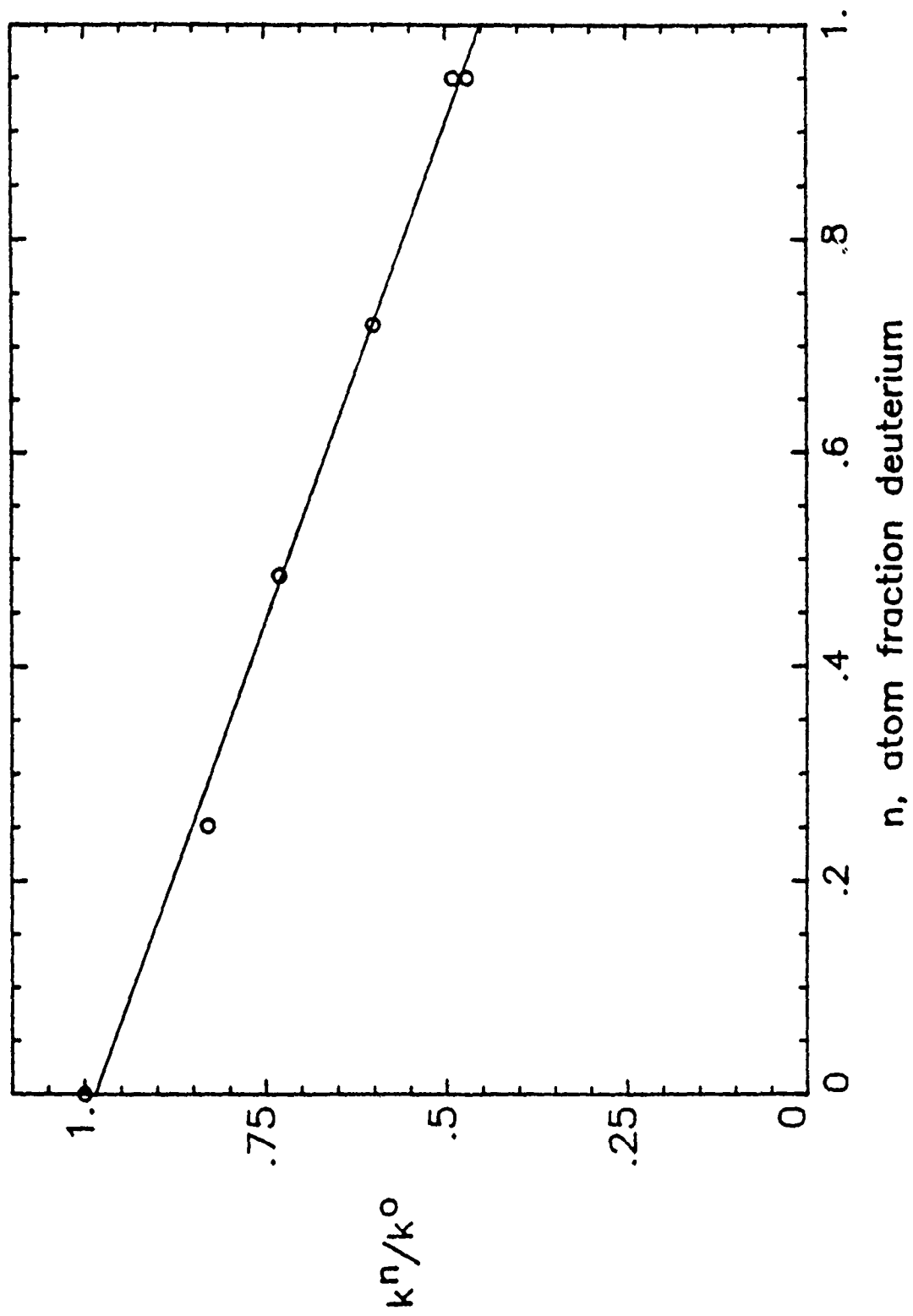


Figure 23. Proton inventory for the reaction of subtilisin BPN' with soman.

TABLE XVI. Primary Data for Elastase Inhibition by MPN.

Enzyme: Elastase, 2.5×10^{-5} M,^a Sigma Lot No. 73F-81651

Inhibitor: MPN, 1.71×10^{-5} M, Source: synthesis IK8417

Buffer: Trizma, 0.1 M, Sigma Lot No. 32F-5010

Ionic strength: 0.034 M, 2% MeOH

Temperature: $25.00 \pm 0.05^\circ\text{C}$

n	pL	$10^{11}V_0, \text{Ms}^{-1}$	No. of Experiments
0.00	8.43	1368 ± 86	(4)
0.238	8.48	1225 ± 59	(4)
0.500	8.50	1012 ± 5	(7)
0.750	8.50	868 ± 50	(4)
0.950	8.52	718 ± 24	(4)

^aActive site titration by MPN

anilide under the conditions given together with the data in Table XIV. The substrate concentrations are indicated under the heading $10^4 S$; therefore, they represent orders of 10^{-4} M concentrations. The second-order rate constants calculated from the data in Table XVII, according to eq. 17, are tabulated in Table IX and plotted against the fraction of deuterium in Figure 19.

g. Solvent Isotope Effects for the Inhibition of Serine Proteases

The rate ratios (k_n/k_1) for the partial solvent isotope effects at each n, atom fraction of deuterium, were calculated and fitted to eq. 1/b for the model for two hydrogenic sites at the transition state. The two fractionation factors, ϕ , so calculated are listed in Table XVIII.

5. Acetylation and Deacetylation of AChE by Phenyl Acetate

Rates in H_2O and four mixtures with D_2O were measured as a function of substrate concentration and the rates were extrapolated by the Lineweaver-Burke expression to zero concentration (V/K) and infinite concentration (V). The Michaelis-Menten parameters V/K and V signify the bimolecular rate constant between enzyme and substrate and the unimolecular rate constant for the first product release from the Michaelis complex, respectively. In the case of the phenyl acetate reaction, the V/K phase corresponds to acyl: ion and V phase is predominantly deacetylation.³⁶ The data are shown in Table XIX for the electric eel and the erythrocyte enzymes. Figures 24 and 25 show the proton-inventory plots.

The overall solvent isotope effects are:

$$\begin{aligned} k_{cat}(HOH)/k_{cat}(DOD) &= 2.42 \pm 0.03 \text{ eel AChE} \\ &2.28 \pm 0.11 \text{ erythrocyte AChE} \end{aligned}$$

$$\begin{aligned} (k_{cat}/K_m)^{HOH}/(k_{cat}/K_m)^{DOD} &= 1.46 \pm 0.07 \text{ eel AChE} \\ &1.61 \pm 0.11 \text{ erythrocyte AChE} \end{aligned}$$

6. ^{18}O -Leaving Group and β -D Isotope Effects

Figure 26 shows the dependence of the inactivation of AChE on the concentrations of $^{16}O^-$ and ^{18}O -labeled IMN in the presence of 8.5×10^{-3} M phenyl acetate. The slope of the lines gives $K_i/k_i[1 + [S]/K_m]$, from which k_i/K_i , the second-order rate constants, are calculated. Since the same substrate concentrations were used for both isomers, the ratio of slopes for $^{18}O:^{16}O$ gives the isotope effect $^{16}k:^{18}k = 1.06 \pm 0.03$.³⁷

Figure 27 shows the dependence for CH_3^- and CD_3^- -labeled isomers for the inactivation of AChE by soman in the presence of 8.5×10^{-3} M phenyl acetate.

Similarly, plots of inverse observed rate constants versus the inverse of sarin concentrations are represented on Figure 28.

Second-order rate constants for the inactivation of AChE by OP inhibitors, for their isotopically labeled counterparts, and the respective isotope effects are listed in Table XX. The data for the solvent isotope effects measured for IMN are also included in Table XX.

TABLE XVII. Primary Data for Elastase Inhibition by NPN.

Enzyme: Elastase, 2×10^{-7} M,^a Sigma Lot No. 73F-81651

Substrate: N-succinyl-(Ala)₃-p-nitroanilide, Sigma Lot No. 104F-5875

Inhibitor: NPN, 1.5×10^{-5} M, Source: synthesis IK8417

Buffer: Trizma, 0.05 M, Sigma Lot No. 32F-5010

Ionic strength: 0.017 M, 3% MeOH, 2% CH₃CN

Temperature: $25.00 \pm 0.05^\circ\text{C}$.

n	10 ⁴ S	pL	10 ⁶ k _{obs} , s ⁻¹
0.00	6.25	8.43	2395, 2633, 2483, 2511, 2422
0.00	1.250	8.43	2737, 2651, 2721
0.253	6.25 6.03	8.45	1957, 2003, 1955 2015
0.253	1.210	8.45	2170, 2261
0.495	6.05	8.47	1803, 1832, 1842, 1832
0.495	1.210	8.47	2014, 1957, 2102
0.747	6.03	8.49	1621, 1594, 1593
0.747	1.10	8.49	1827, 1814
1.00	6.05	8.52	1349, 1363, 1380, 1400
1.00	1.21	8.52	1625, 1633, 1534, 1659

^aActive site titration by NPN

TABLE XVIIIa. Second-order Rate Constants and Solvent Isotope Effect Information for Inactivation of Serine Proteases by NPN at 25°C and Appropriate pL.^a

Enzyme (pH), $k_{\text{HOH}}/k_{\text{DOD}}$	$(k_i/K_i)_{\text{HOH}},$ $\text{M}^{-1}\text{s}^{-1}(\text{SD})$	$(k_i/K_i)_{\text{DOD}},$ $\text{M}^{-1}\text{s}^{-1}(\text{SD})$	ϕ_1 (SD)	ϕ_2^b (SD)
Chymotrypsin (7.45) 1.92 ± 0.06	2260(59)	1178(17)	0.57 (0.06)	0.93 (0.09)
Elastase (8.45) 1.65 ± 0.05	1840(50)	1120(20)	0.77 (1.03)	0.66 (1.15)
Trypsin (8.48) 1.83 ± 0.06	264(8)	145(3)	0.58 (0.04)	0.93 (0.05)
Subtilisin (8.40) 1.85 ± 0.07	1330(49)	721(20)	0.50 (0.03)	1.07 (0.05)

^aFor chymotrypsin, a value approximating the pH of maximum rate was used. For other enzymes, a pH in the pH-independent region was chosen. Corresponding pL in mixtures of HOH and DOD was achieved by employment of constant buffer ratios.

^bFractionation factors.

TABLE XVIIIb. Second-order Rate Constants and Solvent Isotope Effect Information for Inactivation of Serine Proteases by MPN at 25°C and Appropriate pL.

Enzyme (pH), $k_{\text{HOH}}/k_{\text{DOD}}$	$(k_i/K_i)_{\text{HOH}},$ $\text{M}^{-1}\text{s}^{-1}(\text{SD})$	$(k_i/K_i)_{\text{DOD}},$ $\text{M}^{-1}\text{s}^{-1}(\text{SD})$	ϕ_1 (SD)	ϕ_2 (SD)
Chymotrypsin (6.90) 2.12 ± 0.05	0.870 (0.016)	0.410 (0.005)	0.40 (0.02)	1.17 (0.05)
Elastase (8.43) 2.01 ± 0.15	3.19 (0.20)	1.59 (0.08)	0.51 (0.07)	0.97 (1.10)
Trypsin (8.50) ---	no reaction observed ($k_i/K_i < 0.1 \text{ M}^{-1}\text{s}^{-1}$)			
Subtilisin (8.40) 2.06 ± 0.05	2.57 (0.01)	1.24 (0.02)	0.50 (0.08)	0.96 (0.13)

^aFor chymotrypsin, a value approximating the pH of maximum rate was used. For other enzymes, a pH in the pH-independent region was chosen. Corresponding pL in mixtures of HOH and DOD was achieved by employment of constant buffer ratios.

TABLE XIX. Kinetic Parameters^a in Mixed Isotopic Waters^b for Hydrolysis of 0.8-8.2 mM Phenyl Acetate by Acetylcholinesterases at pH 7.60 and Equivalent^c at 25.00 ± 0.05°C.

Atom Fraction of Deuterium (n)	<u>Electric Eel</u> ^d		<u>Red Blood Cell</u> ^e	
	10 ⁻⁸ V, Ms ⁻¹	10 ⁵ /K, s ⁻¹	10 ⁷ V, Ms ⁻¹	10 ⁴ V/K, s ⁻¹
0.000	403(3)	168(2)	181(6)	152(7)
0.238	350(6)	153(4)	155(3)	142(3)
0.475	293(4)	139(3)	134(3)	122(5)
0.713	232(2)	130(3)	104(1)	110(2)
0.950	180(2)	117(3)	86(0.5)	101(2)

^aMaximal velocity V and its ratio to substrate concentration at half-maximal velocity V/K, determined by extrapolation from data at no less than three substrate concentrations, each velocity reproduced at least three times. Errors in parentheses are standard deviations.

^bContaining 1 percent by volume of methanol.

^cAll solutions contained 0.0434 M K₂HPO₄, 0.0066 M KH₂PO₄.

^dSigma V-S, 10 units/L.

^eSigma XIII, further purified, 12.5 units/L.

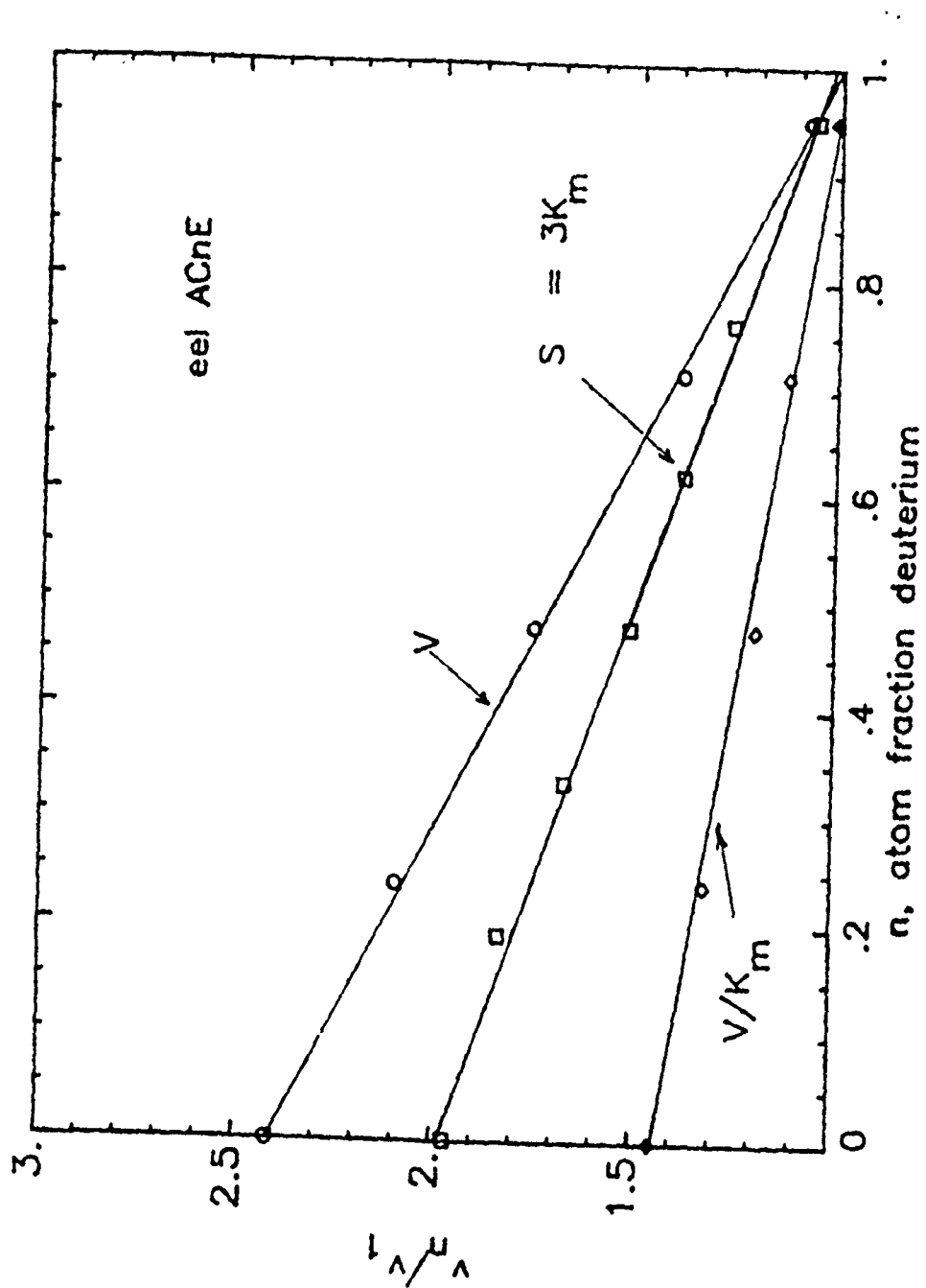


Figure 24. Proton inventory for the reaction of phenyl acetate with eel AChE.

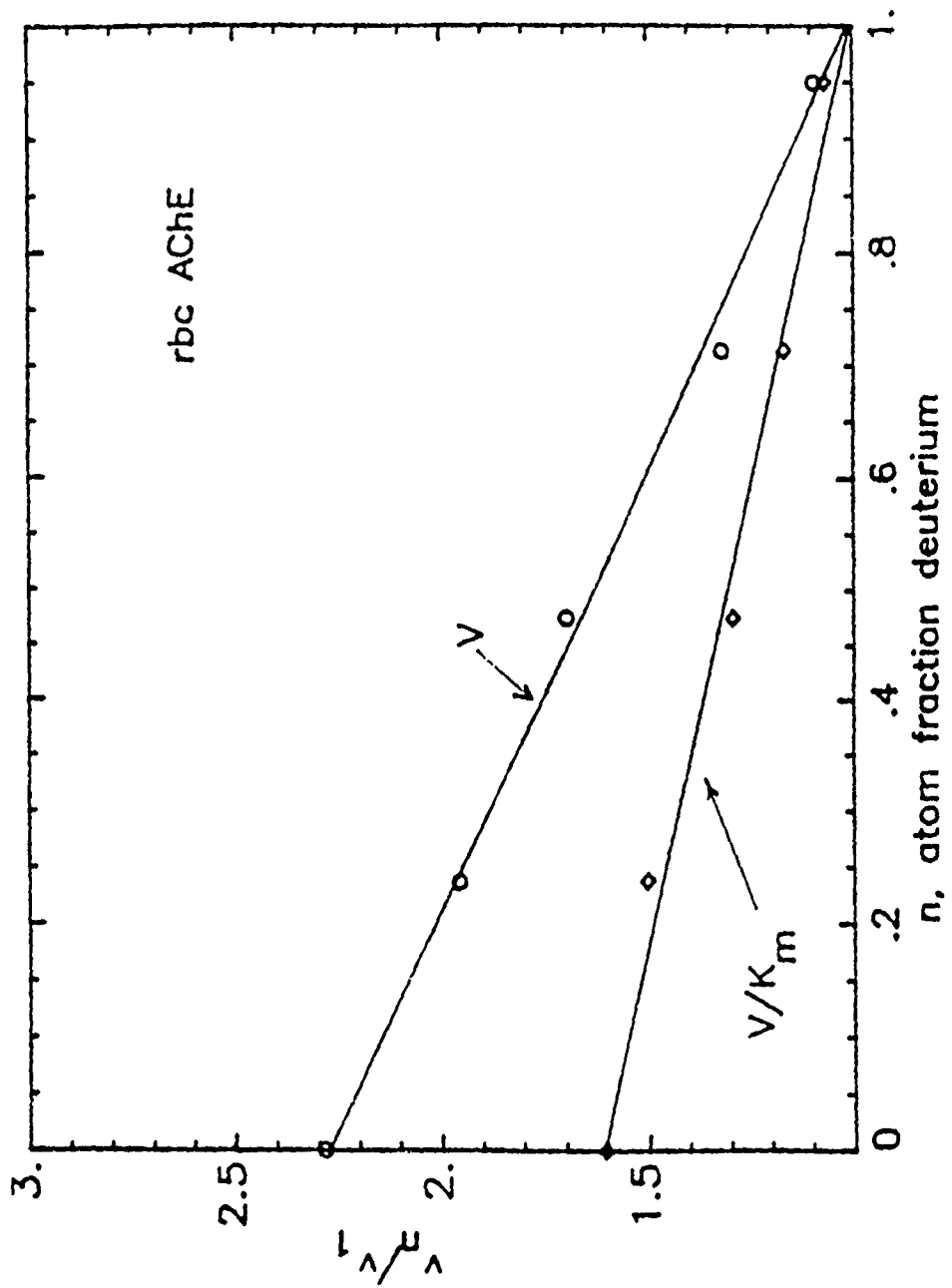


Figure 25. Proton inventory for the reaction of phenyl acetate with AChE (RBC).

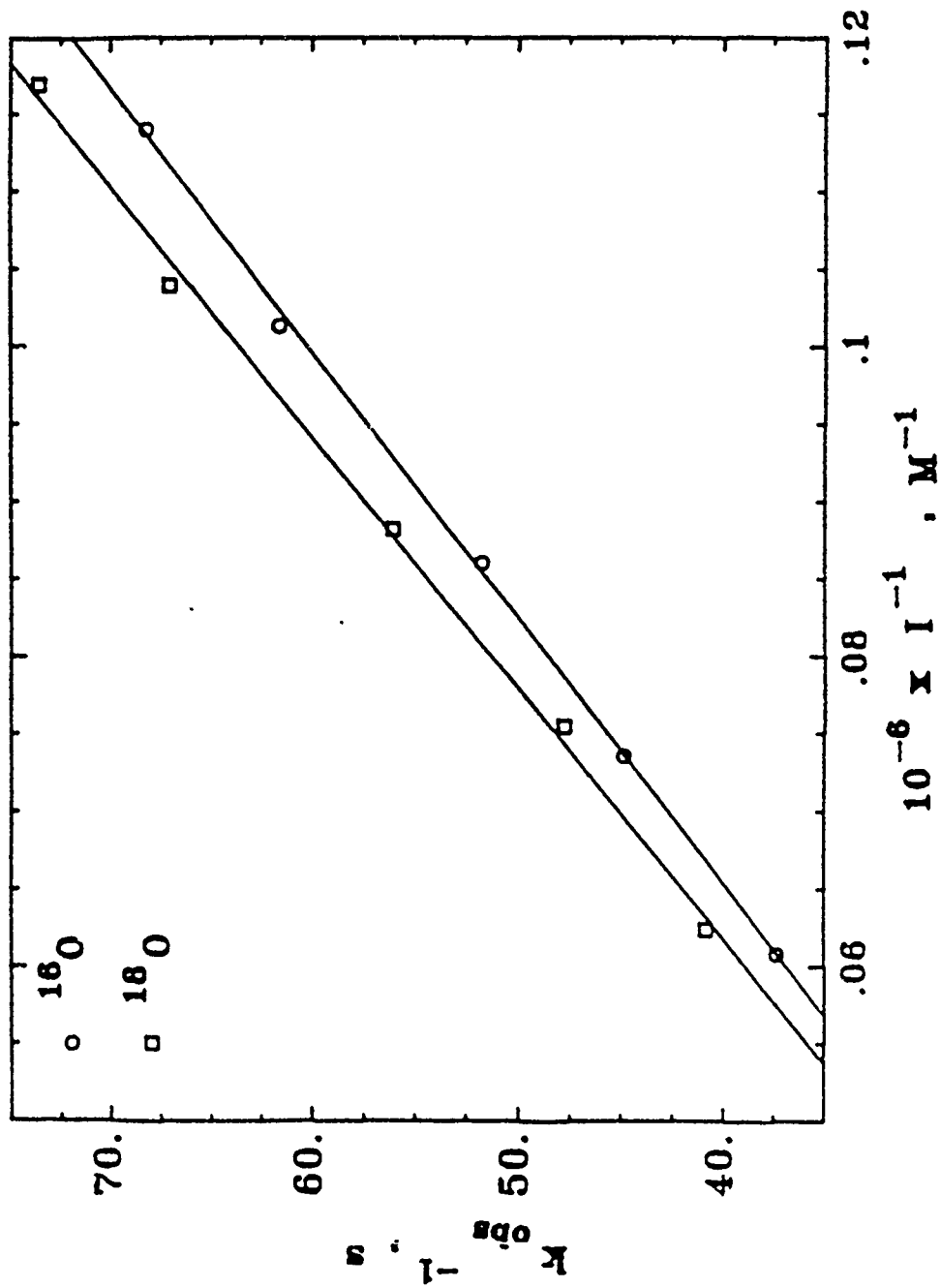


Figure 26. Inactivation of AChE by IMN.

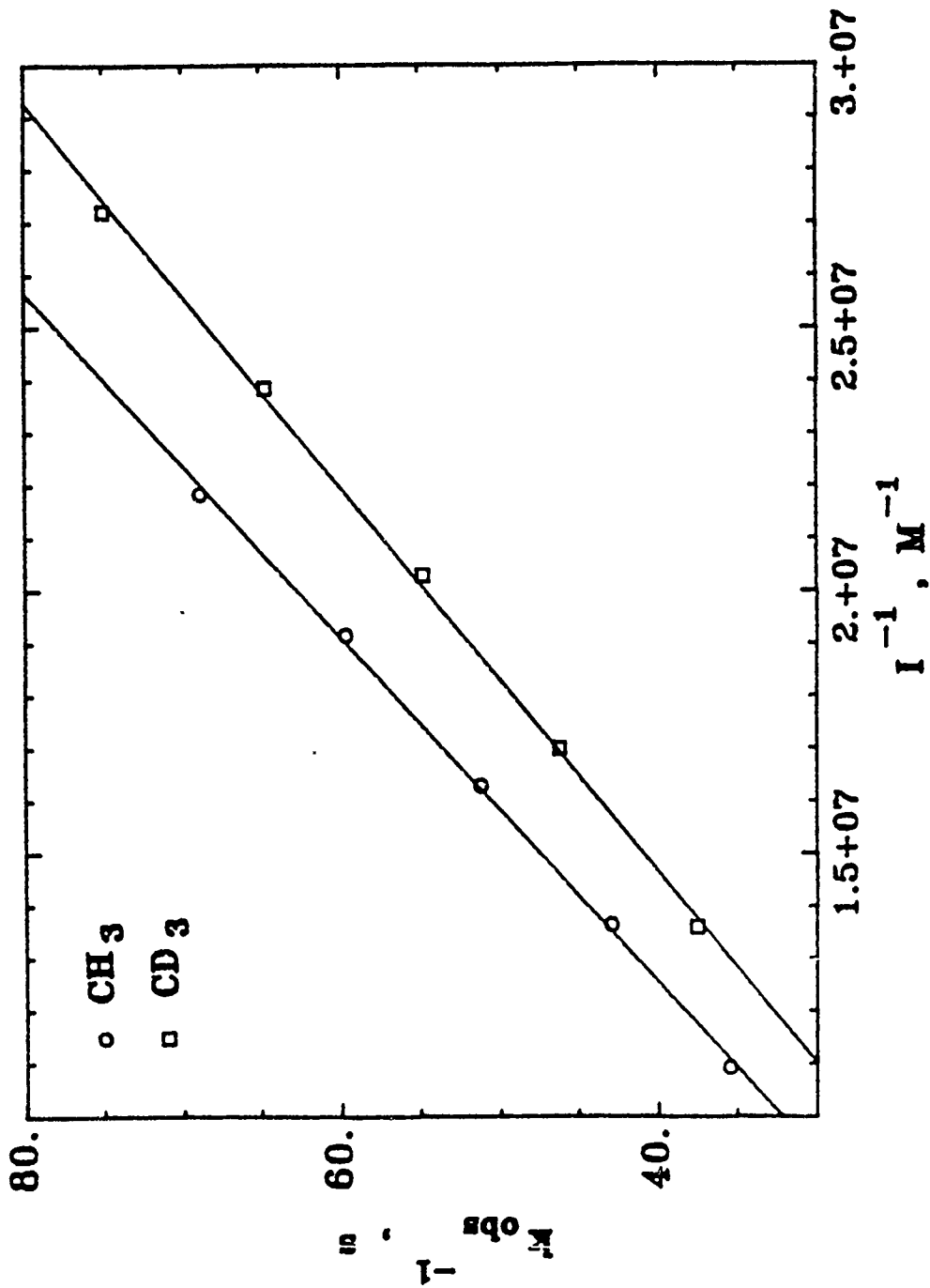


Figure 27. Inactivation of AChE by soman.

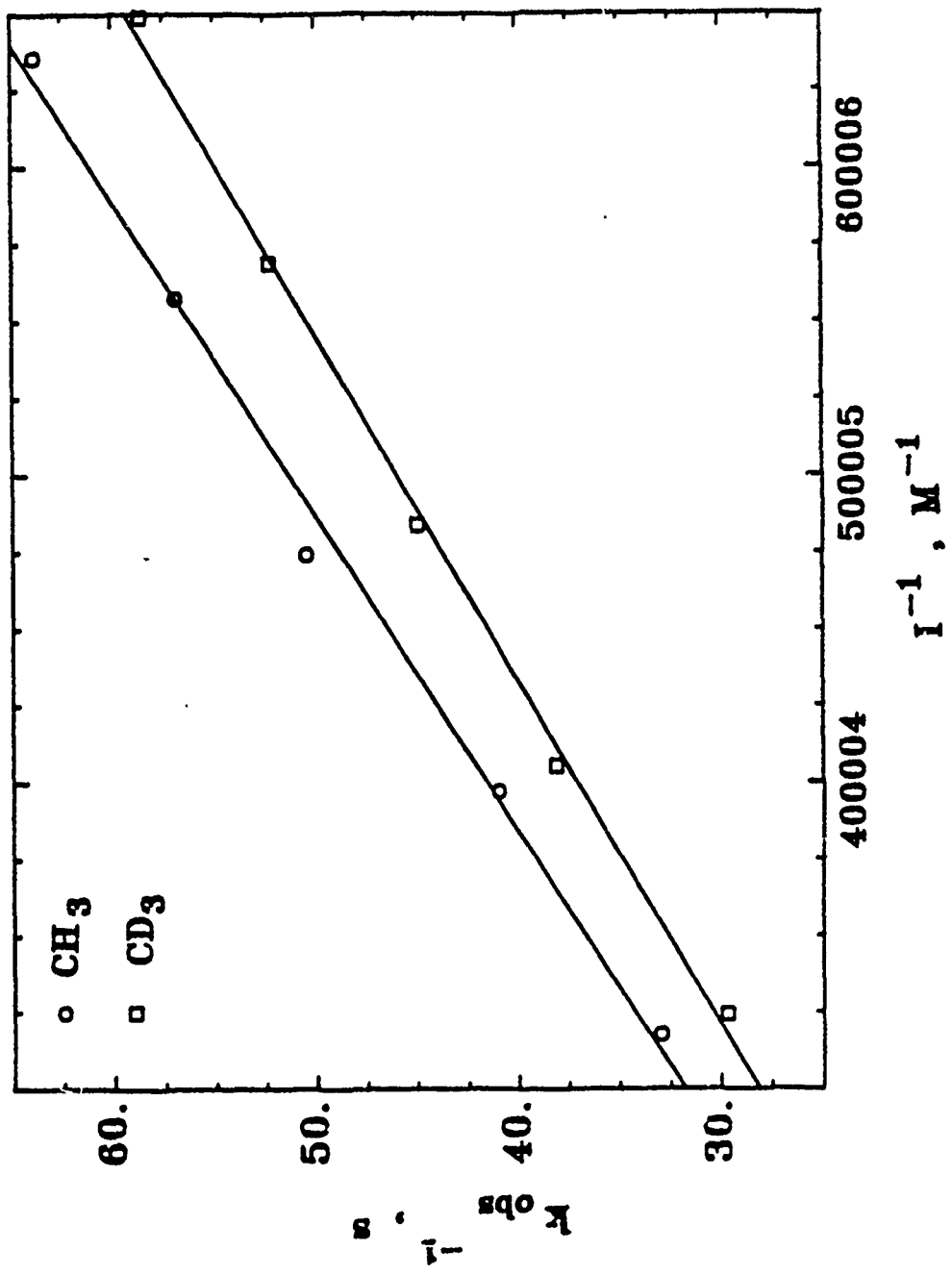


Figure 28. Inactivation of AChE by sarin.

TABLE XX. Second-order Rate Constants for Inactivation of AChE.

Inhibitor	Isotopic Label	(k_i/k_i) light, $M^{-1} S^{-1}$ (SD)	(k_i/K_i) heavy, $M^{-1} S^{-1}$ (SD)	Kinetic Isotope Effect	(SD)
soman	β -CD ₃	1.56 (0.03) x 10 ⁶	1.74 (0.02) x 10 ⁶	0.90	(0.02)
sarin	β -CD ₃	4.61 (0.16) x 10 ⁵	5.03 (0.16) x 10 ⁵	0.91	(0.04)
IMN	solvent D ₂ O	8.13 (0.38) x 10 ³	6.52 (0.10) x 10 ³	1.25	(0.06)
IMN	4-nitrophenol ¹⁸ O	8.07 (0.20) x 10 ³	7.60 (0.23) x 10 ³	1.06	(0.03)

7. Hydrolytic Reactions of 4-Nitrophenyl 2-Propyl Methyl-phosphonate (IMN).

Figure 29 demonstrates the dependence on pH of aqueous hydrolysis of IMN. In the strongly basic solutions in these experiments, hydroxide ion attack predominates, with a second-order rate constant of $14 \text{ M}^{-1} \text{ s}^{-1}$ at 25°C .

Hydrolytic reactions of IMN were also studied in phosphate buffer in the concentration range 0.05-0.2 M, at $\text{K}_2\text{HPO}_4/\text{KH}_2\text{PO}_4$: 6 (pH 7.65) and 1 (pH 7.2) and at temperatures $52\text{-}73^\circ\text{C}$ to facilitate the reaction. The rate law under these conditions includes the following terms:

$$k_{\text{obs}} = k_{\text{H}_2\text{O}}[\text{H}_2\text{O}] + k_{\text{HO}^-}[\text{HO}^-] + k_{\text{HPO}_4^-}[\text{HPO}_4^-] + k_{\text{H}_2\text{PO}_4^-}[\text{H}_2\text{PO}_4^-]$$

At any particular constant ratio of $\text{K}_2\text{HPO}_4:\text{KH}_2\text{PO}_4$, a plot of the dependence of the hydrolysis rate on phosphate concentration yields the terms for water and hydroxide attack as intercepts and the slope equals $k_{\text{HPO}_4^-} (f_b) + k_{\text{H}_2\text{PO}_4^-} (1-f_b)$, where f_b is the fraction of HPO_4^- . The general acid catalysis by H_2PO_4^- of aqueous hydrolysis is negligible. As it is portrayed in Figure 30, the intercept is very small and poorly defined, the values are 4.2 ± 1.5 and $5.4 \pm 0.6 \times 10^{-6} \text{ s}^{-1}$, at 65°C , for f_b 0.5 and 0.86, respectively, which correspond to ~25% specific base hydrolysis and 75% water attack. From the slope of the two lines at f_b 0.50 and 0.86, the catalysis constant $k_{\text{HPO}_4^-} = 1.05 \times 10^{-4} \text{ M}^{-1} \text{ s}^{-1}$ can be calculated. The much smaller rate constant, $k_{\text{H}_2\text{PO}_4^-}$, cannot be evaluated.

The temperature dependence of the rate constants for phosphate-catalyzed hydrolysis of IMN at pH 7.65 is shown in Figure 31. The Eyring plots for first-order hydrolysis rate constants are shown in Figure 32. The activation parameters calculated from the Eyring equation for hydrolysis of IMN at different phosphate concentrations are shown in Table XXI.

8. Solvent Isotope Effects for the Aging and Spontaneous Reactivation of 2-Propyl Methylphosphonyl-AChE

The aging reaction of 2-propyl methylphosphonyl-AChE has been reported to be relatively slow and acid-catalyzed with a pH maximum around 5.³⁸ It is also known to be species-dependent. We began with a preliminary investigation of the pH dependence of this reaction. At pH 7.7 and 25°C , the aging of 2-propyl methylphosphonylated AChE (from the electric eel) took place with a half-life of 13 hours, $k_{\text{obs}} = 8.8 \times 10^{-4} \text{ min}^{-1}$. At lower pH, 4.2-5.3, enzyme instability prevented us from conducting kinetic measurements. The solvent isotope effects were measured at pH 6.4, pD 6.9, and 37°C , where rates were followed conveniently for 8 hours.

We also established that inhibited AChE can be reactivated with either 0.1 or 1 mM solution of tetramethyl benzidine (TMB4) at pH 7.7 in 0.05 M phosphate buffer in 10 minutes at 25°C to 60-70% and at 37°C to 70-80% of the AChE activity. This 20-40% loss of enzyme activity has been measured with controls and appears to stem from an inhibition of AChE activity toward substrates such as acetylthiocholine (ACTCh), which is used in the Ellman assay. The hydrolysis of ACTCh is also catalyzed by the oxime, TMB4, which requires a slight correction (2-5% of the rate) when a 0.1 mM concentration is used in the assay mixture.

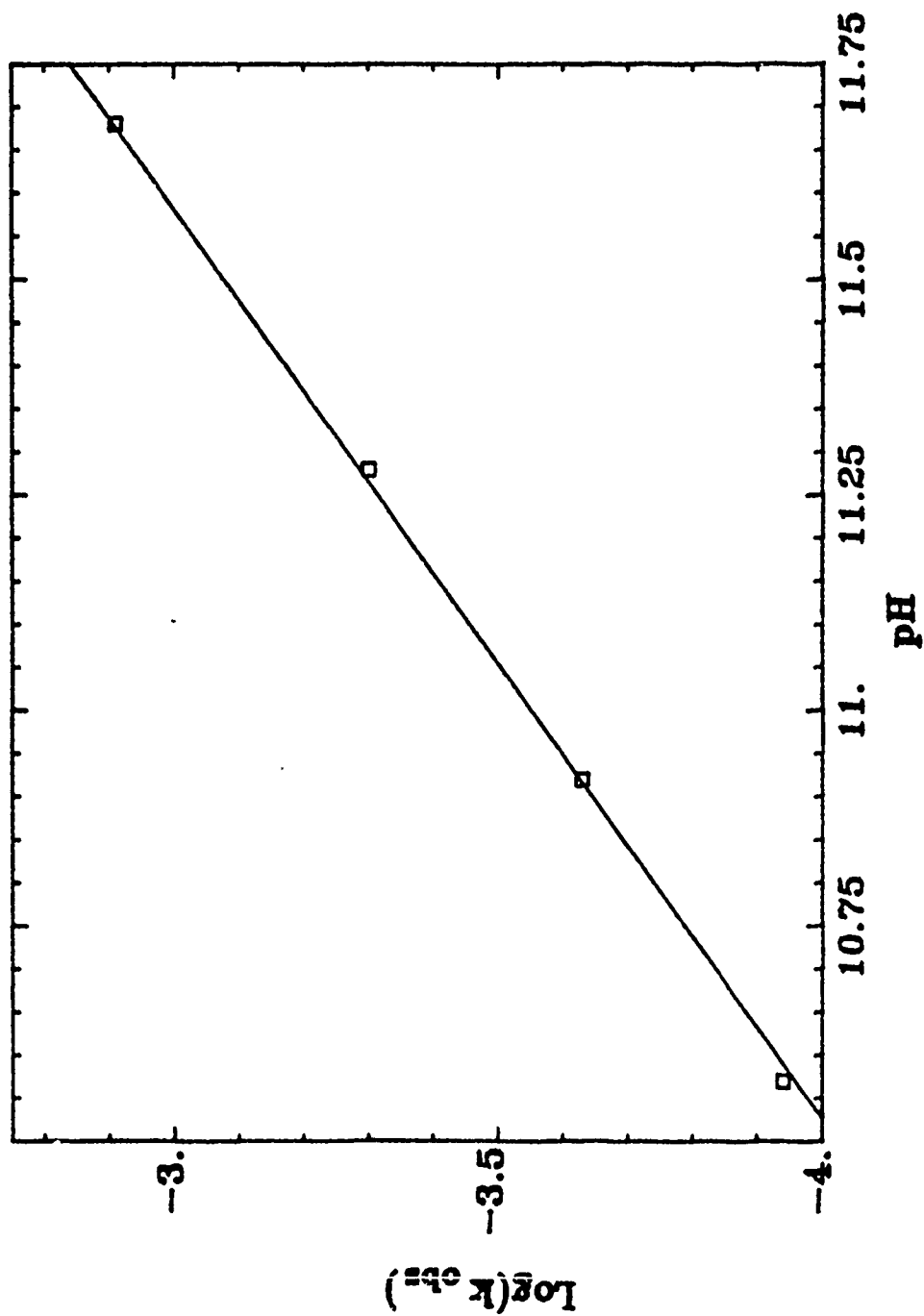


Figure 29. pH dependence of the aqueous hydrolysis of IMN.

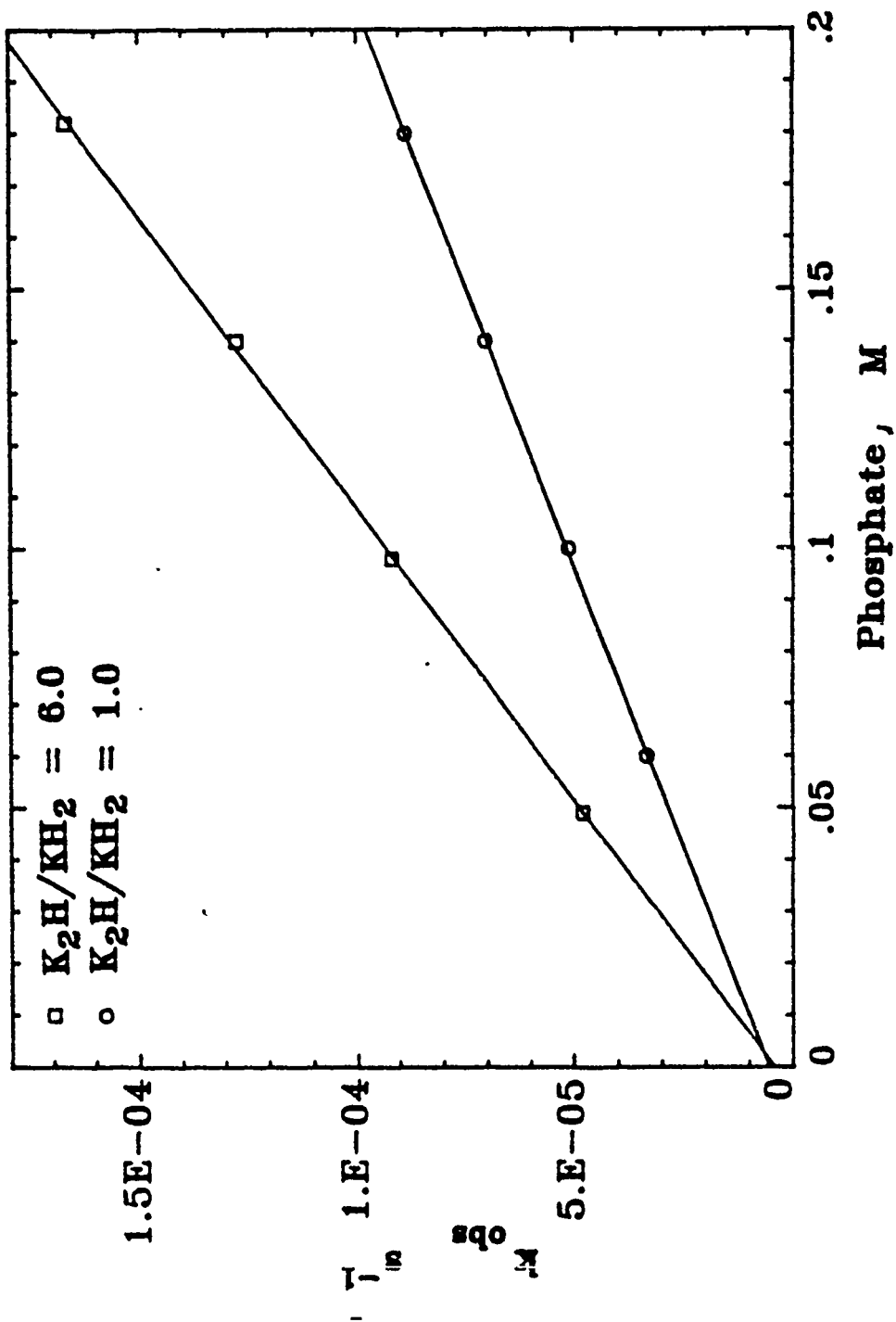


Figure 30. Phosphate-catalyzed hydrolysis of IMN.

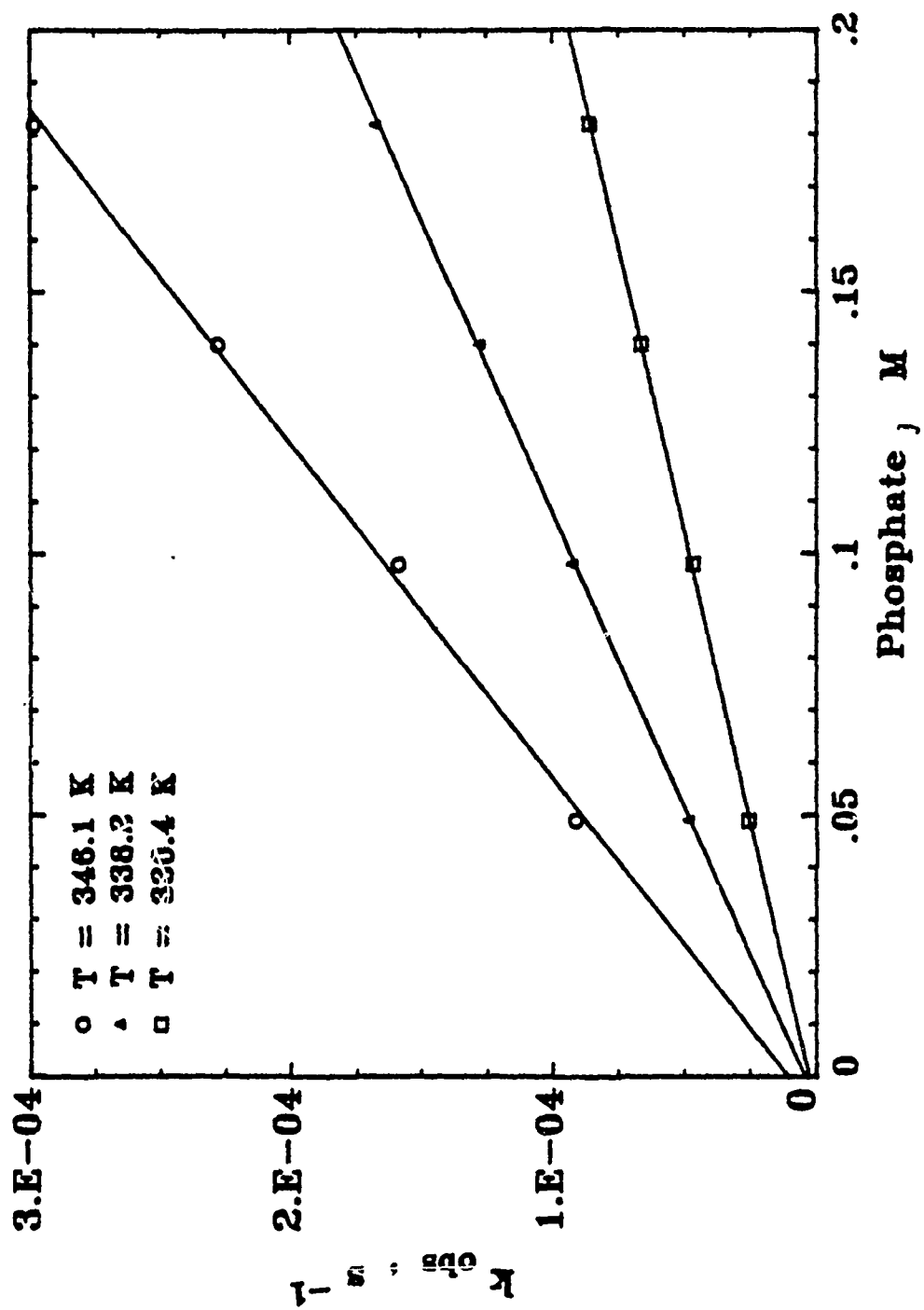


Figure 31. Phosphate-catalyzed hydrolysis of IMN at three temperatures.

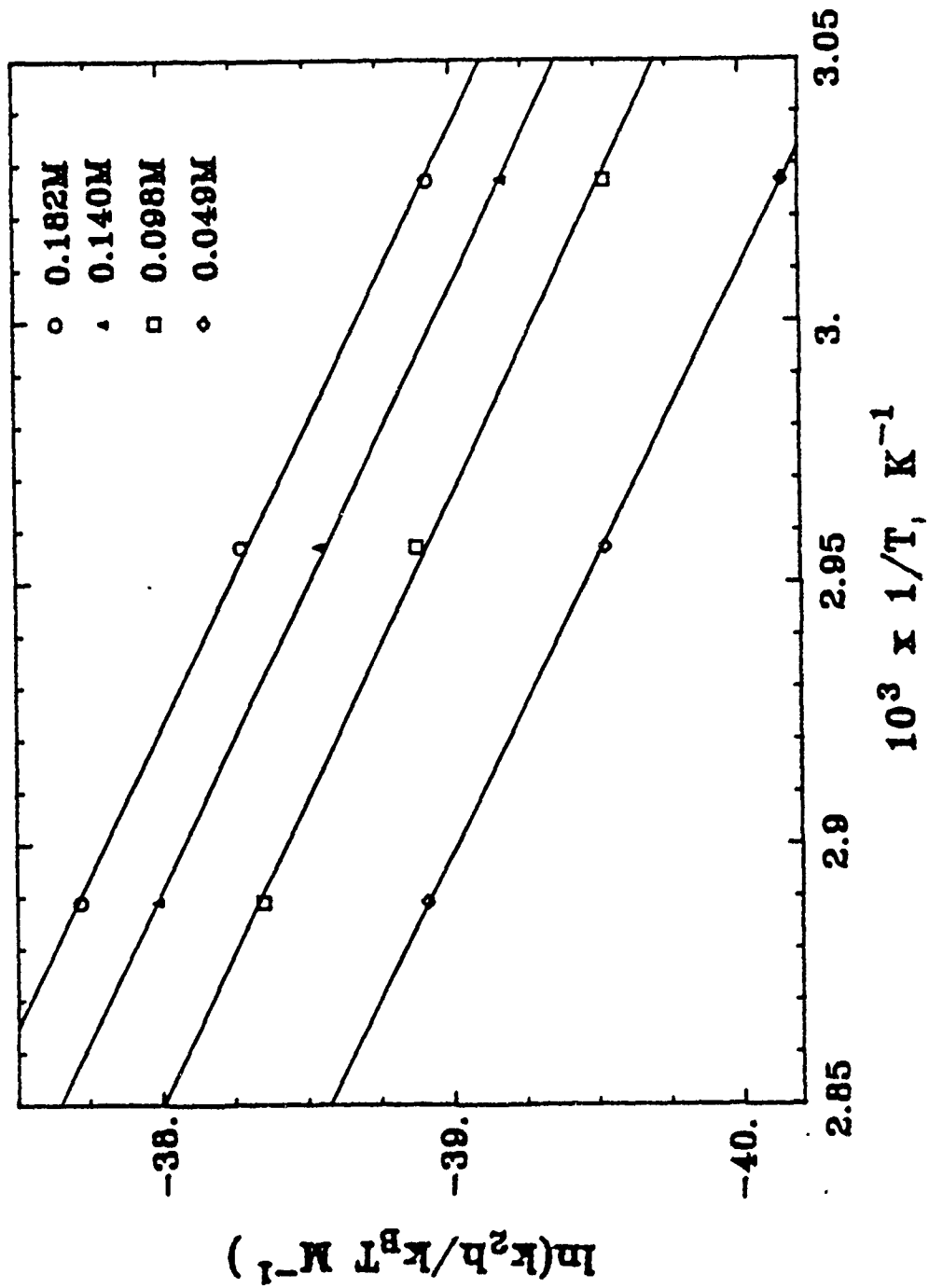


Figure 32. Eyring plots for the phosphate-catalyzed hydrolysis of IMN.

TABLE XXI. Activation Parameters for Nonenzymic Hydrolysis of IMN.

Phosphate conc, M	ΔH^\ddagger , Kcal mol ⁻¹ (SD)	ΔS^\ddagger , e u (SD)
0.182	17.35 (0.52)	-24.8 (1.6)
0.140	17.17 (0.41)	-25.9 (1.2)
0.098	17.01 (0.90)	-27.0 (2.7)
0.049	17.82 (0.25)	-25.8 (0.7)

2-Propyl methylphosphonochloridate has been used initially for inhibition; however, some slow inhibitor or its hydrolysis product contaminating the compound, obtained from commercial source. This contaminant apparently prevented reactivation to any measurable extent in our experience. The much purer isosteric phosphonohalide, sarin, has given good results in the protocol described in the Experimental Procedures.

Figure 33 shows the time course of AChE activity for spontaneous reactivation and reactivation by TMB⁴, and for their difference in water and in heavy water. AChE activities are indicated in units of OD/min (ACTCh hydrolyzed). Figure 34 gives the semilog plot of the aging reactions in H₂O and in D₂O. Figure 35 gives the data for aging of the H₆ and D₆ isopropyl compounds. The slopes of the lines for aging in water and in heavy water and for the AChE adduct containing D₆ in the methyl groups of the isopropyl moiety give the first order rate constants listed in Table XXII, which also contains the values of the solvent and β-secondary deuterium isotope effects.

9. ¹⁸O-Exchange in the Aging of Soman-inhibited AChE from the Electric Eel

AChE (1 nmole, 1,000 units) was inhibited with 20 nmol soman in 0.11 ml pH 7.65, 0.05 M phosphate buffer 45% in H₂¹⁸O. The solution was incubated at 25°C for 30 minutes to allow the aging reaction to be completed. The pH was then raised to 10.00 by the addition of 0.1 M TAPS buffer, which brought the volume to 1 ml. Excess soman was thus destroyed rapidly. The dimethyl-2-butanol product, which is reported to be 40% of all products of aging,³¹ was then extracted with CH₂Cl₂, dried and concentrated. A 1 μl sample of the solution was used for separation by gas chromatography (GC) on a DB5 column and the eluent was introduced into the mass spectrometer. Incorporation of ¹⁸O was monitored in the (CH₃)₂COH fragment by measuring the 59:61 ratio. Figure 36 shows a mass fragmentogram. A 42±3% ¹⁸O content can be calculated from the mass-spectral results, which compares well with the 45% ¹⁸O content of the reaction mixture for aging.

10. Solvent Isotope Effect for the Nucleophilic Reactivation of AChE Inhibited by Sarin

Figure 37 gives the time course of reactivation in H₂O and in D₂O in the presence of 8.3 x 10⁻³ M pralidoxime chloride (2-PAM). Enzyme activities are plotted in units of OD/min ACTCh hydrolyzed. The rate constants, calculated from the nonlinear least-squares fit of the data to the first-order rate law, are listed in Table XXIII.

A similar procedure to what has been used in the aging studies has also been used for studies of reactivation and is detailed in the Experimental Procedures. Figure 38 shows the time-course of reactivation in H₂O and D₂O in 5.7 x 10⁻⁴ M TMB⁴. Enzyme activities are plotted in units of OD/min ACTCh hydrolyzed. The kinetic profile is not of a simple pseudo first-order reaction giving a constant infinity point. Instead, it has the characteristics of a quick equilibrium followed by a slower reaction, i.e., a shifting equilibrium. The tangent drawn to the semilog plot of the last points of the reaction in D₂O gives infinity values (A_i) for each time coordinate where an enzyme activity measurement was taken (A_t). Therefore, (A_i-A_t) gives the difference in enzyme activity between the equilibrium

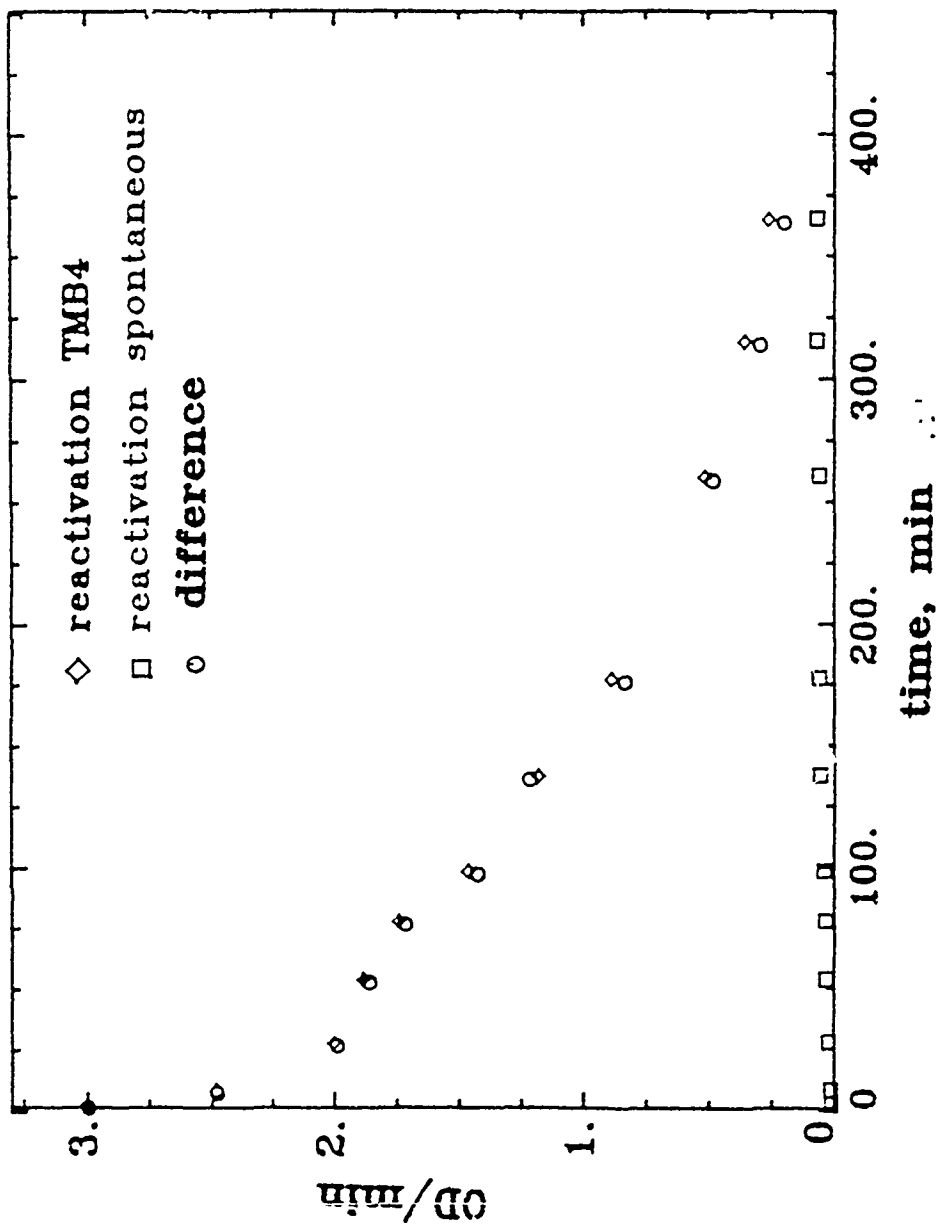


Figure 33. Reactivation and aging of 2-propyl methylphosphonyl-AChE.

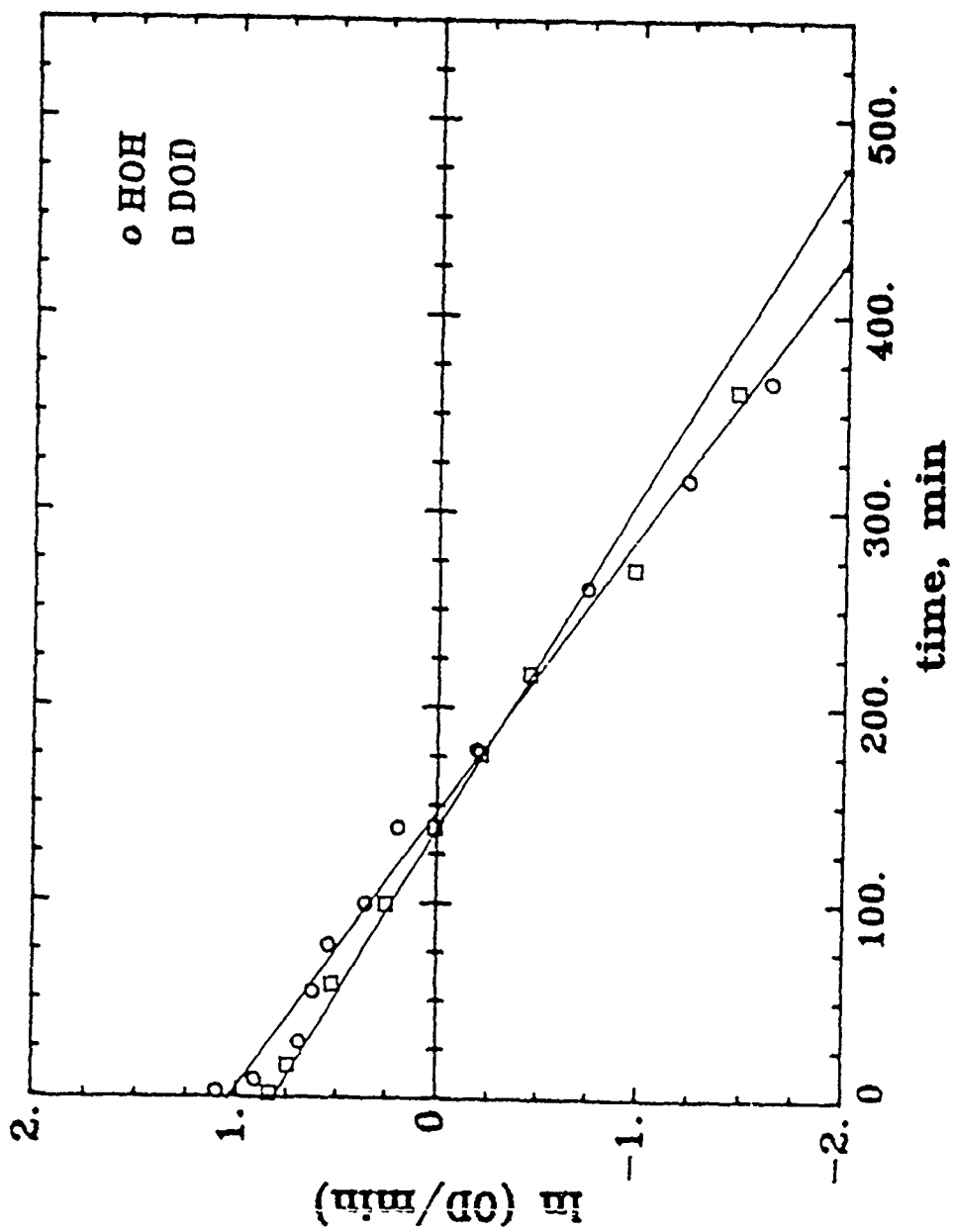


Figure 34. Aging of 2-propyl methylphosphonyl-AChE.

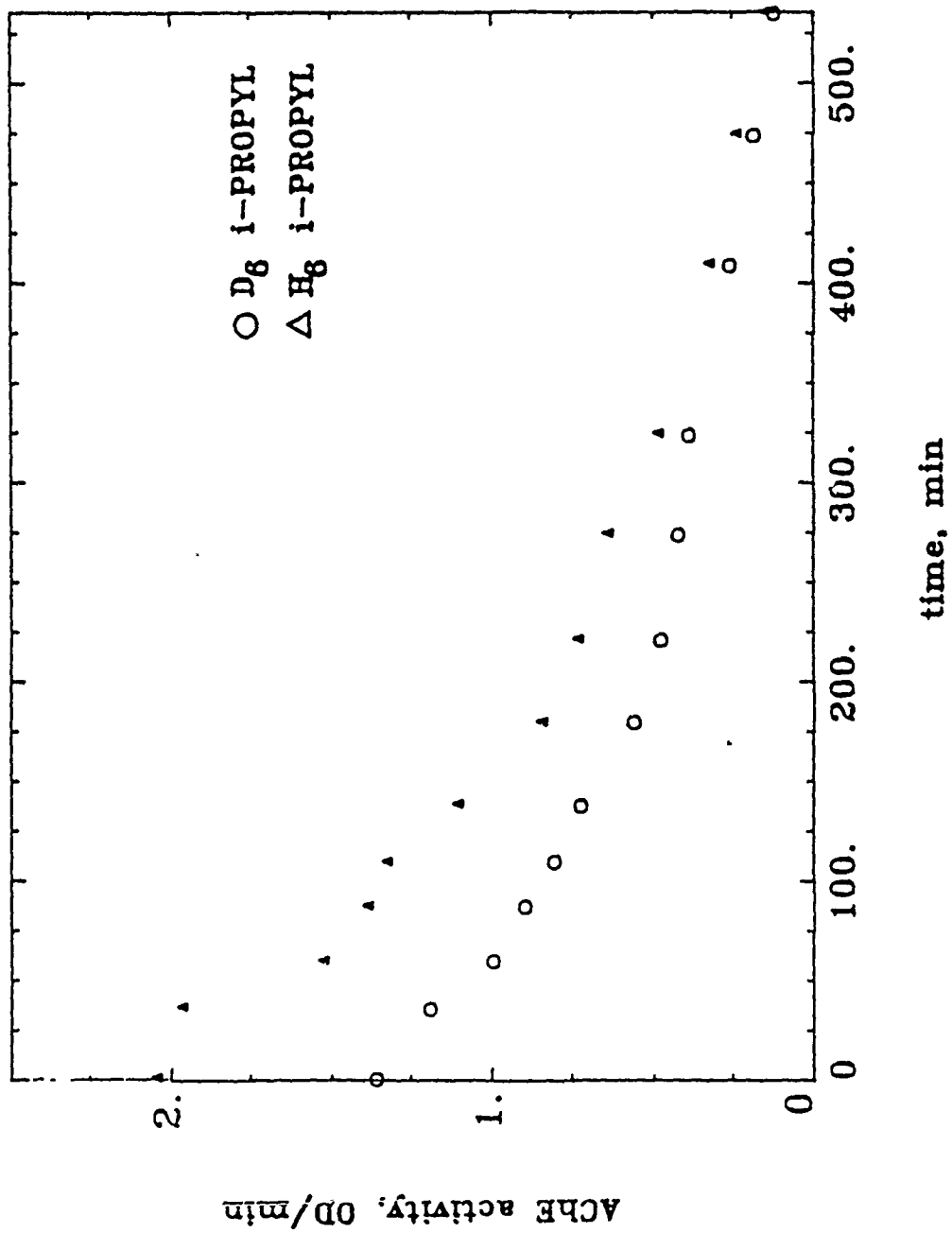


Figure 35. Aging of L₆-2-propyl methylphosphonyl-AChE.

TABLE XXII. First-Order Rate Constants and Isotope Effects for the Aging of L₆-2-Propyl Methylphosphonyl-AChE (Electric Eel, L=H,D) in pH 6.43 (pD 6.93), 0.13 M Phosphate Buffer

Isotopomer	Solvent	Temp, °C	$10^3 k_a$ (SD), m^{-1}	Isotope Effect (SD)
H ₆	HOH	37.5	7.0 (0.2)	
D ₆	DOD	37.5	5.8 (0.2)	1.20 (0.06)
H ₆	HOH	37.3	5.0 (0.4)	
D ₆	HOH	37.3	4.7 (0.6)	1.08 (0.16)

TABLE XXIII. Pseudo-First-Order Rate Constants and Solvent Isotope Effects for the Reactivation of 2-Propyl Methylphosphonyl-AChE (Electric Eel) by Oximes in pH 7.60 (pD 8.10), 0.05 M Phosphate Buffer at 25°C.

Oxime 10^5	[Oxime], M	$10^3 k_{HOH}$ (SD), m^{-1}	$10^3 k_{DOD}$ (SD), m^{-1}	k_{HOH}/k_{DOD} (SD)
2-PAM	8.33	45.6 (4.3)	43.1 (5.2)	1.06 (0.15)
2-PAM	16.7	78.0 (9.3)	78.1 (8.4)	1.00 (0.16)
2-PAM	33.3	148 (16)	---	---
TMB4	5.7	8.19 (0.14)	5.12 (0.19)	1.60 (0.06)

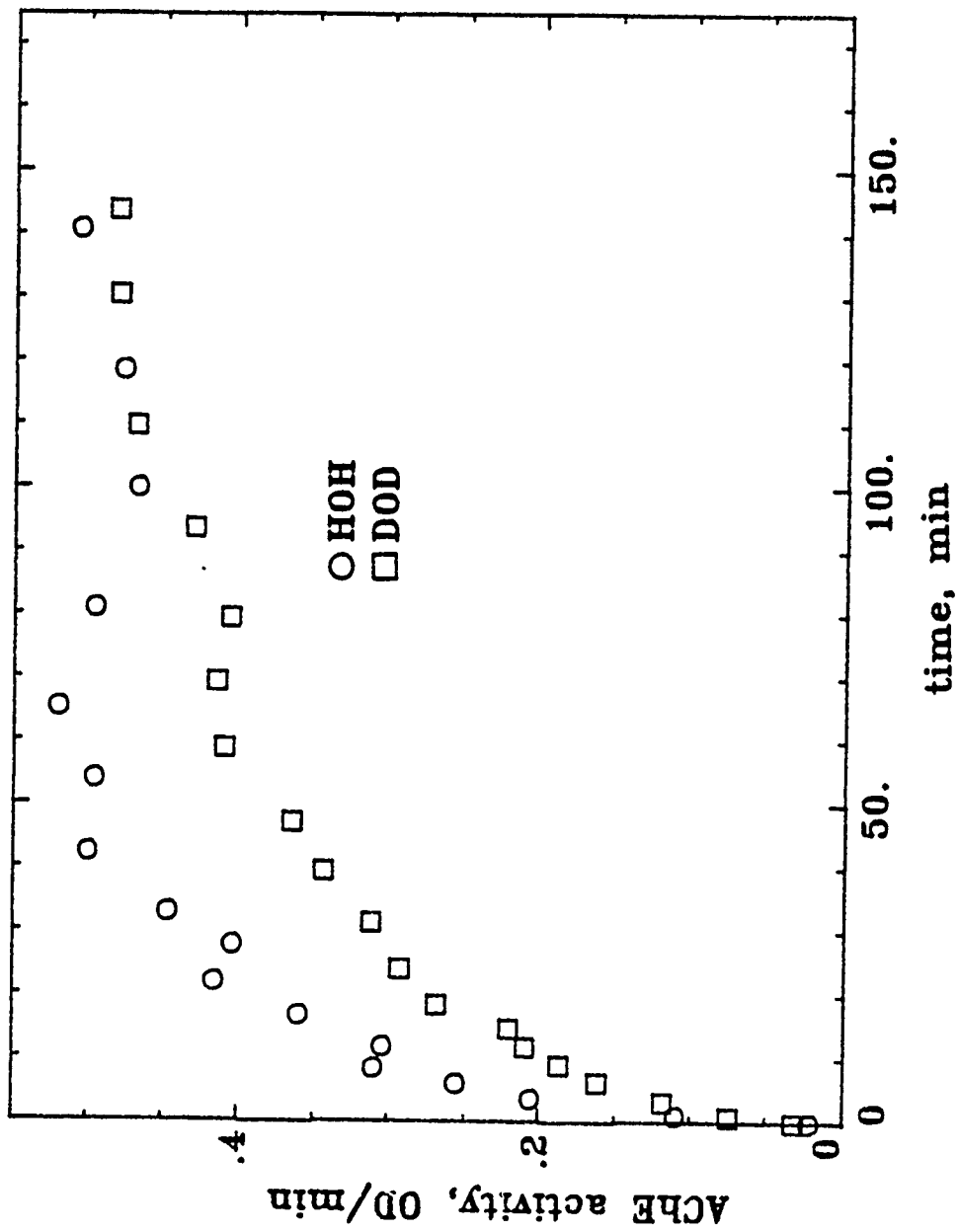


Figure 37. Reactivation of 2-propyl methylphosphonyl-AChE with 2-PAM.

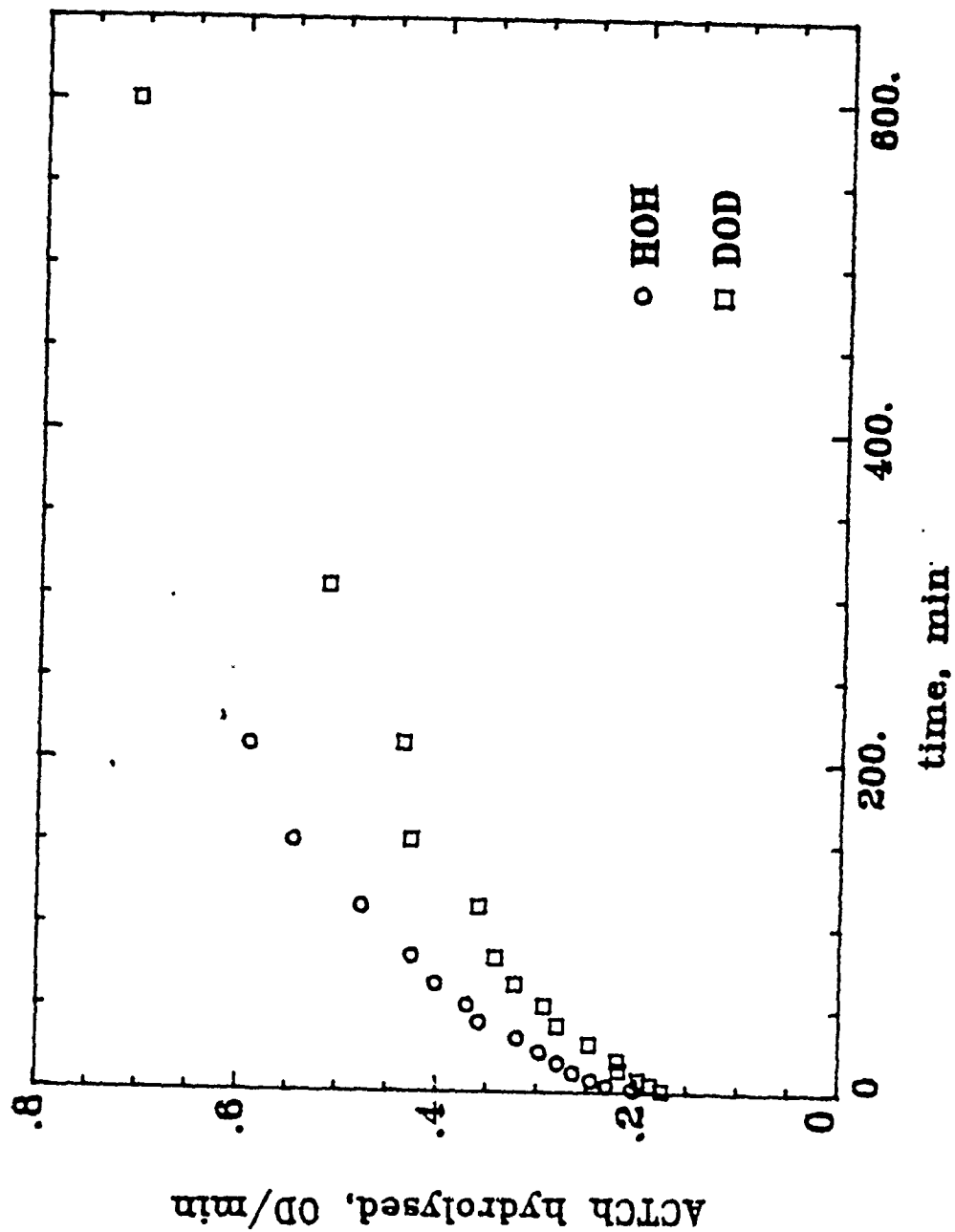


Figure 38. AChE activity recovered by TMB4 after inhibition by sarin.

value at infinity and the corresponding value at time t . Figure 39 shows the semilog plot of $(A_i - A_t)$ as a function of time, which abides by a first-order form, and the slopes give the rate constants. The rate constants and isotope effects from these data appear in Table XXIII.

11. Chemical Model Reactions for Aging

Structural analogs of sarin (R = isopropyl) and soman (R = pinacolyl) were subjected to methoxide attack in methanol or acetonitrile and the appearance of their low molecular weight products was monitored by gas-liquid chromatography (GLC). As shown in scheme I, production of an alcohol would entail P-O bond cleavage, whereas C-O bond cleavage should result in the formation of the methyl ester of the leaving alcohol. These compounds were used here as models of the serine phosphorylated enzymes. The nonenzymic basic decomposition mode of models were looked at for comparison to the enzymic reaction.

I. Isopropyl methyl methylphosphonate (IMPP) was prepared in situ from isopropyl methylphosphonochloridate in methanol with sodium methoxide. The sodium chloride byproduct was filtered out and the ~0.3 M methanolic solution of IMPP with two equivalents of sodium methoxide was sampled on a Porapak Q column. No evidence of any reaction was obtained after a day. The reaction volume was then reduced to half and two more equivalents of sodium methoxide was added with 0.1 mol 1,4,7,10,13,16-hexaoxacyclooctane (18-crown-6) to facilitate the dissolution of sodium methoxide. The appearance of a peak was followed through 50 hours; the mixture was then heated to 40°C and refluxed for 72 hours until no more increase in the isopropanol peak intensity was discernible. Addition of ~1.5 mol 18-crown-6 brought about the dissolution of all sodium methoxide and the clear solution was further kept at 40°C for several hours. This did not change the peak intensity, nor did it bring out any other peaks. The retention time of the product was identical with that of isopropanol and spiking with isopropanol resulted in complete overlap with the product peak. An isopropyl methyl ether standard for GLC was also prepared from sodium isopropionate in excess isopropanol and methyl iodide. The retention time of this compound was distinctly different from that of the product of the methoxide displacement reaction. These ethers seemed to be resistant to basic hydrolysis.

II. EPPP (1 mmol) and 0.5 mmol 18-crown-6 were dissolved in dry acetonitrile and an aliquot was drawn and injected to a free fatty acid phase (FFAP) column. Sodium methoxide (1 mmol) was added and the mixture was stirred for 3 days with intermittent sampling. Another 0.5 mmol 18-crown-6 was also added after 5 hours, but no reaction could be detected in 2 days. Then the mixture was heated in a bomb to 50°C for 1 day, which resulted in the production of pinacolyl alcohol. Identification of the product was based on matching the peaks of the product and of pinacolyl alcohol and on spiking the product with pinacolyl alcohol before analysis. A pinacolyl methyl ether standard has also been made as described for the isopropyl-methyl ether. The retention time of the methyl ether was significantly different from that of the product or of pinacolyl alcohol.

III. Another structural analogue dipinacolyl propylphosphonate of soman was subjected to methoxide attack in methanol and the low molecular weight products of the reaction were monitored by GLC.

Dipinacolyl propylphosphonate, 1 mmol; (18-crown-6), 1 mmol; and sodium methoxide, 1 mmol, were dissolved in dry acetonitrile and refluxed at 40°C for several hours, which resulted in the production of pinacolyl alcohol. The reaction was monitored by the injection of aliquots into an FFAP column. Identification of the product is based on peak-matching with pinacolyl alcohol and on spiking with pinacolyl alcohol. Pinacolyl methyl ether has also been synthesized, and the retention time of this species was found to be markedly different from that of the product.

12. Molecular Graphics Modeling of the Interactions of OP Agents with Serine Proteases

Figure 40 shows the plotted computer-screen image of the x-ray crystallographic topography of the catalytic triad and the binding site of the DFP-inhibited trypsin as retrieved from the Brookhaven data base.

The interaction of the 4-nitrophenyl and propyl groups with the trypsin active site on inhibition of trypsin with NPN has been modeled for both optical isomers, i.e., P(R) and P(S), on the serine-phosphonylated adduct. The oxygen on phosphorus was oriented toward the oxyanion hole and the two other ligands were rotated to optimal distances from the active site protein residues. As Figure 41 shows, the specificity pocket is large enough to accommodate either orientation of the 4-nitrophenyl group.

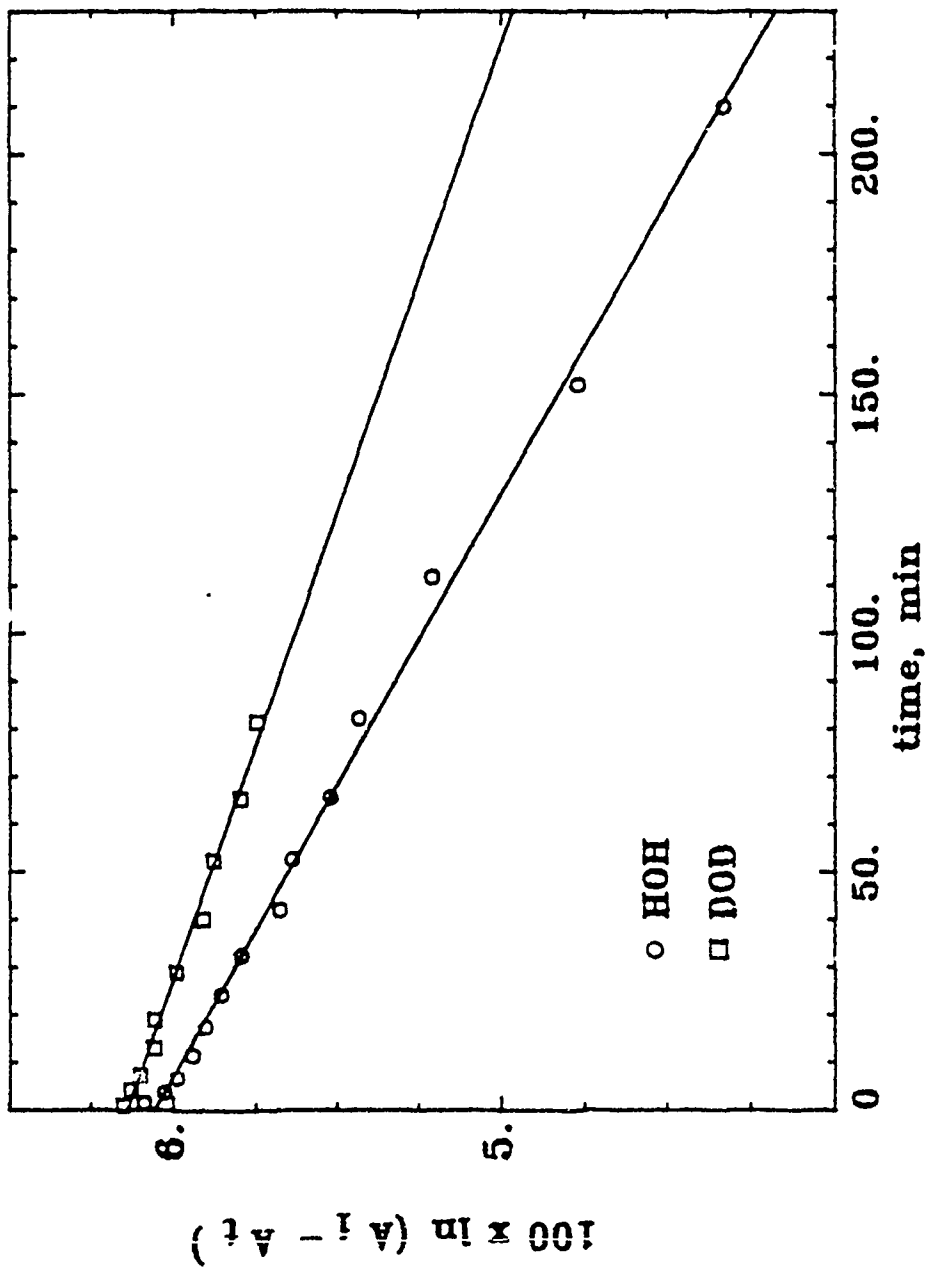


Figure 39. Evaluation of the first-order rate constants for reactivation from data in Figure 38.

Legend: The active site His 57 for the uninhibited and inhibited x-ray structures are superimposed.

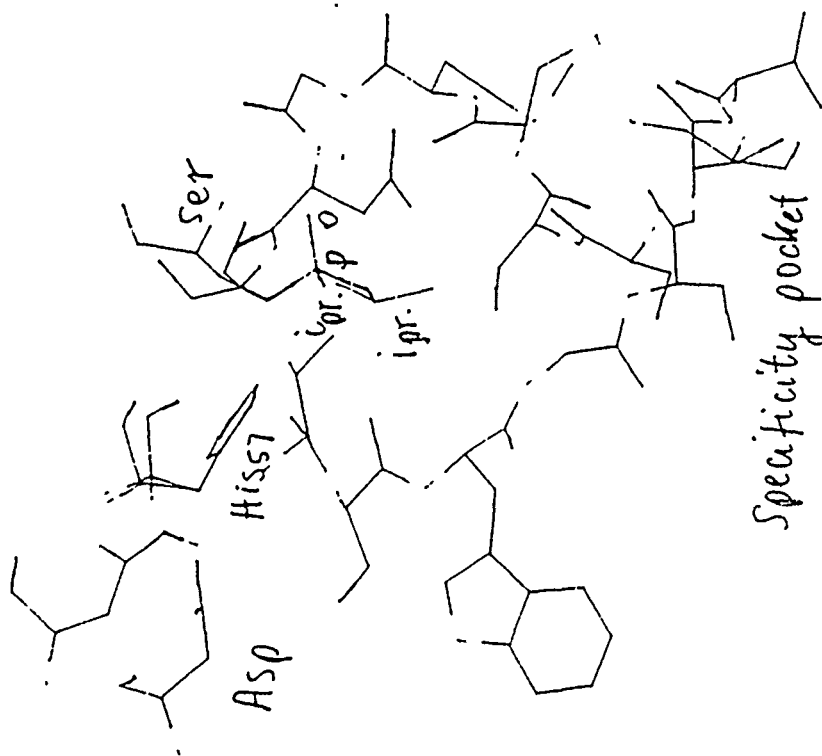
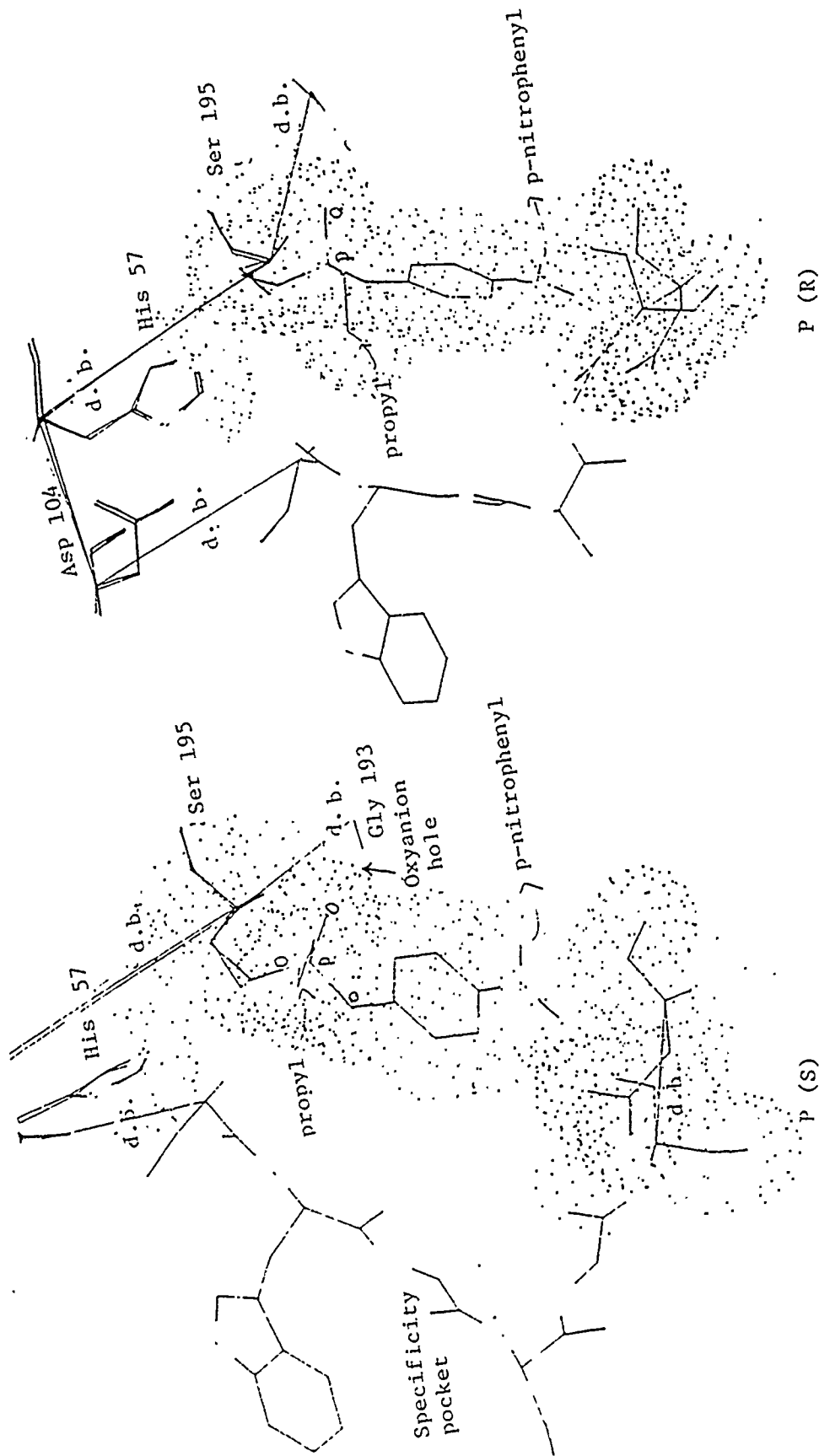


Figure 40. DFP-inhibited trypsin active site and specificity pocket.



Legend: The active site Asp 104, His 57, and Ser 195 residues for the inhibited and uninhibited trypsin x-ray structures are superimposed. d.b. = dummy bonds to tie together fragments.

Figure 41. 4-Nitrophenyl trypsin O-serinyl propylphosphonate.

E. Discussion

1. Rates, Solvent Isotope Effects and Proton Inventories for AChE Inhibition by OPs

In the concentration range of the inhibitors in this investigation, saturation of AChE by any of the inhibitors has not been detectable; therefore, deductions can be made only about the nature of the bimolecular combination of AChE with the appropriate agent.

The rate accelerations observed for the OP inhibition of AChE in pH 7.7, 0.0 5M phosphate buffer are of the order of 10^{11} times faster than the corresponding general base-catalyzed hydrolyses for all three inhibitors. Enzymic acceleration of the hydrolysis of acetylcholine, the natural substrate, is 10^{18} by AChE.¹⁸ Thus these OP compounds seem to mobilize 60% of the catalytic power of AChE. The second-order rate constants for the inhibition of AChE by the inhibitors are given in Table I and II. The differences in potency can be related to the electronic characteristics of the leaving groups and beyond to the capacity of the other ligands for proper steric and hydrophobic interactions with the enzyme.

The reactivity of AChE with three reagents is remarkably different. The rate constant for soman in Table I is larger than what has been reported³⁹ and it is 3,000 and 200,000 times larger than those of MPN and NPN, respectively. Soman is 10^4 more reactive toward the nucleophile of AChE than toward hydroxide ion ($k_{OH} \sim 20$).⁴⁰ An approximate value of $K_a = 5-8 \times 10^{-7}$ M and an estimate for the phosphorylation rate of $k_2 = 0.57^{26}$ have clearly shown that the predominant factor in catalysis is the high affinity of soman for AChE. MPN reacts with AChE at comparable velocity to that of paraoxon³⁹ and 3 times faster than diisopropyl-fluorophosphate (DFP). This might partially reflect the similar length of the n-propyl group in MPN to those of the ethoxy and isopropoxy groups in paraoxon and DFP, respectively, for hydrophobic attachment to the AChE transition state. The other opposing factors may cancel out as follows: the methoxy substituent may not provide as much transition state stabilization as the other substituents, but MPN is a phosphonate with greater electrophilic character of the phosphorus than is present in an analogous phosphate. The second-order rate constant for MPN with hydroxide ion is $0.210 + 0.001 \text{ M}^{-1} \text{ s}^{-1}$, relative to which AChE enhances its reaction with MPN by 1,770 fold. Replacement of the methoxy group of MPN by a bulky p-nitrophenoxy moiety, as in NPN, creates a surprisingly poor inhibitor of AChE. The inductive effect accompanying this change would be expected in the opposite direction, making MPN less reactive, as is seen in their hydrolysis rates. The second-order rate constant for NPN with AChE is almost the same as with hydroxide ion (an approximate value is $3 \text{ M}^{-1} \text{ s}^{-1}$). This organophosphonate presumably is sterically unfit to use most or all of the catalytic capability of AChE.

Solvent isotope effects on all inhibition reactions of AChE are smaller than typical values of one proton transfer in general acid-base catalysis (2.5).²¹ Such small effects are frequently observable when acid-base catalysis is only partially rate-determining or when a generalized solvation, i.e., the transfer of protons from many solvent molecules at the transition state, is in effect. In the latter case, an exponential dependence of k^n/k^0 on n ($[\text{DOD}]/([\text{HOH}] + [\text{DOD}])$), otherwise, small solvent

isotope effects can also result from complex mechanisms such as with enzymes, when more than one rate-determining step occurs along the reaction path. If one of these steps does not involve protonic reorganization while the other does, then the weighted average of the two (or more) will give a reduced effect. Physical steps such as induced-fit conformational changes have been known to involve high energy barriers comparable to transition states for covalent or protonic reorganizations. A rate-limiting diffusion of substrate to active site precedes the reactions of AChE with its natural substrate, whereas the acid-base catalytic steps presumably are so fast that they are not revealed in a solvent isotope effect (1.0).^{8,9} A small solvent isotope effect of 1.41 was measured with PA, another good substrate, because an isotopically insensitive rate-determining induced-fit conformational change dominates acylation.^{8,9,36} It is likely that the induced-fit conformational change is also partially rate-limiting in the inhibition of AChE.

The rate of phosphorylation by soman is similar to these acylation rates ($k_2 = 1.6 \times 10^8 \text{ M}^{-1} \text{ s}^{-1}$ for acetylcholine and $1.76 \times 10^7 \text{ M}^{-1} \text{ s}^{-1}$ for PA) and also to the magnitude of the solvent isotope effects.⁸ The rate data at the midpoint, $n = 0.5$, gives $k^{0.5}/k^0 = 0.78 \pm 0.08$ (1/1.28). With the use of $k^n/k^0 = \phi_T^{2n} = 0.71$, from eq. 1b, one calculates $\phi_T^2 = 0.85$ and $k^{0.5}/k^0 = (1-0.5+0.5 \times 0.71)^2 = 0.85 \pm 0.08$. The exponential and linear models predict $k^{0.5}/k^0 = 0.84$ and 0.86 , respectively. Consequently, it is difficult to distinguish between the three models in a case like this when the solvent isotope effect is so small. The transferring proton at the catalytic transition state most likely is from the serine hydroxyl to the histidine residue. As described below, the participation of a single-proton transfer in catalysis, supposedly by the imidazole residue, of the deacetylation of acetyl-AChE was observed. The enzymatic results can be compared with a solvent kinetic isotope effect of 2.3 for the general base-catalyzed hydrolysis of a bis-(4-nitrophenyl) phosphonate by imidazole, which shows that the base-catalyzed attack of water is rate-determining.⁴¹

Rates of inhibition of the erythrocyte AChE by both soman and 4-nitrophenyl methoxy n-propylphosphonate (MPN) are ~6 times slower than those of the eel AChE. The solvent isotope effects, however, are very similar around 1.5 and, as judged from one measurement at $n = 0.5$, they probably are linear. Our previous observation with the eel enzyme¹ on the dependence of the partial isotope effect on deuterium content in the buffer was inconclusive with soman and clearly linear with MPN. The difficulty involved in the distinction between quadratic and linear dependence might be understandable if the very small value of the partial isotope effect is considered. The distinction to be made is approximately between 1.2 and 1.18, for which precision much greater than that obtainable by the competitive method is needed. Thus the mechanism of phosphorylation of the eel AChE and erythrocyte AChE is a partially rate-limiting protolytic catalysis, most likely by one proton.

The temperature dependence of the eel AChE is similar in HOH and DOD, i.e., the solvent isotope effect is not sensitive to the temperature gradient between 5° and 45°C. The activation enthalpy is the same within experimental error in H₂O and D₂O and the solvent isotope effect seems to stem from the difference in entropy. Thus, contrary to common expectation, the origin of the solvent isotope effect could be something else than the change in zero point energies during reaction. It could be solvent

reorganization that is isotope-sensitive. Proton tunneling has been found to cause similar isotopic discrimination that is manifested in differences in activation entropy of some reactions of proteases⁴². Because of the very small differences in rate between water and heavy water, the enthalpies and entropies are very similar and the inference about the greater difference in entropy than in enthalpy remains vague.

Activation Parameters. This information provides further aid in unraveling the character of the transition states for the hydrolytic decomposition of OP compounds in enzymic and nonenzymic reactions. Inactivation of AChE by soman and 4-nitrophenyl diethyl phosphate (paraoxon) involves $\Delta H^* \sim 7-10$ kcal/mol and $\Delta S^* -6-3$ eu, as reported by us³⁵ and Aldridge,⁴³ respectively. For the phosphate-catalyzed hydrolysis of IMN, we measured $\Delta H^* 17.2$ kcal/mol and $\Delta S^* -18$ eu; and for paraoxon, Aldridge⁴³ reported $\Delta H^* 18.5$ kcal/mol and $\Delta S^* -25.8$ eu. Enzymic catalysis is manifest in more favorable values for both enthalpy and entropy. The entropy in the enzymic case is small and negative, supposedly because of a much more loose structure of the transition state than in regular bimolecular reactions.

2. Kinetic Isotope Effect Probes for the Inactivation of AChE^{37,44}

Precise measurements of these effects became possible through the development of sensitive analytical techniques for the determination of intact inhibitor used in the actual kinetic experiments. The most satisfactory results for the analytical concentrations of soman and sarin are obtained by the spectrofluorimetric technique for the difference in active site concentrations between native and inhibited chymotrypsin.

The heavy atom, ¹⁸O isotope effect is 1.06 ± 0.3 and the secondary deuterium effects are 0.90 ± 0.04 , both indicative of extensive bond-breaking processes occurring at the phosphorus atom in the transition state for the inactivation of AChE.

The kinetic solvent isotope effects for the inhibition of AChE measured so far all lie in the range 1.3-1.5, which suggests that general base catalysis by the imidazole of the histidine residue at the active-site is partially rate determining. These effects, together with the heavy atom and secondary deuterium kinetic isotope effects, are supportive of the proposition that extensive bond breaking and bond making take place at the phosphorus atom in the transition state. They also suggest that steps preceding covalent rearrangement are probably not rate-limiting, as in the case of acylation of AChE.

In conclusion, results from both isotope effect probes and activation parameters support a mechanism of phosphorylation, for the inhibitors investigated here, in which imidazole-catalyzed attack by the active site serine residue and breakage of the bond to the leaving group either occur at the same transition state or have transition states with energy barriers of similar magnitude.

3. Acetylation and Deacetylation of AChE by Phenyl Acetate

The proton inventories for some substrate reactions were studied for comparison with the results obtained with the inhibitors. A meaningful

interpretation of the inhibition data requires the knowledge of the behavior of typical substrates with the same probes.

The proton inventory data give the appearance of linearity and thus of one-site catalysis throughout. This is substantiated by statistical treatment. None of the plots can support a second-order term in n at a confidence level above 90%.

For the V/K effects, which are around 1.5, it might well be true that contributions from other sites are concealed in the noise of the fit. Thus one cannot exclude strongly multi-site contributions to these isotope effects.

The V effects are more easily interpreted, especially that for the eel enzyme. The straightforward interpretation is that one protonic site and one site only is involved in catalysis. The real test as to whether the data can, on the other hand, accommodate a second-site contribution to the isotope effect is to obtain a best-fit set of parameters (fractionation factors) to the two-site form of eq. 1:

$$k_n/k_0 = (1 - n + n\phi_1)(1 - n + n\phi_2). \quad b$$

When this expression was used to fit the data for the electric-eel enzyme, the values obtained for the parameters were: $\phi_1 = 1.03 \pm 0.04$; $\phi_2 = 0.40 \pm 0.02$. Since one of these values is unity, the isotope effect is in fact, even on a two-site model, arising from a single site. A similar fit for the erythrocyte-enzyme data yields values of 0.87 ± 0.15 , and 0.50 ± 0.10 . Again, one factor is within experimental error of unity and the effect comes essentially wholly from the other site. The data thus indicate no concealment of a second-site contribution within the noise of the observed linear dependence. Rather, they favor one-site catalysis.

It is known from the work of Froede and Wilson⁴⁵ that k_{cat} for the electric-eel enzyme is not wholly determined by one step, but rather that acylation and deacylation contribute, with the weighting factors being 0.26 for acylation and 0.74 for deacylation (thus deacylation is "74% rate-limiting"). When using these weighting factors and the assumption of more than one proton catalysis in the deacetylation step, a curvature is generated that is inconsistent with the experimental result. If, however, one uses the solvent isotope effects for V/K and V along with the weighting factors for a one-proton catalysis in each step, the agreement between calculated and experimental points is excellent⁴⁵. Deacylation thus appears to involve one-site catalysis.

4. Inhibition of Serine Proteases³²

Kinetics and Stoichiometry. In our kinetic studies of the inactivation of these four serine proteases by soman, bis-4-nitrophenyl n-propylphosphonate (NPN), and MPN, no departure from second-order kinetics was observed. Up to the highest concentrations employed by us (around 10 μ M), there was therefore no sign of saturation through the formation of enzyme-reagent complexes. Although these complexes probably form, their dissociation constants apparently exceed about 100 μ M.

Both NPN and MPN liberated 1 mol of p-nitrophenol per mol of enzyme-

active sites upon inactivation of the enzymes. This is an indication, for both reagents, that phosphorylation of only the active-site serine is occurring, and for NPN, that after initial phosphorylation of serine, the liberation of a second mol of 4-nitrophenol occurs relatively slowly, if at all. Liberation of a second leaving group, when one is present in the derivatized enzyme, is known for other reagents^{4,6} and is called "aging." Aging thus appears to be slow for 4-nitrophenyl n-propylphosphonyl enzymes ("NP-enzymes"), a feature we will attempt to explain below.

Specificity. Some specificity is observed in these reactions: Each reagent discriminates among the four enzymes, and each enzyme reacts differentially with the three reagents. Because the structures of these enzymes and the interactions responsible for their substrate specificity are so well understood, some conclusions are possible about the origins of the rate differences.

For example, the presence of the second aryloxy group in NPN (as opposed to the methoxy group in MPN) is obviously advantageous: NPN reacts with every enzyme at least 400-fold more rapidly than MPN. With chymotrypsin, trypsin and subtilisin, a logical hypothesis would have been that this aromatic group inserted itself into the "pocket" that accommodates a relatively large C-alpha side chain of the natural substrate for each of these enzymes. This hypothesis is excluded by the large rate constant for elastase; only a small "pocket" is present in the active site of this enzyme, not capable of accepting a p-nitrophenyl group.

An alternative hypothesis we favor is that the second aryloxy group binds to one of the N-acyl binding sites which normally accommodates the amide linkages of residues along the "polypeptide tail" of the natural substrates. The rate factor of 400 or more between NPN and MPN would then arise from the loss of transition-state binding energy of 3.6 kcal/mol or more when p-nitrophenyl is replaced by methyl. It may further be suggested that the n-propyl group occupies the C-alpha side-chain pocket; this is clearly possible with chymotrypsin, trypsin and subtilisin, while it should be possible with elastase to orient the (relatively small) n-propyl group to lie in the depression which customarily accommodates the C-alpha methyl group of an alanine residue.

This idea has stereochemical consequences. First, with MPN, binding of the n-propyl group in the C-alpha pocket and the aryloxy group at an N-acyl site forces the methoxy group into the site opposite (across the phosphorus from) the serine hydroxyl. Since the serine hydroxyl probably cannot displace this relatively poor leaving group, this is an example of "wrong-way binding." The compound must rebind with the methoxy and aryloxy groups exchanged in order to allow the displacement reaction. If this occurs, the S-enantiomer of this chiral compound should be able to react faster. We are now in the process of testing this prediction.

The concept explains the failure of the NP-enzyme to age rapidly. The aryloxy leaving group which must depart in the aging reaction is held in the N-acyl binding site, presenting the opposing face of the phosphorus (the target of a backside, "on-line" nucleophilic attack) to a part of the active site distant from the active-site histidine. The latter is the likely nucleophile for the aging reaction, and the enzyme thus cannot age without interruption of favorable interactions.

Soman is not as efficient an inhibitor of the serine proteases as of the AChEs. Its stereochemical resolution by chymotrypsin has been observed^{4,7} and used. Subtilisin BPN' is much more poorly inhibited by soman than chymotrypsin is and the stereoselectivity of this reaction is unknown.

Recruitment of Acid-base Catalytic Machinery. The solvent isotope effect and proton-inventory results for all systems studied are essentially the same; the overall solvent isotope effects are in the range 1.7-2.1 and the proton inventories are linear, indicating that the solvent isotope effect arises from a single transition-state site. This is exactly the result which is obtained with serine proteases and substrates¹⁵⁻¹⁶ which do not adequately simulate the natural polypeptide substrates; an overall solvent isotope effect, around 2 in magnitude, produced by a single site in the transition state. It is true that the demonstration of one-site catalysis for elastase with NPN is not convincing because the two-site fit gives very large errors. Nevertheless, in the context of the other results and with recognition of the good linear fit of the elastase data, there is no basis for assuming any more complex model for this enzyme.

With both truncated peptide-analogue substrates, which give one-site catalysis, and the inhibitors, the most straightforward assumption is that the single site involved in acid-base catalysis is the hydrogen bridge between the active-site serine hydroxyl and the imidazole nitrogen of the active-site histidine. This component of the catalytic power of the enzyme has therefore been recruited by the organophosphorus reagents. The likelihood of this interpretation is further increased by the dependence of the rate on what is apparently the histidinium ionization, as seen in the pH/rate profiles^{4,5,8}.

On the other hand, the inhibitors have not recruited the multi-proton catalytic capability of the enzyme, seen with good simulators of the natural substrates^{16,17}. Oligopeptides of sufficient length usually "couple" the acid-base catalytic entity of the serine proteases to produce multi-proton catalysis and therewith nonlinear ("bowl-shaped") proton inventories. Since the inhibitors, even in the cases with the greatest rates, give linear proton inventories, the multi-proton component of the catalytic apparatus remains unrecruited.

5. Comparison of AChE and Serine Protease Catalysis

a. Substrates

Mechanistic analogies between the serine proteases and AChE do not extend to the acid-base catalytic machinery and its activation by the natural substrate structure of the enzyme.

b. Inhibitors

I. Soman and sarin react with AChEs by a rapid, perhaps complex, mechanism with little protonic involvement in catalysis. The data are consistent with either a rate-determining induced-fit conformational change accompanied by solvent reorganization or a "solvent-bridge" type of acid-base catalysis. In this latter type of protolytic catalysis, the proton has a passive role, it transfers with relatively small motion in the reaction

coordinate. The inhibition of serine proteases by soman is not as efficient as with the AChEs and proceeds with the recruitment of one-proton catalysis, presumably by the active-site imidazole.

II. MPN reacts efficiently with the AChEs, but very poorly with all serine proteases and uses the participation of one proton on the enzyme active site.

III. While NPN has been found to be a poor inhibitor of eel AChE, it is very efficient with all serine proteases. One-proton catalysis is observed for the serine proteases provided, presumably, by the active-site imidazole.

6. Nonenzymic Hydrolyses of Phosphonate Esters⁴¹

The activation parameters calculated from the Eyring equation for hydrolysis of IMN at different phosphate concentrations are shown in Table II. The enthalpies are indistinguishable within experimental error at 17.2 kcal/mol. The entropies are -18 eu when the correction is applied to bring them to the 1 M standard state for phosphate dianion. Entropies of this magnitude can arise from tighter transition state structures than expected when based on just the loss of translational and rotational freedom on reaction. These negative entropies can originate from a greater degree of structural order of water molecules at the transition state compared to the reactant state. Phosphate dianion, the predominant catalyst under the experimental conditions, seems to act as a nucleophile in this reaction much as bis-4-nitrophenyl methylphosphonate, studied by Brass and Bender.³⁴ Further support for this claim comes from the solvent isotope effects for this reaction, measured at 56 and 70°C to be 1.11 and 1.15, respectively. The low extent of the solvent isotope effect is consistent with the lack of proton transfer, i.e., no general catalysis, at the transition state.

Further characterization of the transition-state properties of non-enzymic hydrolytic reactions of IMN will include studies of general base-catalyzed hydrolysis by imidazole, for which the ¹⁸O leaving group effect may also be determined. A direct comparison of the transition-state structure for such an appropriate nonenzymic model to the available information on the nature of the transition state for inhibition of AChE by not only IMN but other organophosphonates will be truly revealing.

7. Solvent Isotope Effects for the Aging of AChE Inhibited by Sarin

The aging process for this inhibitor does not seem to involve an extensive solvent isotope effect. This information was needed for a characterization of the nature of enzymic catalysis involved in dealkylation of the phosphorylated AChE. A solvent isotope effect of 1.2 ± 0.06 may arise from a general acid catalysis of the departure of the isopropyl group by the imidazolium ion, which occurs with a low frequency motion of the hydronium ion at the transition state. Alternatively, it may not involve proton transfer at the transition state, but it may stem from solvent reorganization. The β -deuterium isotope effect for six deuterium atoms, between 1.2 and 0.85, is consistent with a fairly small degree of rehybridization toward sp^2 character, which is expected for a transition state with a slight carbonium ion character.

8. ^{18}O Exchange Studies of Aging of Soman-inhibited AChE

The results of these experiments is essentially complete incorporation of the ^{18}O label from the labeled solvent into the pinacolyl moiety. This is in agreement with the previous finding³¹ of tritium incorporation from $^3\text{H}_2\text{O}$ into reaction products of aging of soman-inhibited AChE. The exchange studies lend support to a mechanism in which water traps an intermediate carbonium ion. The carbonium ion is likely to be derived directly from the aging process.

9. Solvent Isotope Effects for the Nucleophilic Reactivation of Sarin-inhibited AChE

The nucleophilic reactivation of sarin-inhibited AChE by 2-PAM is associated with a solvent isotope effect of one within experimental error. This is exactly what might be expected for a protolytically unassisted nucleophilic reaction.

In the nucleophilic reactivation of sarin-inhibited AChE by TMB4, a phosphonyl oxime is generated along with the free enzyme. The oxime formed from sarin and TMB4 is an even more potent inhibitor of AChE than sarin is; therefore, it rapidly inactivates the liberated enzyme. The equilibrium formed initially, however, is slowly offset by the decomposition of the oxime of sarin. The reaction follows the rate law for a preequilibrium consecutive scheme in which the slow second step dominates the late phases. From the slow portion, the rate constant for the decomposition of the oxime can be calculated and used for the generation of the apparent infinity values at the earlier points in the time course of reactivation. By such a technique the rate constants for the reactivation can be calculated. The solvent isotope effect calculated from the rate constants indicates some solvent reorganization in the course of reactivation.

10. Chemical Modeling of Aging

The methoxide displacement reactions of isopropanol and pinacolyl alcohol from methyl isopropyl methylphosphonate, EPPP and the sterically hindered compound dipinacolyl propylphosphonate respectively, in methanol were surprisingly slow. In all cases, bond cleavage took place at the P-O bond to the branched alcohol, although, a slight amount of methyl ethyl ether was also generated from EPPP indicating an SN_2 attack at $-\text{CH}_2\text{CH}_3$. The dipinacolyl derivative is free of labile alcohol fragments other than the pinacolyl group to be split off from the phosphonate. If indeed the process of aging goes with C-O bond cleavage and follows a different mechanism when catalyzed by AChE, which is different from the alkaline hydrolysis; it is most likely not a simple nucleophilic displacement or caused by a basic residue on the enzyme.

11. Molecular Graphics Modeling of the Interactions of OP Agents with Serine Proteases

An explanation of the higher reactivity of the P(S) isomer of soman over that of the P(R) isomer with chymotrypsin will be attempted by visual inspection and energy calculations of the interactions between the enzyme and each isomer. For reliable molecular mechanics calculations of the energy differences, the macromolecule will be completely hydrated and the

phosphonate fragments will then be inserted into the active site. Thus the nonbonded energies between protein and water and inhibitor and water will also be included in the energy profile. These interactions can also be significant and make a difference in the stability of the diastereomers of serine hydrolase-OP adducts. The calculations involved, however, are not trivial and can not be completed within the remainder of this project.

F. Experimental Procedures

UV and Visible spectra were recorded on either a Cary 118, Cary 16, or Perkin Elmer Lambda-7 spectrophotometer. Nuclear magnetic resonance (NMR) spectra were obtained with a Varian T-60 spectrophotometer. GLC measurements were carried out on a Varian Aerograph instrument. Capillary melting points were obtained on a Thomas-Hoover apparatus.

GLC sorbents were Porapak Q and FFAP. Porapak Q is a nonpolar porous polymer of small pore size composed of ethyl vinyl benzene cross-linked with divinyl benzene. FFAP is a chromosorb, w 80/100, solid-coated with 10% nitrophthalic acid on Carbowax 20 M. Thin layer chromatography (TLC) was carried out on an Analtech GF 1000 silica gel plate.

Materials. Inorganic salts, buffer components and preparative reagents were reagent-grade chemicals, which were used as purchased or dried, recrystallized, or distilled as necessary. HOH was distilled, deionized, and degassed with nitrogen. DOD (99.9 % deuterium, Norell, Inc., Landisville, NJ) was distilled (100-102°C fraction) and stored under nitrogen. Acetonitrile for stock solutions of kinetic measurements was purified by a three-step procedure^{4,9}. Absolute methanol used in kinetic measurements was also distilled from magnesium turnings and benzoic acid.⁵⁰ PA (Eastman Chemicals, Kingsport, TN) was purified by column chromatography and vacuum distillation. N-succinyl-(Ala)₃-p-nitroanilide was purchased from Sigma Co. (St. Louis, MO) and used without further purification. GLP was a gift from Professor A. Barth and his coworkers.

The starting materials, n-propylphosphonodichloridate, pinacolyl alcohol, and isopropyl methyl-phosphonochloridate, were purchased from Aldrich Company (97% purity) and were used without further purification. Potassium p-nitrophenolate was synthesized by us earlier³⁰ and purified by recrystallization from dry methanol followed by drying over P₂O₅. AChE from the electric eel organ, 1000 unit/mg, and chymotrypsin type III from bovine pancreas were obtained from Sigma Co.

Methyl or ethyl n-propylphosphonochloridate

This synthesis is an adaptation of reported methods.^{38,51} The n-propylphosphonodichloridate, 0.11 mol, was stirred vigorously in 50 ml pentane under N₂ while 0.095 mol each of dry lutidene and methanol, or ethanol, in 50 ml of pentane was added dropwise over a 1 hour period. Stirring was continued for 48 hours and then the solid was filtered and washed well with pentane. The supernatant was evaporated at reduced pressure and the product distilled to give 10.0 g (67%) of an oil, bp. 75°C, 3.2-4 Hg-mm. The distilled product was estimated to be 70% of the methoxy compound by NMR. NMR: CCl₄, 2% TMS, δ 0.8-1.4 (m, 3H, CH₃), 1.4-2.9, (m, 4H, CH₂-CH₂), 3.85 (d, 3H, OCH₃) J (P-H) = 11 Hz.

Ethyl pinacolyl n-propylphosphonate

Pinacolyl alcohol, 7.2 mmol in 5 ml of dry pentane, was stirred with 4.7 mmol (1.3 equivalents) NaH (washed with pentane) overnight. To this mixture, 3.6 mmol ethyl n-propylphosphonochloridate in pentane was added dropwise and the mixture was allowed to stir overnight. The reaction mixture was centrifuged, the supernatant removed, the residue filtered and

washed with pentane. The pentane solution of products was treated with a small amount of Dowex 50 x 8 50 mesh (Biorad), and the solvent removed under reduced pressure. The pinacolyl alcohol-free product distilled at 95°C, 1.2 Hg-mm. GLC analysis showed no evidence of the alcohol. NMR: CCl_4 , 2% TMS, δ 0.92 (s, 9H, tbut), 0.8-2.0 (m, 13H nprop + $\text{CH}_3\text{-C-H}$ + OCH_2CH_3), 4.1 (g, 3H, OCH_2CH_3 + O-C-H).

4-Nitrophenyl methyl n-propylphosphonate and Bis 4-nitrophenyl n-propylphosphonate (NPM and NPN).

To potassium 4-nitrophenolate, 2.06 mmol in 5 ml dry benzene, 1.45 mmol methyl n-propylphosphonochloridate in 3 ml benzene was added dropwise under constant stirring at room temperature. The progress of the reaction was monitored on TLC. After several days, the supernatant solution was decanted and the yellow residue was washed with benzene. The KCl was filtered out and the benzene was removed at reduced pressure. The pasty residue was taken up in 15 ml methanol and the insoluble product was filtered out to give a white powder, mp 132-40°C. The solid was recrystallized from ethylacetate-pentane and was identified by base hydrolysis of an aliquot to two equivalents of p-nitrophenoxide as monitored at 400 nm (102%) mp 132-133°C.

The methanol was removed from the filtrate and a yellow oil was obtained, which separated into four components on TLC. The oil was placed on a preparative TLC plate and double-developed until MPPP was completely isolated from other contaminants: TLC: ethylacetate:cyclohexane 3:2, ethylacetate:pentane 3:2; Rf: p-nitrophenol, 0.74; BPPP, 0.64; MPPP, 0.42. The MPPP product was scraped off the plate and eluted with ethylacetate. Hydrolysis in 1 M NaOH produced 1.05 equivalents of 4-nitrophenolate as monitored spectroscopically. NMR: CCl_4 , 2% TMS, δ 1.1-2.0 (m, 4H CH_2CH_2), 3.6 (d, 3H, OCH_3) J (P-H) = 11 Hz, 7.15 (d, 2H, Ar_{1,6}) J_{2,3} = 5 Hz, 8.0 (d, 2H, Ar_{3,5}) J_{5,6} = 5 Hz.

4-Nitrophenyl (2-propyl) methylphosphonate (IMN)^{32a}

To dry potassium 4-nitrophenolate (9.66 mmol) in dry benzene (5 ml), 2-propyl methylphosphonochloridate (10.0 mmol, Aldrich Co., Milwaukee, WI) in dry benzene (5 ml) was added dropwise with stirring at ambient temperature. The reaction was left stirring overnight, the potassium chloride was then filtered and the benzene was removed under reduced pressure. The syrupy residue was distilled under high vacuum (130-135°C, 0.3 mmHg). Yield=65.9% (6.37 mmol).

NMR(¹H): CCl_4 , 2% TMS, δ 1.30 (dd, 6H, CHMe_2) J_{H-H}=12 Hz, J_{P-H}=4 Hz, δ 1.50 (d, 3H, P-Me) J_{P-H}=27 Hz, δ 4.70 (m, 1H, CHMe_2), δ 7.23 (d, 2H, Ar_{2,6}) J_{H-H}=9 Hz, δ 8.04 (d, 2H, Ar_{3,5}).

4-Nitro[¹⁸O]phenyl (2-propyl) methylphosphonate

Methanol[¹⁸O]^{33a}. Trimethyl orthoformate (20 ml) was added to dry butan-1-ol (55 ml) containing 4-toluenesulfonic acid (100 mg). This mixture was heated while the theoretical amount of methanol was removed by distillation. The remaining solution was distilled under high vacuum to yield tri-(1-butyl) orthoformate (b.p. 128-130°C, 15 mm Hg). A mixture of tri-(1-butyl) orthoformate (16 ml) and dry diglyme (10 ml) was stirred under dry nitrogen as water ¹⁸O (1.0 g, 99.0 atom%, Stohler-KOR batch # B-30641) was

added followed by dry hydrogen chloride gas (5 ml). This mixture was distilled immediately through a small Vigreux column. 1-Butyl formate-carbonyl- ^{18}O and butan-1-ol were collected over the range b.p. 107-118°C. This mixture was added to a cooled solution of lithium aluminium hydride (2.0 g) in dry diglyme (75 ml); this was left stirring for 30 minutes, when water (1.45 ml) was added slowly, followed by ethan-1,2-diol (10 ml). Distillation gave methanol- ^{18}O (b.p. 64.5-66.0°C). Yield=2.00 ml (93.0% based on H_2^{18}O).

4-Nitro[^{18}O]anisole^{33b}. Lithium hydride (2.0 g) was added to dry dimethyl sulfoxide (75 ml) and the suspension was stirred at 70-80°C until reaction ceased. The solution was allowed to cool to room temperature, methanol[^{18}O] (2.0 ml) was added and the solution was stirred for 20 minutes. To this solution was added 1-fluoro-4-nitrobenzene (5.4 ml); the mixture was stirred at 50-55°C for 16 hours, cooled, poured into aqueous tetrahydrofuran (150 ml), and extracted with ether (3 x 150 ml). The ethereal extracts were washed with saturated brine (2 x 150 ml), and distilled water (150 ml), dried (MgSO_4), and evaporated. The residue was recrystallized to afford 4-nitro[^{18}O]anisole, in 40.9% yield from methanol.

4-Nitro[^{18}O]phenol^{33b}. Dry pyridinium hydrochloride (8.0 g) was fused with the labeled anisole (2.95 g) at 180-190°C for 2.5 hours. The reaction mixture was then allowed to cool to room temperature, when water (40 ml) was added. The solution was then extracted with ether (2 x 50 ml); the ethereal extracts were washed with dilute hydrochloric acid (0.1 M, 50 ml), dried (MgSO_4), and evaporated to yield after recrystallization from dry toluene 1.93 g (71.9%) of pure 4-nitro[^{18}O]phenol.

Potassium 4-nitro[^{18}O]phenolate⁴⁹. To a solution of potassium hydroxide (1.5 equivalents) in dry methanol (5 ml) was added dropwise a solution of the labeled phenol (1.93 g) in dry methanol (2 ml); the resulting crystalline salt was filtered and dried to give a 60.0% yield of the potassium salt (1.47 g). Concentration of the mother liquor produced more of the labeled potassium salt.

The labeled inhibitor was produced in 29.8% yield in an analogous manner to the unlabeled phosphonate.

Enzymes. AChE from Electrophorus electricus was obtained with an activity of 1,000 mol units/mg (Sigma type V-S) lyophilized powder. Solutions of AChE from the eel were prepared in 0.1 M phosphate buffer at pH = 6.9, 46 ng/ml, by dilution of the Sigma lyophilized preparation and were frozen until use. Reactions were conducted at enzyme concentrations of 0.005-0.01 unit/mL of AChE from the eel and 0.0125 unit/mL of AChE from human erythrocytes based on the Ellman assay, contained in 50 μl of a stock solution. The pH was maintained at 7.60 in HOH (0.0065 M KH_2PO_4 , 0.0434 M K_2HPO_4). AChE from human erythrocytes was obtained with an activity of 1 unit/mg solid (Sigma XIII) and was further purified by affinity chromatography according to Rosenberry and Scoggins⁵². The progression of enzyme purification was monitored with the Ellman assay. The enzyme (purified about 20-fold) was stored in 0.01 M phosphate buffer at pH = 7.00 with 0.1% Triton X-100 (peak fraction; 7-10 unit/ml) and kept frozen until use. Bovine pancreatic α -chymotrypsin (EC 34.21.1) was obtained from Sigma Chemical Co. as a salt-free, lyophilized, three times recrystallized powder with an activity of 52 BTEE units/mg. Bovine pancreatic trypsin (EC

3.4.21.4) from Sigma Chemical Co.--dialyzed, recrystallized, salt-free powder with an activity of 7500 BAEE units/mg--was treated by storing buffered aqueous solutions of it at room temperature for at least 2 hours to obtain autolytically stable solutions. Elastase (pancreatopeptidase E, EC 3.4.21.11, from hog pancreas--chromatographically purified, lyophilized, water-soluble powder with an activity of 90 elastin units/mg) and subtilisin BPN' (protease nagarse; EC 3.4.21.3; from Bacillus amyloliquefaciens, crystallized and lyophilized with an activity of 10 tyrosin units/mg) were both obtained from Sigma Chemical Co.

Kinetics. Rate measurements involved the automated acquisition of 500-1000 data points with one of the Cary spectrophotometers interfaced to a DEC-Heathkit H-11 microcomputer or with the Perkin Elmer Lambda-7 interfaced to a Zenith Z-100 microcomputer. Reaction temperatures were controlled by a Lauda K4/RD circulating bath connected to the cell jacket of the Cary instruments or by a Peltier system for the Perkin Elmer Lambda-7 instrument. Temperatures were monitored by a digital thermometer.

Solutions for Kinetics. Corresponding pL in H₂O/D₂O mixtures was achieved by use of the same buffer composition throughout. H₂O/D₂O mixtures were made up by volume from buffer stock solutions in the pure isotopic solvents. MPN, NPN and IMN solutions were prepared in methanol freshly for each experiment and an aliquot was hydrolyzed to one equivalent of p-nitrophenol for MPN and IMN and to two equivalents of p-nitrophenol for NPN to determine the actual concentration spectroscopically at 400 nm. PA stock solutions were hydrolyzed to phenol and the liberated phenoxide ion was measured at 286.9 nm (ϵ 2544 M⁻¹ cm⁻¹) to verify concentrations. Nonenzymatic hydrolysis of PA was completely negligible under our conditions.

General Kinetic Protocol. In a typical kinetic experiment, the appropriate volume of buffer was equilibrated at 25.00 ± 0.05°C (as monitored with a thermistor probe) in a quartz cuvette in the cell compartment of the instrument. Substrate and/or inhibitor were added from stock solutions and the absorbance recorded after each injection to monitor decomposition of chromogenic, labile species. The reaction was initiated with the injection of the enzyme in 20-50 µl volume to bring the total to 1 ml. The total concentration of cosolvents was kept constant at < 5% (mostly MeOH); any decomposition in the substrate or inhibitor was monitored and the results discarded or corrected.

Irreversible inhibition of enzymes in the presence of a modifier was studied under pseudo-first-order conditions with a 20-1000-fold excess of inhibitor over enzyme concentration to obtain a signal < 10% decomposition of the substrate. First-order rate constants were calculated by a least-squares fit of absorbance time coordinates. Substrate-independent, second-order inhibition constants were calculated by a linear least-squares fit of the inverse observed rate constants to substrate concentration according to eq. 17.

AChE Reactions. In the inhibition experiments, soman and sarin were injected in 50 µl volume from a 2-5 x 10⁻⁷ M cold H₂O or D₂O (pH=4, HCl) solution, NPN, MPN and IMN were from a ~10⁻³ M methanolic stock solution in 40 µl volume, and PA was delivered in 10 µl volume from 0.2-1.0 M methanolic stock solutions.

Remaining AChE activities after inhibition by NPN or MPPN were determined by initial rates not exceeding 5% consumption of PA. Initial velocities, $\Delta\text{Abs}/\Delta t$, were converted to units of s^{-1} by dividing with $\Delta\epsilon = 1356 - 15 = 1340 \text{ M}^{-1} \text{ cm}^{-1}$. Appropriate amounts of buffer to give a total volume of 1 ml per run were pre-equilibrated at 25°C for 15 minutes. PA was then introduced in 10-50 μl aliquots from a 0.1 M methanolic stock solution.

For the substrate reactions, 10 μl PA was delivered from a methanolic stock solution and mixed; its absorbance was recorded; and then the reaction was initiated by the introduction of 50 μl of the AChE stock solution. Initial rates were calculated from the computer-stored data by a linear least-squares method. Enzyme kinetic parameters, V and V/K_m , were obtained by linear least-squares fit of the reciprocal rates to the reciprocal of PA concentration.

Serine Proteases. Stock solutions were made in 10^{-3} M concentration in pH=4 (HCl) H_2O or D_2O for chymotrypsin and trypsin, in pH=7.0 phosphate buffer for subtilisin BPN', and in pH=5.0 acetate buffer for elastase. A 50 μl aliquot of the enzyme stock solution was injected to start a kinetic run. The buffers used for kinetic measurements were: 0.05 M phosphate, pH = 7.4, pD = 7.9 for chymotrypsin and 0.05 - 0.1 M trizma pH = 8.4, pD = 8.9 for trypsin, elastase and subtilisin. Soman was used in a 50 μl volume from 10^{-6} - 10^{-4} cold, pH = 4.0 stock solutions. NPN and MPN were introduced from 10^{-3} methanolic stock solutions in 40 μl volume. Substrate solutions were prepared in 10^{-3} M stock solutions with 10% acetone or acetonitrile cosolvent at pH < 7.0 (NaOH) and used in 0.1-0.5 ml volume in a kinetic run.

Direct measurements of inhibition of chymotrypsin, elastase, and subtilisin by MPN were conducted under zero order conditions, the release of 4-nitrophenol was monitored at 400 nm, and data were fit to a linear dependence on time by linear least squares. Second-order rate constants were calculated from:

$$k_2 = (\delta\text{Abs}/\delta t)/[E_0][I]\delta\epsilon$$

where E_0 = initial concentration of the enzyme

I_0 = initial concentration of the inhibitor

and ϵ (400 nm); $6.33 \times 10^3 \text{ M}^{-1} \text{ cm}^{-1}$ pH = 6.90

$17.40 \times 10^3 \text{ M}^{-1} \text{ cm}^{-1}$, pH = 8.40⁵³

The inhibition of trypsin by NPN was studied under pseudo-first-order conditions with trypsin in > 20-fold excess. The inhibitions by soman and NPN were studied in the presence of 5×10^{-5} to 5×10^{-4} M GLP with chymotrypsin and subtilisin BPN' and in the presence of N-succinyl-Ala-Ala-Ala-4-nitroanilide with elastase, both at 390 nm. Aliquots of the substrate solutions were also hydrolyzed to 4-nitroanilide and read at 390 nm (ϵ 11,520).

Experiments for the Aging and Spontaneous Reactivation of 2-Propyl Methylphosphonyl-AChE (Electric Eel) In each of two 1 ml volumetric flasks, ~ 10 units (10^{-11} mol) AChE from electric eel contained in 50 μ l, pH 10.0, 0.1 M TAPS buffer was incubated at 37.4°C for at least 30 minutes. One of these, the test solution, also contained 2 μ l of a 10^{-4} M (2×10^{-10} mol) sarin solution. The hydrolysis rate of sarin at pH 10.0 has $k_{\text{obs}} = 0.054 \text{ s}^{-1}$; $t_{1/2} = 2$ minutes; thus 99.9 % of the sarin added is destroyed in 30 minutes. Both test solution and control were diluted to 1 ml with the buffer used for aging and were placed back in the incubator at 37.4°C. The buffer was made in H_2O or D_2O to contain 0.115 M KH_2PO_4 , 0.052 M K_2HPO_4 , 0.1% gelatin, and 0.01% MgCl_2 . Sampling for the time course of spontaneous reactivation and aging began immediately and was continued at 20-40 minute intervals for 8 hours. At each time, two aliquots of 20 μ l of each solution were drawn. One of these was incubated for 20 minutes with 100 μ l of 1 mM TMB4 solution in a pH = 7.7, 0.05 M phosphate buffer, which had also been preincubated in a 1 cm cuvette. To this solution was added 880 μ l, pH 7.7, 0.05 M phosphate buffer and it was allowed to equilibrate for another 10 minutes before it was assayed. The other aliquot was added directly to 980 μ l, pH 7.7, 0.05 M phosphate buffer that had been preequilibrated at 37°C in a cuvette. The Ellman assay was carried out by injecting 30 μ l 0.01 M dithiobisnitrobenzoate (DTNB) solution and 20 μ l, 0.05 M ACTCh solution into the cuvette. Initial velocities were recorded for the first < 5% of the substrate reaction. The correction for the TMB4 reaction with the substrate was 0.21 OD/min, less than 10% of the rate of the reaction with the uninhibited enzyme. This correction was applied to all measurements for reactivation; then the rates were factored to correct for the inhibition of AChE activity as measured in the Ellman assay.

Experiments for the Nucleophilic Reactivation of 2-Propyl Methylphosphonyl-AChE (Electric eel). AChE, ~7-8 units (7-8 pmol), dissolved in 50 μ l, pH 10.0, 0.1 M TAPS buffer, was inhibited with 5 μ l 10^{-4} (500 pmol) sarin solution and was incubated for 1 hour at 25°C. A 25-fold dilution of aliquots of this solution into pH 7.65, 0.05 M phosphate buffer, pH 7.65 in HOH, pD 8.15 in DOD, was performed and the solution was reincubated at 25°C for 15 minutes before TMB4 was introduced into the reaction mixture in 10 μ l volume. The most feasible concentration range for following the kinetics of reactivation was $2-8 \times 10^{-5}$ M for TMB4. Aliquots of 20 μ l were drawn from the reaction mixture as a function of time for assay with the Ellman reagent. In the assay mixture, 3×10^{-4} M DTNB and 10^{-3} M ACTCh were used in a pH 7.65, 0.05 M phosphate buffer.

GLC Experiments. Separation of isopropanol and its methyl ether from other components was accomplished by the injection of 0.5 μ l samples of the supernatant of the reaction mixtures into the Porapak Q column at 120°C followed by ramping to 140°C (2°C/min) at $t = 5$ minutes, then to 200°C (10°C/min) at 15 minutes. The N_2 carrier gas flow was 20 ml/minute and the elution times were as follows: MeOH, 2 minutes; iPrOH, 7 minutes; iPrOMe, 9 minutes. Separation was also attained on an FFAP column at 30°C with ramping to 200°C (20°C/min) at $t = 10$ minutes with the following retention times: iPrOMe, 0.7 minutes; iPrOH and MeOH, 3 minutes; phosphonates, 16 minutes.

Separation of pinacolyl alcohol and its methyl ether from other components was accomplished by injection of 1 μ l samples of the supernatant (filtered through a nylon millipore filter) into the FFAP column. Elution

with the N₂ carrier gas (20 ml/min) began at 25°C and was subsequently ramped to 200°C (20°C/min) at t = 18 minutes. The retention times were as follows: MeOpinacolate, 1.5 minutes; MeOH, 3.5 minutes; pinacolyl alcohol, 14 minutes; phosphonates, 27 minutes.

G. References

1. Schowen, R. L.; Kovach, I. M., Molecular Origins of Selective Toxicity. Annual Report for USAMRDC Contract DAMD17-83-C-3199, November 10, 1984.
2. a. Rosenberry, T. L., Catalysis by Acetylcholinesterase. The Rate-Limiting-Steps Involved in the Acylation of Acetylcholinesterase by Acetic Acid Esters and Phosphorylating Agents, Croatia Chemica Acta, 1975, 47, 235.
b. Rosenberry, T. L., Acetylcholinesterase, Adv. Enzymol. Relat. Areas Mol. Biol., 1975, 43, 103.
c. Rosenberry, T. L., Catalysis by Acetylcholinesterase: Evidence that the Rate Limiting Step for Acylation with Certain Substrates Precedes General Acid Base Catalysis, Proc. Natl. Acad. Sci., USA, 1975, 72, 3834.
3. O'Brien, R. D., Toxic Phosphorus Esters. Chemistry, Metabolism, and Biological Effects, Academic Press, New York, 1960.
4. Heath, D. F., Organophosphorus Poisons. Anticholinesterases and Related Compounds, Pergamon Press, Oxford, 1961.
5. Koelle, G. B., ed., Cholinesterase and Anticholinesterase Agents, Handbuch der Experimentellen Pharmacologie, Ergänzungs-werk XV, Springer-Verlag, Berlin, 1963.
6. a. Aldridge, W. N.; Reiner, E., Enzyme Inhibitors as Substrates. Interactions of Esterases with Esters of Organophosphorus and Cartemic Acids, American Elsevier Publishing Company, Inc., New York, 1972.
b. Aldridge, W. N., Survey of Major Points of Interest About Reactions of Cholinesterases, Croatia Chemica Acta, 1975, 47, 215.
7. Johnson, M. K., Neurotoxicity: Mechanisms Explored and Exploited, Nature, 1980, 287, 105.
8. Kraut, J., Serine Proteases: Structure and Mechanism of Catalysis. Ann. Rev. Biochem., 1977, 46, 331-358.
9. Lockridge, O.; Bartels, C. F.; Vaughan, T. A.; Wong, C. K.; Norton, S. E.; Johnson, L. L., Complete Amino Acid Sequence of Human Serum Cholinesterase. J. Biol. Chem., 1987, 262, 549-557.
10. Fersht, A. R., Enzyme Structure and Mechanism, 2nd ed., Freeman, New York, 1985. Chap. 1.
11. Hogg, J. L.; Elrod, J. P.; Schowen, R. L., Transition State Properties and Rate-Limiting Processes in the Acylation of Acetylcholinestrerase by Natural and Unnatural Substrates, J. Am. Chem. Soc., 1980, 102, 2082.

12. Schowen, K. B.; Smissman, E. E.; Stephen, W. F. Jr.; Conformational Aspects of Acetylcholine Receptors Sites: III. Base-Catalyzed and Acetylcholinesterase-Catalyzed Hydrolysis of the Isomeric dl-3-Tri-methyl Ammonium-2-acetoxy-trans-decalin Halides and the Isomeric dl-1-Methyl-3-acetoxy-trans-dexoquinoline Methiodides, *J. Med. Chem.*, 1975, 18, 292.
13. Bauer, C. A.; Thompson, R. C.; Blout, E. R., The Active Centers of *Streptomyces griseus* Protease-3 and α -Chymotrypsin: Enzyme-Substrate Interactions Remote from the Scissile Bond, *Biochemistry*, 1976, 15, 1291.
14. Hunkapiller, M. W.; Smallcombe, S. H.; Whitaker, D. B.; Richards, J. H., Carbon Nuclear-Magnetic Resonance Studies of the Histidine Residue in α -Lytic Protease. Implications for the Catalytic Mechanisms of Serine Proteases, *Biochemistry*, 1973, 12, 4723.
15. Quinn, D. M., Acetylcholinesterase: Enzyme Structure, Reaction Dynamics and Virtual Transition States. *Chem. Rev.* 1987, 87, 955.
16. Elrod, J. P.; Hogg, J.L.; Quinn, D.M.; Venkatasubban, K.S.; Schowen, R.L., Protonic Reorganization and Substrate Structure in Catalysis by Serine Proteases, *J. Am. Chem. Soc.*, 1980, 102, 3917.
17. a. Quinn, D. M.; Venkatasubban; K. S. Kise, M.; Schowen, R. L., Protonic Reorganization and Substrate Structure in Catalysis by Amidhydrolases, *J. Am. Chem. Soc.*, 1980, 102, 5365.
b. Quinn, D. M.; Elrod, J.P.; Ardis, R.; Friesen, P; Schowen, R.L., Protonic Reorganization in Catalysis by Serine Proteases: Acylation by Small Substrates, *J. Am. Chem. Soc.*, 1980, 102, 5358.
18. Kovach, I. M., Structure and Dynamics of Serine Hydrolase-Organophosphorus Adducts. *J. Enzyme Inhib.* 1988, 2, 199.
19. Stein, R. L.; Elrod, J. P.; Schowen, R. L., Correlative Variations in Enzyme-Derived and Substrate-Derived Structures of Catalytic Transition States. Implications for the Catalytic Strategy of Acyl-Transfer-Enzymes, *J. Am. Chem. Soc.*, 1982, 105, 2446.
20. Benkovic, S. J.; Shray, K. J., in Gandour, R. D.; Schowen, R. L., Eds; Transition States of Biochemical Processes, Plenum, New York, 1978. Chapter 13.
21. Schowen, R. L., Isotope Effects on Enzyme-Catalyzed Reactions, University Park Press, Baltimore, 1977, Chap. 3.
22. Gorenstein, D. G., Oxygen-18 Isotope Effect in the Hydrolysis of 2,4-Dinitrophenyl Phosphate. A Monomeric Metaphosphate Mechanism, *J. Am. Chem Soc.*, 1972, 94, 2523.
23. Gorenstein, D. G., Lee, Y. G., and Kar, D., Kinetic Isotope Effects in the Reactions of Aryl- ^{18}O -2,4-Dinitrophenyl Dibenzyl Phosphate and Aryl- ^{18}O -2,4-Dinitrophenyl Phosphate. Evidence for Monomeric Metaphosphate, *J. Am. Chem. Soc.*, 1977, 99, 2264.

24. Hegazi, M. F. *et al.*, α -Deuterium and Carbon-13 Isotope Effects for Methyl Transfer Catalyzed by Catechol O-Methyltransferase. S_N2 -Like Transition State., *J. Am. Chem. Soc.*, 1979, 101, 4359.
25. Rozenberg, S. and Kirsch, J. F., Direct Spectrophotometric Measurement of Small Kinetic Isotope Effects., *Anal. Chem.*, 1979, 51, 1379.
26. Rozenberg, S. and Kirsch, J. F., Measurement of Heavy Atom Kinetic Isotope Effects by Direct Mass-Spectrometric Analysis, *Anal. Chem.*, 1979, 51, 1375.
27. Burton, C. W. *et al.*, Calculation of Carbon-14, Chlorine-37, and Deuterium Kinetic Isotope Effects in the Solvolysis of Tertiary Butyl Chloride, *J. Am. Chem. Soc.*, 1977, 99, 337.
28. Kaplan, E. D. and Thornton, E. R., Secondary Deuterium Isotope Effects, *J. Am. Chem. Soc.*, 1967, 89, 6644.
29. Carter, R. F. and Melander, L., Experiments on the Nature of Steric Isotope Effects, *Adv. Phys. Org. Chem.*, 1973, 10, 1.
30. Smith, T. E. and Usdin, E., Formation of Nonreactivable Isopropyl Methylphosphonofluoridate-Inhibited Acetylcholinesterase, *Biochemistry*, 1966, 5, 2914.
31. Michel, H. O. *et al.*, Ageing and Dealkylation of Soman (Pinacolyl Methylphosphonofluoridate)-Inactivated Eel Cholinesterase, *Arch. Biochem. Biophys.*, 1967, 127, 29.
32. Kovach, I. M.; Larson M.; Schowen, R. L., Catalytic Recruitment in the Inactivation of Serine Proteases by Phosphonate Esters. Recruitment of Acid-Base Catalysis. *J. Am. Chem. Soc.*, 1986, 108, 5490.
33. a. Sawyer, C. B.; Kirsh, J. F. Kinetic Isotope Effects for Reactions of Methyl Formate-Methoxyl- ^{18}O . *J. Am. Chem. Soc.*, 1973, 95, 7375.
b. Bennet, A. J.; Sinnott, M. L.; Wijesundera, S., ^{18}O and Secondary 2H Kinetic Isotope Effects Confirm the Existence of Two Pathways for Acid-Catalyzed Hydrolyses of α -Arabinofuranosides. *J. Chem. Soc. Perkin Trans. II*, 1985, 1233.
34. Kovach, I. M., Competitive Irreversible Enzyme Inhibition in the Presence of a Substrate. Submitted to *J. Enzyme Inhibition*.
35. Kovach, I. M.; Huber Harmon-Ashley, J.; Schowen, R. L., Catalytic Recruitment of Acetylcholinesterase by Soman: Temperature Dependence of the Solvent Isotope Effect. *J. Am. Chem. Soc.*, 1988, 110, 590.
36. Kovach, I. M.; Larson, M. L.; Schowen, R. L. One Proton Catalysis in the Deacetylation of Acetylcholinesterase. *J. Am. Chem. Soc.*, 1986, 108, 3054-3056.

37. Bennet, A. J.; Kovach, I. M.; Schowen, R. L., Rate-Limiting P-O Fission in the Self-stimulated Inactivation of Acetylcholinesterase by 4-Nitrophenyl 2-Propyl Methylphosphonate. *J. Am. Chem. Soc.*, 1988, 110, 7892.
38. Hovanec, J. W. and Lieske, C. N., Spontaneous Reaction of Acetylcholinesterase Inhibited with Substituted Phenyl Methylphosphonochloridates, *Biochemistry*, 1972, 11, 1051.
39. Forsberg, A. and Puu, G., Kinetics for the Inhibition of Acetylcholinesterase from Electric Eel for Some Organophosphates and Carbomates, *Eur. J. Biochem.*, 1984, 140 153.
40. Epstein, J., Callahan, J. J. and Bauer, V. E., Kinetics and Mechanisms of Hydrolysis of Phosphonothiolates in Dilute Aqueous Solution, *Phosphorus*, 1974, 4, 157.
41. Bennet, A. J., Bibbs, J. A. and Kovach, I. M., Buffer-catalyzed Hydrolysis of Phosphonate Esters: Activation Parameters and Solvent Isotope Effects, to be submitted to *J. Am. Chem. Soc.*
42. Khoshtariya, D. E.; Topovlev, V. V.; Krishtalik, L. I., A Study of Proton Transfer in Enzymatic Hydrolysis by Means of the Temperature-Dependent Kinetic Isotope Effect. I. Hydrolysis of the Ethyl Esters of N-Acetyl and N-Benzoyl-L-Tyrosin by α -Chymotrypsin. *Russian Bioorg. Chem.* 1979, 964 (English).
43. Aldridge, W. N., The Inhibition of Erythrocyte Cholinesterase by Triesters of Phosphoric Acid, *Biochem. J.*, 1953, 54, 442.
44. Bennet, A. J., Kovach, I. M. and Bibbs, J. A., Catalytic Recruitment by Phosphonyl Derivatives as Inactivators of Acetylcholinesterase and as Substrates for Imiazole-catalyzed Hydrolysis: β -Deuterium Isotope Effects, *J. Am. Chem. Soc.* 1989, 110, 0000.
45. Froede, H. C.; Wilson, I. B., Direct Determination of Acetyl- enzyme Intermediate in the Acetylcholinesterase-catalyzed Hydrolysis of Acetylcholine and Acetylthiocholine. *J. Biol. Chem.*, 1984, 259, 11010.
46. Bender, M. L.; Weddler, F. C., Phosphate and Carbonate Ester Aging Reactions with α -Chymotrypsin. Kinetics and Mechanism. *J. Am. Chem. Soc.*, 1972, 94, 2101.
47. Boter, H. L.; Ooms, A. J., Stereospecificity of Hydrolytic Enzymes in their Reaction with Optically Active Organophosphorus Compounds II. *J. Biochem. Pharmacol.* 1967, 16, 1563
48. Bender, M. L.; Clement, G. E.; Kezdy, F. J.; Heck, H. D. A., The Correlation of pH (pD) Dependence and the Stepwise Mechanism of α -Chymotrypsin-catalyzed Reactions. *J. Am. Chem. Soc.*, 1964, 86, 3680.
49. Kovach, I. M., Kinetics and Some Equilibria of Transacylation between Oxy Anions in Aprotic Solvents, *J. Org. Chem.*, 1982, 47, 2235.

50. Kovach, I. M., et al, The B-Hydrogen Secondary Isotope Effect in Acyl Transfer Reactions. Origins, Temperature Dependence, and Utility as a Probe of Transition State Structure, J. Am. Chem. Soc., 1980, 102, 1991.
51. Lacy, C. I. and Loew, L. M., A Simple Synthesis of Choline Akkyl Phosphates, Tetrahedron Letters, 1980, 21, 2017.
52. Rosenberry, T. L.; Scoggins, D. M., Structure of Human Erythrocyte Acetylcholinesterase. Characterization of Intersubunit Disulfide Bonding and Detergent Interaction. J. Biol. Chem., 1984, 259, 5643.
53. Kovach, I. M.; Elrod, J. P.; Schowen, R. L., Reaction Progress at the Transition State for Nucleophilic Attack on Esters, J. Am. Chem. Soc., 1980, 102, 7530.

DISTRIBUTION LIST

1 copy Commander
US Army Medical Research and Development Command
ATTN: SGRD-RMI-S
Fort Detrick
Frederick, MD 21701-5012

5 copies Commander
US Army Medical Research and Development Command
ATTN: SGRD-PLE
Fort Detrick
Frederick, MD 21701-5012

2 copies Administrator
Defense Technical Information Center
ATTN: DTIC-DDA
Cameron Station
Alexandria, VA 22314

1 copy Commandant
Academy of Health Sciences, US Army
ATTN: AHS-CDM
Fort Sam Houston, TX 78234

1 copy Dean, School of Medicine
Uniformed Services University
of the Health Sciences
4301 Jones Bridge Road
Bethesda, MD 20014

Oral Presentations and Abstracts

"Molecular Origins of Selective Toxicity: Protonic Reorganization in the Phosphorylation of Serine Hydrolases." I.M. Kovach and R.L. Schowen, Fifth Annual Chemical Defense Bioscience Review, The Johns Hopkins University Applied Physics Laboratory, Columbia, Maryland 29-31 May, 1985 (Poster).

"Molecular Origins of Selective Toxicity: Protonic Reorganization in the Phosphorylation of Serine Hydrolases." I.M. Kovach, Gordon Research Conferences on Enzymes, Coenzymes, and Metabolic Pathways, Meriden, New Hampshire, July 8-12, 1985.

"Catalytic Recruitment in the Inactivation of Serine Hydrolases by Phosphonate Esters." I.M. Kovach and R.L. Schowen, 191st National Meeting ACS, New York City, NY, April 17-23, 1986.

"Catalytic Recruitment in the Inactivation of Serine Hydrolases by Phosphonate Esters." I.M. Kovach, Seminar at the Central Research Institute for Physics of the Hungarian Academy of Sciences, Budapest, Hungary, July 1986 - Invited Presentation.

"Catalytic recruitment in the Inactivation of Serine Hydrolases by Phosphonate Esters." I.M. Kovach, 2nd International Meeting on Cellular Regulation and Enzyme Mechanism, Halle an der Salle, German Democratic Republic, August 17-23, 1986 - Invited Presentation.

"The Extent of Catalytic Involvement in the Inhibition of Acetylcholinesterase by Phosphonate Esters." I.M. Kovach, J. Ashely-Huber, and R.L. Schowen, 21st Midwest Regional Meeting ACS, Kansas City, MO, June, 1986.

"Serine Hydrolase Phosphyl Ester Interactions." I.M. Kovach, 30th National Organic Symposium, Vancouver, B.C., Canada, June 21-25, 1987 (Poster).

"Serine Hydrolase Phosphyl Ester Interactions." I.M. Kovach, 22nd Midwest Regional Meeting ACS, Wichita, KS, November 5, 1987.

"Structure Dependent Elimination of 4 Nitrophenol from 4 Nitrophenyl Alkylphosphonyl Chymotrypsin Adducts." K. Hall and I.M. Kovach, 22nd Midwest Regional Meeting ACS, Wichita, KS, November 5, 1987 (Poster).

"Computational and Kinetic Studies of the Energetics of Serine Hydrolase Organophosphate Interactions." I.M. Kovach, Third Chemical Congress of North America and the 195th National Meeting ACS, Toronto, Canada, June 5-10, 1988.

"Characterization of Transition States and Stable Intermediates in the Phosphorylation of Serine Hydrolases." I.M. Kovach, 9th Mechanisms Conference, Pittsburgh, PA, June 11-15, 1988 (Poster).

"Computational and Kinetic Studies of the Energetics of Serine Hydrolase Organophosphate Interactions." I.M. Kovach, 9th IUPAC Conference on Physical Organic Chemistry, Regensburg, FDR, August 21- 27, 1988.

"Characterization of Transition States for Phosphonylation of Serine Hydrolases by Isotopic Probes." I.M. Kovach, 9th IUPAC Conference on Physical Organic Chemistry, Regensburg, FDR, August 21-27, 1988 (Poster).

"Comparative Study of Nucleophilic and Enzymic Reactions of 2-Propyl Methylphosphonate Derivatives." I.M. Kovach and A.J. Bennet, XI International Conference on Phosphorus Chemistry, Tallin, USSR, July 3-7, 1989 - Invited Presentation.

"Kinetic Isotope Effect Probes for the Elucidation of the Mechanism of Organophosphonate Hydrolysis and Inactivation of Acetylcholinesterase." A. Bennet, I.M. Kovach, and R.L. Schowen, 193th ACS National Meeting, Denver, CO, April 5-10, 1987.

Publications

I.M. Kovach , M. Larson and R.L. Schowen, One Proton Catalysis in the Deacetylation of Acetylcholinesterase, J. Am. Chem. Soc. 108, 3054 (1986).

I.M. Kovach, M. Larson and R.L. Schowen, Catalytic Recruitment in the Inactivation of Serine Proteases by Phosphonate Esters. Recruitment of Acid-Base Catalysis, J. Am. Chem. Soc. 108, 5490 (1986).

I.M. Kovach and R.L. Schowen, Catalytic Recruitment in the Inactivation of Serine Hydrolases by Phosphonate Esters, in Peptides and Proteases: Recent Advances, R.L. Schowen and A. Barth (Eds.), Pergamon, Oxford, England, 1987.

I.M. Kovach , J. Harmon-Ashley Huber and R.L. Schowen, Catalytic Recruitment in the Inactivation of Acetylcholinesterase by Soman: Temperature Dependence of the Solvent Isotope Effect, J. Am. Chem. Soc. 110, 1002 (1988).

I.M. Kovach, Serine Hydrolase Phosphyl Ester Interactions: Molecular Modeling, J. Mol. Struct. (Theochem), 170, 159 (1988).

I.M. Kovach, Structure and Dynamics of Serine Hydrolyase-Organophosphate Adducts, J. Enz. Inhib. 2, 198 (1988).

A.J. Bennet, I.M. Kovach , and R.L. Schowen, Enzymic Determination of the Concentrations of Intact Soman and Sarin in Aqueous Solutions, Pesticide Biochem. Physiol. 33, 78 (1989).

A.J. Bennet, I.M. Kovach and R.L. Schowen, Rate-Determining P-O Fission in the Self-Stimulated Inactivation of Acetylcholinesterase by 4-Nitrophenyl 2-Propyl Methylphosphonate, J. Am. Chem. Soc. 110, 7892 (1988).

I.M. Kovach and A.J. Bennet, Comparative Study of Nucleophilic and Enzymic Reactions of 2-Propyl Methylphosphonate Derivatives, Phosphorus and Sulfur, 000 (1989).

A.J. Bennet, I.M. Kovach and J.A. Bibbs, Catalytic Recruitment by Phosphonyl Derivatives as Inactivators of Acetylcholinesterase and as Substrates for Imidazole-catalyzed Hydrolysis: β -Deuterium Isotope Effects, J. Am. Chem. Soc., 110. 6424 (1989).

A.J. Bennet, J.A. Bibbs and I.M. Kovach; Buffer-Catalyzed Hydrolysis of Phosphonate Esters: Activation Parameters and Solvent Isotope Effects, J. Am. Chem. Soc., submitted.

I.M. Kovach and J.H.-A. Huber, Basic Methanolysis of Pinacolyl and Isopropyl Derivatives of Alkyl Phosphonates with P-O Fission, manuscript in preparation for submission to J. Org. Chem.

I.M. Kovach, Substrate Competition for Enzyme Activity as a Measure of Rates of Irreversible Inhibition: Scope and Limitations, submitted to J. Enzyme Inhib.